

TRACING *TRITURUS* THROUGH TIME:
PHYLOGEOGRAPHY AND SPATIAL ECOLOGY

Biense Marinus Wielstra

Examining committee:
Prof. dr. V.G. Jetten
Prof. dr. ir. A. Veldkamp
Prof. dr. M. Vences
Prof. dr. P.C. van Welzen

University of Twente
University of Twente
Technical University of Braunschweig
Leiden University



ITC dissertation number 212
ITC, P.O. Box 6, 7500 AA Enschede, The Netherlands

ISBN 978-90-6164-337-1
Cover designed by Ben Wielstra
Printed by ITC Printing Department
Copyright © 2012 by Ben Wielstra



TRACING *TRITURUS* THROUGH TIME:
PHYLOGEOGRAPHY AND SPATIAL ECOLOGY

DISSERTATION

to obtain
the degree of doctor at the University of Twente,
on the authority of the rector magnificus,
prof. dr. H. Brinksma,
on account of the decision of the graduation committee,
to be publicly defended
on Wednesday 3 October 2012 at 14.45 hrs

by

Biense Marinus Wielstra

born on 7 September 1982

in Terneuzen, The Netherlands

This thesis is approved by
Prof. dr. A.K. Skidmore, promoter
Dr. J.W. Arntzen, assistant promoter
Dr. A.G. Toxopeus, assistant promoter

To my parents

Preface:

This PhD research was supported by a partnership between the University of Twente, Faculty of Geo-Information Science and Earth Observation (ITC) and Naturalis Biodiversity Center.

ITC dissertation list:

http://www.itc.nl/Pub/research/Graduate-programme/Graduate-programme-PhD_Graduates.html

Personal webpage of Ben Wielstra (with biography and publication list):

<http://science.naturalis.nl/research/people/cv/wielstra>

Acknowledgements

I am most indebted to Pim Arntzen. Pim already acted as my supervisor during several projects, in collaboration with Naturalis Biodiversity Center, while I was still studying Biology at Leiden University. Pim managed to motivate me and opened my eyes: Biology was not so bad after all! Pim's supervision during my PhD was invaluable. I consider Pim a mentor and an example.

My PhD was a collaboration between Naturalis Biodiversity Center and ITC. The city of Enschede became my base for four years. My supervisory team at ITC consisted of Andrew Skidmore and Bert Toxopeus, who helped shape my concept of Science. Many thanks. My office mate Sukhad Keshkamat provided mental support and supplied the GIS training I needed. Our suffering has come to an end Dr. Kesh! I thoroughly enjoyed the friendship of my fellow PhDs and the staff at ITC. But, of course, the best thing that happened to me at ITC was meeting Yali Si! You are awesome!

During my PhD I still regularly worked in Leiden too, first at the van der Klaauw Laboratory and later at the Sylvius Laboratory. I could always count on good discussions with many colleagues from Naturalis Biodiversity Center and the Institute of Biology Leiden. Aline, Amy, Camiel, Dick, Frank, Gonçalo, Janine, Kevin, Marcel, Natasha, Rene, Sander (and the many people I undoubtedly forgot to mention, please forgive me): thanks! I especially want to thank Niels Raes, whose plentiful advice helped me familiarize myself with the field of spatial ecology.

By meeting at conferences, conducting fieldwork together, visiting museums, and a hell of a lot of correspondence, I came in contact with a lot of colleagues working on *Triturus* newts. The many people listed as co-authors and mentioned in the acknowledgements of the individual chapters illustrate the importance of collaboration during my PhD. A special thanks to Wouter Beukema for helping me to tackle chapter 3. Graham Wallis' critical reviews helped me improve several of my papers and we managed to find some good ponds during a fun field trip!

My biggest supporters are and have always been my parents. They have continuously stimulated me to pursue the line of work that I like. A son doing newt modeling for a living... how do you explain *that?! To express my gratitude, I dedicate this thesis to my parents.*

Table of Contents

Introduction.....	1
Chapter 1: Unraveling the rapid radiation of crested newts (<i>Triturus cristatus</i> superspecies) using complete mitogenomic sequences.....	11
Chapter 2: Cryptic crested newt diversity at the Eurasian transition: The mitochondrial DNA phylogeography of Near Eastern <i>Triturus</i> newts.....	25
Chapter 3: Corresponding mitochondrial DNA and niche divergence for cryptic crested newt species.....	43
Chapter 4: Tracing glacial refugia of <i>Triturus</i> newts based on mitochondrial DNA phylogeography and species distribution modeling.....	53
Chapter 5: Postglacial species displacement in <i>Triturus</i> newts deduced from asymmetrically introgressed mitochondrial DNA and ecological niche models.....	77
Chapter 6: A multimarker phylogeography of crested newts (<i>Triturus cristatus</i> superspecies) reveals cryptic species.....	95
Synthesis.....	111
References.....	117
Summary.....	131
Samenvatting.....	131

Introduction

Biogeography: studying the shaping of biodiversity patterns

Earth is a heterogeneous place, both in space and in time. An environmental gradient stretches from pole to pole and on a finer scale, a mosaic of biotopes exists. Climate is in a constant state of flux and geomorphological processes continually change the surface of the Earth. Differences in the spatial and temporal composition of community structure result in shifting interactions among biota. Aforementioned factors do not function independently, but form an intricate web of interactions. The versatility of the face of the Earth is reflected in the non-random distribution of life. Whereas only the current situation can be directly witnessed, past processes which caused the structuring of life have to be inferred.

Biogeography is the branch of Biology that seeks to understand the spatio-temporal distribution of biodiversity (1). Two distinct classical schools of thought, 'Ecological' and 'Historical Biogeography', emphasize the importance of active and passive dispersal, respectively. It is nowadays recognized that only a synthesis of both would manage to grasp the complexity of biogeography (2-4); present distribution of biodiversity has been molded by a reticulation of historical factors. From a species' point of view, distribution during the course of history depends on variation in the extent and accessibility of suitable surface: in the face of extinction, a species must continually 'track' the habitat it prefers. This train of thought presumes that a species is bound to a particular partition of the biosphere.

The ecological niche: linking species to the environment

The ecological niche of a species enfolds the suite of conditions under which it can maintain self-sustaining populations: areas not satisfying the niche are uninhabitable (5). The range of environmental conditions a species can tolerate – the width of its niche – determines the extent of its distribution. Generalist species thrive under a wide range of conditions, sharing resources with an assemblage of other species, whereas specialist species are constrained to localized habitat, with the benefit of having a monopoly on resources.

The presence of other organisms influences a species' distribution. Different species with an identical niche cannot co-occur, they competitively exclude on another. Colonization of an area is hampered when a species with a similar niche is already established (6): unless the newcomer is superior (i.e. capable to outcompete the resident), it is beforehand left disadvantaged (i.e. first-come, first-served).

Co-occurrence can only be accomplished by niche partitioning: in areas of overlap, a narrower niche is exploited (ecological character displacement; 7, 8) than outside of sympatric zones (competitive release; 7). Similarly, other types of biotic interactions (e.g. predators, parasites, pathogens and prey) pose either positive or negative pressures on a species. The presence of particular ecological interactions may alternate over a species' distribution range (9).

A distinction is made between the potential niche (the set of abiotic conditions suitable) and the realized niche (a narrower niche as pressured by biotic interactions). Species do not occupy every speck on earth where suitable conditions happen to prevail (the potential distribution); only a part of the area predicted to be suitable is inhabited (the realized distribution), leaving the remainder unpopulated. Tracts of inhospitable terrain can act as discontinuities and pose limits to distribution. Whether a feature acts as a barrier to distribution depends on the vagility of a species.

Contrast between suitable and non-suitable area does not only occur in space, but also in time: barriers of inhospitable terrain can be raised or demolished and the composition of community structure shifts (2). Alterations in surface characteristics may either facilitate expansion (dispersal/colonization) or cause regression (contraction/extinction). From a historical perspective, the distinction between potential and realized distribution is therefore not surprising: the extent to which the potential distribution is saturated depends on the dispersal opportunities encountered by a species during its evolutionary history and the time which has been available.

Distribution dynamics through time have determined the current state of affairs. Clues on biogeography are left in the patterns in which contemporary biodiversity is distributed. For these clues to be unlocked, first biodiversity and its distribution have to be determined.

Deriving biogeographical hypotheses: a move towards genetic information

Human perception of biodiversity has traditionally been biased towards morphological heterogeneity (10). This approach, whether applied out of ignorance (implying only morphological features are evolutionary relevant) or necessity (morphology providing the only noticeable and therefore exploitable variation), inevitably underestimates the true extent of biodiversity. A solution to this problem came with the opportunity to explore the genotype instead of the phenotype. With the advance of molecular approaches, a wealth of hitherto cryptic biodiversity was revealed, hidden in organisms' genomes (10). Randomly arisen mutations provide an objective way of assessing diversity.

Molecular systematics places genetic variation in an evolutionary context by tracing genealogical histories. By examining the spatial distribution of genetic lineages, biogeographical hypotheses can be formulated (10). The spatio-temporal scale involved ranges from macro- to microevolutionary processes; from the large-scale phylogenetics (10), dealing with relationships among species and more inclusive taxa, to the fine-grained landscape genetics (11), dealing with population interactions. Such sub-disciplinary terms are employed for the classification of what should in fact be seen as a continuum. The distribution of intraspecific genetic differentiation is the subject of the somewhat intermediate field of phylogeography (12) and will be the subject of the present research.

Phylogeography: biogeography based on intraspecific gene geography

The study of gene pedigrees within a species was pioneered in the 1970's. In order to distinguish this exciting branch of genetics, John C. Avise and co-workers, in a landmark paper published in 1987, coined the term phylogeography – a contraction of phylogeny and geography (13). The name has stuck. Phylogeography combines elements of population genetics and phylogenetics, thereby placing population structure in a historical context. Phylogeographical research has seen a surge of attention since its relatively recent germination and is now considered a full-fledged branch of biogeographical science (12).

The tremendous amount of attention addressed to phylogeographical research is imputed to its interesting scale. The field homes in on what has been referred to as 'the evolutionary twilight zone' (14): the boundary between macro- and microevolutionary processes. Extracting biogeographical patterns is hampered in phylogenetics as subsequent distribution changes diluted the patterns which initiated cladogenesis: it is hard to determine whether barriers to genetic interaction arose in allopatry or sympatry (15). Landscape genetics studies connections among populations in mosaic landscapes: it focuses on the cohesiveness of populations despite barriers rather than the growing apart because of barriers. Phylogeography provides the most direct way of looking at the forces driving distribution. The field focuses on the genesis of evolutionary lineages as triggered by environmental processes: the essence of biogeography.

Key to gene-based biogeography is the generation of genetic variation. But how does this process work? Within a species' gene pool – comprising the genomes of its individual members – many copies of each gene occur. Through mutation, various variants of the same gene arise, which differ slightly in sequence, but not in function (they are selectively neutral).

These different gene versions are known as haplotypes. The spread of new haplotypes in the gene pool during the next generations is a stochastic process. Chances for a newly arisen haplotype to increase in frequency are influenced by gene flow and genetic drift. Gene flow homogenizes the gene pool; in the extreme case, panmixia forestalls genetic variation. Partitioning of the gene pool, on the other hand, hampers the free exchange of genetic material; as genetic isolation takes action, genetic drift drives deviation among spatially separated subdivisions. The extent in which these opposite forces act determines population structure.

Mutation is a random process. Two forces act on sequence evolution: genetic drift and (either negative or positive) natural selection. Which of the two plays a dominant role, has been a matter of heated debate (10). The upholding view is that the majority of the evolutionary change is ascribed to genetic drift, acting on selectively (nearly-) neutral mutations. According to the molecular clock theory, on average, mutations arise at a constant rate (10). By estimating this rate, topological data can be placed into a temporal context. Time intervals for cladogenetic events can be acquired by calibration of the phylogenetic network, by appointing a fixed age to a particular node (based on a dated fossil, for example). The existence of a universal molecular clock is disputed, but at the taxonomic level which is the subject of phylogeography, assuming a molecular clock seems reasonable (16).

Gene flow and genetic drift have left their marks on the current geographical distribution of genetic information. In order to extract the biogeographical data imprinted in genomes, for a sample of individuals from across the distribution range, the basepair arrangement for a particular gene is determined – a procedure known as sequencing (10). The individual DNA sequences are appointed to haplotypes. By inferring relationships among the different haplotypes, the history of a gene is reconstructed. Patterns of differentiation and similarity among populations suggest past conditions facilitating vicariance and connectivity.

Advances in phylogeography: more data and improved ways to analyze it

Different genetic transmission systems are used in phylogeographic studies, presenting different advantages and considerations (12). Mitochondrial DNA has traditionally dominated the field of phylogeography, but the application of autosomal nuclear DNA is becoming increasingly implemented (12). Both sources present their limitations and advantages (17, 18). Due to its recombining nature, the nuclear genome is composed of a reticulation of genealogical lineages; each gene has a unique history. For mitochondrial DNA, however, all genes express a linked inheritance.

Mitochondrial DNA is present in only one copy per cell (haploid), whereas for autosomal nuclear DNA, two copies are present (diploid). Mitochondrial DNA is transmitted matrilineally, whereas autosomal nuclear DNA is inherited from both parents. Therefore the effective population size of mitochondrial DNA is a fourth of that of autosomal nuclear DNA. This results in a shorter coalescence time for mitochondrial DNA than for autosomal nuclear DNA; lineage sorting until attaining reciprocal monophyly takes less time for mitochondrial DNA, autosomal nuclear DNA will retain patterns of ancestral polymorphism longer.

Stochasticity in the genetic process – variance in coalescent time and population affiliation of alleles – means that the history of a single gene is different from population history: each gene tells its own variation on a story. Including multiple, unlinked markers, allows more reliable inferences; averaging over gene trees enables the distillation of the true species tree (16). Phylogeographic studies show a trend towards a multi-marker approach. Genealogical concordance – corroboration across multiple unlinked loci within a species – is a strong indication of an underlying causal event.

A case study on a single species provides insight into situations which would have influenced contemporary biota. Events which have shaped genetic patterns in a particular species are not expected to have left co-distributed species entirely unaffected. Comparing the genetic structuring within multiple sympatric species – an approach known as comparative phylogeography – may reveal concordant patterns (19, 20). Congruent patterns suggest shared causality: a prevailing scenario of biogeography.

An ever increasing amount of information is extracted from genomes. As sequencing becomes increasingly cheaper and faster, the use of denser sampling and inclusion of more genetic markers is enabled. Analytical methods are getting more and more sophisticated (14). In other words, the acquisition and analysis of genetic data is well developed. As the term implies, phylogeography explicitly deals with the geographical distribution of phylogenetic lineages. So how is this wealth of genetic information paired with geography?

A challenge to 'traditional' phylogeography: the missing link with geography

Present day genetic structuring is a derivative of the evolutionary history of the species under study. In phylogeographic studies, biogeographical scenarios are inferred, by inductive reasoning. Paleogeomorphological information provides insight in the formation of the area in which the species under study is distributed. Based on this knowledge, historical operators are appointed to explain the current geographic distribution of genotypes.

Coarsely put, the researcher searches for historical events fitting the uncovered phylogenetic framework. The resulting 'just so story' may very well be correct, but lacks statistical support and alternative explanations are not explored. Contrasting with the sophisticated, quantitative methods for obtaining a phylogenetic tree, the geographical aspect is addressed (dismissed, one could argue) in a subjective, qualitative, over interpreted way.

Concern about this disentanglement of phylogeography with geography is increasingly being expressed in the literature (21-24). The lack of statistical rigor, underlines the problem facing current phylogeographical approaches. Paraphrasing Kidd and Ritchie (21): "*Spatial-geographic aspects of phylogeographic research are underdeveloped: the emphasis lays on the 'phylogeny' component of phylogeography and the 'geography' component has a subordinate role.*"

There is an obvious need in phylogeographical research for a way to incorporate spatial information in a quantitative way. As a result of the experimental set-up of phylogeographic research – recording geographical coordinates of localities from which samples are extracted with a global positioning system – the spatial distribution of gene lineages is known quite exact. Now, would it not be great if there was a tool available with which this information could be exploited? Well, actually there is.

The use of a geographic information system (GIS) – a computer system that facilitates the integration and interrelation of different geographically referenced data sets (21) – has been suggested to be playing an important role in future approaches, in order to quantify the role of geographical factors (14, 21, 22, 25). A GIS environment can aid in the visualizing of the distribution of biodiversity by (simply put) overlaying phylogenetic networks over a map (26-29). But geographic information systems have much more potential in evolutionary research (see 22 for an overview). Most promising in a phylogeographical context is the procedure known as ecological niche modeling.

Ecological niche modeling: predicting species distributions through time

Occurrence data can be used for an educated extrapolation of a species' range. Based on the characteristics linked to georeferenced populations, environmental correlates which determine distribution can be extracted. In other words, it is possible to approximate the niche of a species (30). Based on a species' preferences, the total surface of the Earth which suits the species can be assessed. This is, in short, the procedure known as ecological niche modeling (also often referred to as species distribution modeling).

In order to capture the width of a species' environmental tolerances, multiple data points are required as input (31, 32). Both presence and absence of the focal species can be incorporated. However, establishing true absence is problematic (33) – when can one be sure to have looked hard enough? Erroneous omission can be circumvented by only using presence data, with the disadvantage of having less data points available (34).

Niche modeling is prone to over-prediction of distribution range, as it will identify the potential distribution instead of the realized distribution (35). This distinction between potential and realized distribution is most interesting from a biogeographical perspective as it enables identification of the factors which pose barriers to a species in fulfilling its potential distribution.

Current distribution is only a snapshot of the history of a species' distribution over the surface of the Earth. In theory, the extent of suitable surface area could be traced back in time, by conducting ecological niche modeling in conjunction with paleogeographical and -climatological reconstructions. The reliability of hindcasting distributions depends on the explanatory potential of the current niche. Past adaptation would distort the signal (36, 37). To what extent can a niche be assumed to have remained stable over evolutionary timescales? The restriction of major taxonomical divisions (i.e. orders or even classes) to long isolated fragments belonging to a certain climate zone (e.g. the three tropical regions) has been interpreted as indicating stasis over extensive time spans (3, 38). A strict interpretation of niche conservatism would exclude the possibility of any adaptation to 'new conditions' taking place (which would enable the 'breaching' of dispersal barriers). But, by definition, adaptation would be expected during an evolutionary trajectory (39). The upholding view is that ecological distance is correlated with genetic distance (opposed to geographic distance).

An estimation of niche stability can be obtained by comparison of related taxa. There are indications that stability occurs within species (40), at the level of sister species (41, 42), over genera (43, 44) and even among genera within families (45, 46). Some studies, however, have shown departure from niche conservatism for all the different hierarchical levels of biological classification discussed (47-52). Niche stability within species has been shown directly – albeit over relatively short time spans – by linking comparing contemporary species and Ice Age fossil data with synchronic environment (53, 54). Even when the fundamental niche has remained stationary, changes in the realized niche (i.e. by fluctuating biotic interactions) may complicate niche modeling through time (55, 56). Communities are not likely to move as an entity: individual species respond idiosyncratically to changes (35). The recreation of entire past communities seems an impossible task and may even involve species which are now extinct.

The modeling of paleodistributions depends on the detail and reliability with which past circumstances can be reconstructed (36). Reconstructions for the past can never be as detailed as for the present day situation. Course grained estimations of past circumstances can be informative, but habitat fragmentation may occur on a scale too fine to distinguish (e.g. rivers may act as dispersal barriers; 57). A growing number of publications is focusing on ecological niche modeling back in time. A real deep time (and very coarse) approach focused on the Cambrium and Devonian Period (58). The subjects of this study have long been extinct. More attention has been paid to the reconstruction of ranges during the Last Glacial Maximum (53, 54, 59-61).

Ecological niche modeling has seen a huge increase in interest and application (62). As in the genetic approach, developments in theoretical, computer and statistical sciences have aided the advance of this GIS approach to uncover species level biogeography (9, 22, 62). If it was to be combined with 'classic' phylogeographic studies, ecological niche modeling has the potential to provide the much needed link of the field with geography.

The context of this thesis: combining phylogeography and spatial ecology

Phylogeography and ecological niche modeling strive towards the same goal: to explain biogeography by uncovering the environmental mechanisms underlying distribution. Both approaches can independently reconstruct the history of distribution, providing a way to cross validate results. Strengths of the two approaches can be combined and weaknesses cancelled out, so increasing the confidence with which biogeographical scenarios are developed. A concerted effort of the two is increasingly being promoted to improve historical biogeographical reconstructions (21, 22, 25, 30). The aim of this thesis is to combine both techniques to increase the yield of biogeographical information from georeferenced genomes.

Using *Triturus* newts as a model

The model system used in the present research is the genus *Triturus*: the marbled and crested newts (Fig. 1). The different *Triturus* species are spatially incompatible: the presence of one species precludes the presence of another (63). This suggests that ecological differences determine which species fares best against which ecological background. *Triturus* newts differ in the number of months they annually congregate in water bodies to fulfill their reproduction cycle, suggesting adaptation to different equilibriums in an aquatic-terrestrial trade-off (63). The ecological variation among the different species is reflected by variation in their body build: the sturdier the species, the more terrestrial it is.



Figure 1 A representative of the genus *Triturus*: a male crested newt.

The area in which *Triturus* occurs, spanning most of Europe and adjacent Asia, has been subjected to a dynamic geomorphological and climatological history. An ecological background in flux combined with territorial tension among taxa makes for an intriguing evolutionary picture across space and time. To explore the spatio-temporal strife among *Triturus* species we first need to determine a phylogenetic framework for *Triturus* and put adaptation in an evolutionary context.

Outline of this thesis

In [chapter 1](#) we investigate the phylogenetic relationships among the different *Triturus* species. For this aim, full mitogenomic sequences are employed. Furthermore, we explore whether the variation in body build in *Triturus* reflects phylogeny. In [chapter 2](#) we develop a historical biogeographical scenario for a newly discovered complex of three distinct mitochondrial DNA lineages comprising the *T. karelinii* group of crested newts. We compare a calibrated phylogeographic framework based on mitochondrial DNA with paleogeological reconstructions of the Mediterranean region. In [chapter 3](#) we test whether the three *T. karelinii* mitochondrial DNA lineages are also ecologically distinct. To be able to interpret our results, we treat the differences among recognized crested newt species as a benchmark. In [chapter 4](#) we investigate whether signatures of population contraction and expansion associated with the glacial-interglacial cycles of the Quaternary Ice Age can be derived from a phylogeographical survey of mitochondrial DNA. We compare this with an independent reconstruction of glacial refugia based on ecological niche modeling. In [chapter 5](#) we study introgression of mitochondrial DNA from one species of crested newt into another in a spatio-temporal context. We first delimit the area of mitochondrial DNA introgression based on a dense phylogeographical survey. Subsequently we use ecological niche modeling to test whether past climate change facilitated outcompetition of the ‘donor’ species by the ‘recipient’ species. In [chapter 6](#) we conduct a multimarker phylogeography of crested newts. We put the question to the test whether the three distinct *T. karelinii* constitute discrete nuclear gene pools.

Chapter 1: Unraveling the rapid radiation of crested newts (*Triturus cristatus* superspecies) using complete mitogenomic sequences

This chapter is based on: Wielstra B, Arntzen JW (2011) Unraveling the rapid radiation of crested newts (*Triturus cristatus* superspecies) using complete mitogenomic sequences. *BMC Evolutionary Biology* 11: 162

Abstract

The rapid radiation of crested newts (*Triturus cristatus* superspecies) comprises four morphotypes: 1) the *T. karelinii* group, 2) *T. carnifex* – *T. macedonicus*, 3) *T. cristatus* and 4) *T. dobrogicus*. These vary in body build and the number of rib-bearing pre-sacral vertebrae (NRBV). The phylogenetic relationships of the morphotypes have not yet been settled, despite several previous attempts, employing a variety of molecular markers. We here resolve the crested newt phylogeny by using complete mitochondrial genome sequences. Bayesian inference based on the mitogenomic data yields a fully bifurcating, significantly supported tree, though Maximum Likelihood inference yields low support values. The internal branches connecting the morphotypes are short relative to the terminal branches. Seen from the root of *Triturus* (NRBV = 13), a basal dichotomy separates the *T. karelinii* group (NRBV = 13) from the remaining crested newts. The next split divides the latter assortment into *T. carnifex* – *T. macedonicus* (NRBV = 14) versus *T. cristatus* (NRBV = 15) and *T. dobrogicus* (NRBV = 16 or 17). We argue that the Bayesian full mitochondrial DNA phylogeny is superior to previous attempts aiming to recover the crested newt species tree. Furthermore, our new phylogeny involves a maximally parsimonious interpretation of NRBV evolution. Calibrating the phylogeny allows us to evaluate potential drivers for crested newt cladogenesis. The split between the *T. karelinii* group and the three other morphotypes, at ca. 10.4 Ma, is associated with the separation of the Balkan and Anatolian landmasses (12-9 Ma). No currently known vicariant events can be ascribed to the other two splits, first at ca. 9.3 Ma, separating *T. carnifex* – *T. macedonicus*, and second at ca. 8.8 Ma, splitting *T. cristatus* and *T. dobrogicus*. The crested newt morphotypes differ in the duration of their annual aquatic period. We speculate on the role that this ecological differentiation could have played during speciation.

Introduction

Understanding the temporal framework in which species have originated is fundamental to historical biogeography and evolutionary studies. However, obtaining a reliable phylogeny for a model system is not always straightforward. Rapid radiations are notoriously difficult in this respect, and the older the radiation, the more pronounced the problem will be (64). The crested newt *Triturus cristatus* superspecies (Amphibia: Salamandridae), distributed in Europe and adjacent Asia (Fig. 1), is an example of a relatively old, rapid radiation, for which it has proved problematic to obtain a resolved phylogenetic tree.

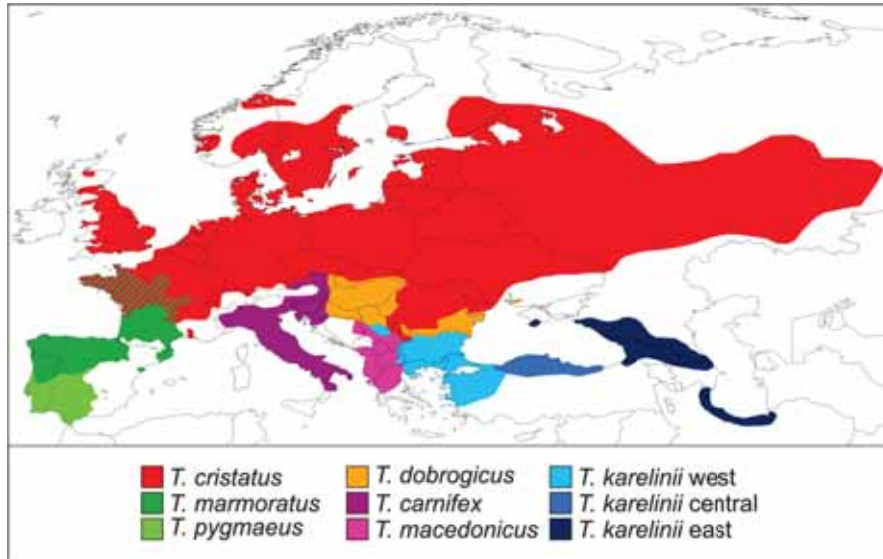


Figure 1 The distribution of the genus *Triturus*. Shown are the ranges for all the different species; the range of the *T. karelinii* group is partitioned according to the three distinct mitochondrial DNA clades the group is composed of (cf. 65). Note the partially overlapping ranges of the crested newt *T. cristatus* and the marbled newt *T. marmoratus*. The map is based on (66) and updated following recent findings.

The crested newt superspecies encompasses four morphological groups, hereafter referred to as ‘morphotypes’. Ordered from a stocky build with sturdy limbs, to slender with small limbs, via two intermediate stages, these are: 1) the *T. karelinii* group, 2) *T. carnifex* – *T. macedonicus*, 3) *T. cristatus* and 4) *T. dobrogicus*. The morphotypes are characterized by discrete differences in the number of rib-bearing pre-sacral vertebrae (NRBV) (67). The typical NRBV count is 13 for the *T. karelinii* group, 14 for *T. carnifex* – *T. macedonicus*, 15 for *T. cristatus* and 16 or 17 for *T. dobrogicus*. The marbled newts, *T. marmoratus* and *T. pygmaeus*, which make up the crested newts’ sister group, have the heaviest body build in the genus and possess a typical NRBV count of 12. Over ninety per cent of these newts can be correctly identified based on NRBV counts alone; interspecific hybridization along parapatric contact zones (Fig. 1) is suggested to account for most of the remaining intraspecific variation (63, 67, 68). Crested newt morphology has been interpreted as reflecting phylogeny (67). A maximally parsimonious interpretation of NRBV (interpreting the ancestral crested newt body shape as relatively robust and the more slender body shapes as derived) suggests a branching order as shown in Fig. 2a.

With the advent of molecular techniques, independent data became available and multiple molecular markers have now been employed to attempt to resolve the crested newt phylogeny. Based on restriction fragment length polymorphism of the mitochondrial genome (employing eleven restriction enzymes), a polytomy was found (Fig. 2b) (69). Similarly, analysis of a suite of forty enzyme loci and 642 bp of mitochondrial sequence data resulted in a polytomous relationship for the four morphotypes (Fig. 2b) (66). A polytomy could simply reflect a lack of phylogenetic resolution in the data. However, as the different datasets both pointed towards a polytomy, it was suggested that the four crested newt morphotypes truly split practically simultaneously (66).

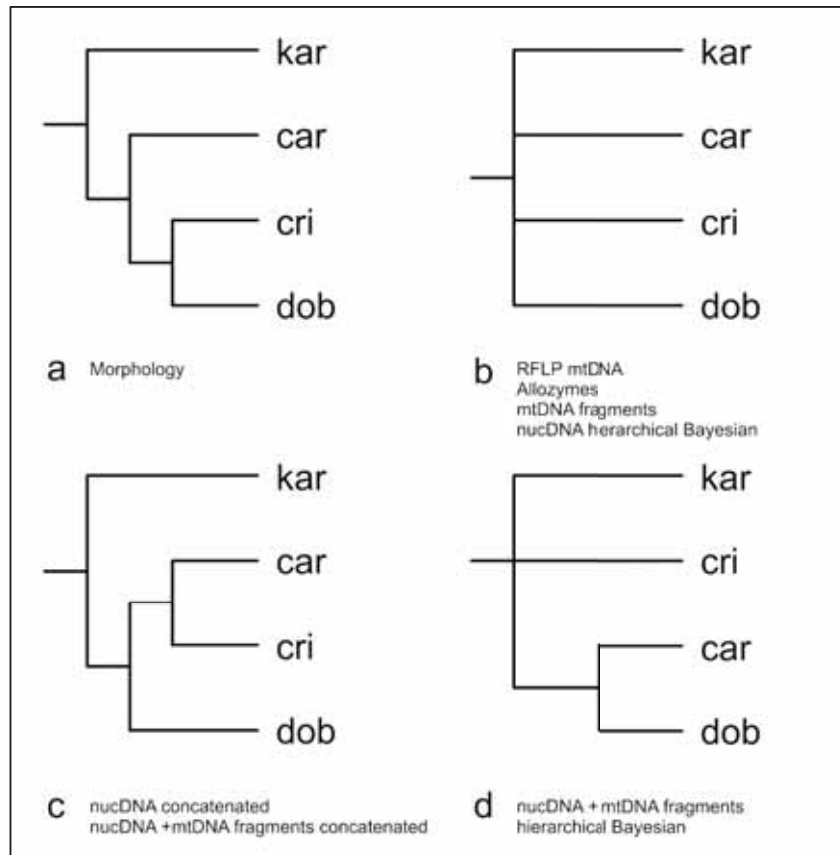


Figure 2 A summary of the different phylogenetic hypotheses for the four crested newt morphotypes as suggested by previous studies. The datasets supporting each tree are noted below it (see the main text for details and references). Abbreviations used for the four morphotypes are: kar = *T. karelinii* group; car = *T. carnifex* – *T. macedonicus*; cri = *T. cristatus*; dob = *T. dobrogicus*.

A later effort using sequence data of five nuclear DNA (2589 bp) and two mitochondrial DNA markers (1747 bp) revealed a more varied picture (70). An analysis using the sequence data concatenated found a fully bifurcating and significantly supported phylogeny (Fig. 2c). There are, however, theoretical objections to data concatenation, as this method does not consider the unique topological history that each individual gene possesses (71). Therefore, phylogenetic inference was also carried out using a hierarchical Bayesian analysis, which does explicitly take the effects of gene tree heterogeneity into account. This analysis indeed produced different results. Based on the five nuclear DNA markers, a fourfold polytomy was found again (Fig. 2b). This fourfold polytomy could be expanded to a trichotomy by incorporating the mitochondrial DNA data, but the single sister relationship found was incongruent with the data concatenation approach (Fig. 2d).

Previous molecular studies have firmly established that the crested newt radiation occurred in a brief time interval. However, they yielded conflicting phylogenetic hypotheses and have been unable to settle the relationship among the morphotypes. Furthermore, all phylogenetic hypotheses found so far are in conflict with the tree suggested by morphology. In this study we further explore the crested newt phylogeny, this time employing complete mitogenomic sequences. As the mitochondrial genome contains tenfold the bp studied up to now (~17 Kbp vs. ~1.7 Kbp), it is a promising source of phylogenetic resolution (cf. 72). We here analyze nine newly-sequenced mitogenomes, representing all *Triturus* species, and manage to obtain a fully-resolved crested newt phylogeny. We discuss this new phylogeny with respect to previous attempts to obtain the *Triturus* tree and speculate on causes for cladogenesis.

Results

We present a mitogenomic *Triturus* phylogeny (Fig. 3) based on a division of the mitogenomic sequence data into 42 data partitions, as this partitioning strategy is preferred over the simpler ones tested (Table 1). Bayesian inference identifies a basal dichotomy in the crested newt superspecies between the *T. karelinii* group and the other morphotypes (node I in Fig. 3). The next bifurcation divides the latter assortment in *T. carnifex* – *T. macedonicus* (node II) versus *T. cristatus* and *T. dobrogicus* (node III). Posterior probabilities are ≥ 0.95 (Table 2). Although Maximum Likelihood inference yields the same branching order and similar branch lengths (tree not shown), the bootstrap support values for two of the three nodes associated with radiation of crested newt morphotypes (nodes II and III) are low (Table 2).

The mitogenomic phylogeny is characterized by long terminal branches, which are connected by short internal branches. The three nodes connecting the crested newt morphotypes represent a narrow time window (approximately 10.4-8.8 Ma) and have small confidence intervals, independent of dating method used (Table 2). Three character state transitions are required to explain the NRBV differentiation across the four crested newt morphotypes, two of which are situated on short internal branches (Fig. 3).

Table 1 Evaluation of the optimal partitioning scheme for the mitogenomic sequence data based on Bayes factor analysis.

	42	6	29	16
16	5,300.00	4,554.12	4,553.18	-
29	746.82	0.94	-	-
6	745.89	-	-	-
42	-	-	-	-

A pairwise comparison of the four tested partitioning strategies (6, 16, 29 or 42 data partitions), which are ordered from highest to lowest marginal likelihood from left to right and vice versa from top to bottom. The marginal likelihoods, in order from highest to lowest, are: 42 = -48316.02, 6 = -48688.96, 29 = -48689.43 and 16 = -50966.02.

Table 2 Support values and temporal estimates for *Triturus* nodes.

Node	Support values		Dating r8s		Dating BEAST	
	MrBayes	RAxML	Mean	95% CI	Mean	95% CI
I	1.0	100	10.3	9.4-11.2	10.4	9.4-11.5
II	1.0	62	9.2	8.5-9.4	9.3	8.3-10.2
III	0.95	46	8.7	8.0-9.4	8.8	7.8-9.7
a #	1.0	100	28.0	24.9-31.1	27.6	24.8-30.8
b	1.0	100	5.9	5.0-6.8	5.6	4.7-6.6
c	1.0	100	8.3	7.3-9.3	8.3	7.3-9.4
d	1.0	100	5.8	5.1-6.6	5.8	5.0-6.7
e #	1.0	100	5.33	n/a	5.33	n/a

The coded nodes correspond to Fig. 2. The nodes of interest, separating the crested newt morphotypes, are coded I-III (the remaining nodes are coded a-e). Nodes marked with a # are used for temporal calibration.

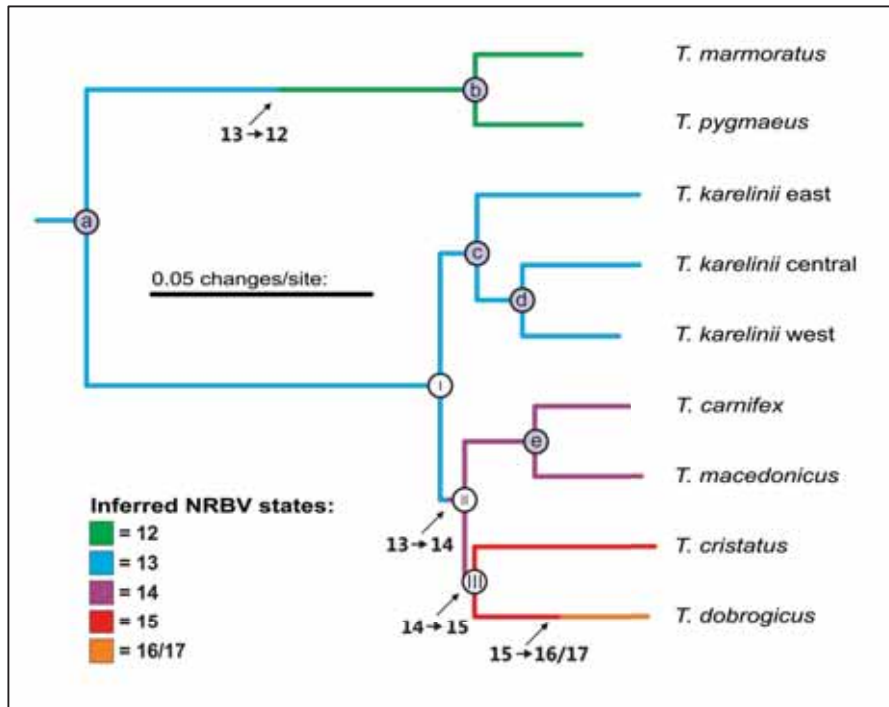


Figure 3 The mitogenomic *Triturus* tree resulting from the Bayesian inference. The *Calotriton asper* outgroup is not shown. Nodes are coded and correspond to table 2; the nodes of interest, separating the crested newt morphotypes, are coded I-III (the remaining nodes are coded a-e). The NRBV additions required to explain the NRBV variation observed in *Triturus* today are noted along the phylogeny (interpreting NRBV = 13 as the ancestral character state, see Additional file 1). The exact timing of inferred NRBV shifts is not known, only that they are positioned on a particular branch.

Discussion

The mitogenomic Triturus tree

The full mitogenomic dataset has provided the phylogenetic resolution that the crested newt case required. Previous approaches using only part of the mitochondrial genome found a polytomy for the four morphotypes, but based on the full mitochondrial DNA sequences we managed to resolve this polytomy. Under Bayesian inference, we find a fully bifurcating phylogeny, with significant support for the three nodes connecting the four crested newt morphotypes (i.e. nodes I-III in Fig. 3 and Table 2). In comparison, Maximum Likelihood bootstrapping finds equivocal results for two of the three nodes (nodes II and III).

Disparity in support values between both methods is known to occur at short internodes, where Bayesian inference appears to better exploit the relatively small number of informative characters (73). Our confidence in the Bayesian phylogeny is increased by its correspondence to the branching order suggested by a maximally parsimonious interpretation of NRBV evolution (Fig. 2a and 3).

The mitochondrial genome, given its non-recombining nature, behaves as a single gene and, due to stochasticity in the coalescent process, the branching order it suggests is not necessarily congruent with the true species tree (74). The motivation behind studying independent gene trees (i.e. multiple nuclear genetic markers) is that these should ultimately converge upon the overarching species tree (71). However, a recent hierarchical Bayesian analysis based on five nuclear markers did not yield a resolved crested newt phylogeny (70). This lack of resolution could be explained by the rapidness of the radiation of the crested newt morphotypes, as repeated cladogenesis within the temporal domain of the lineage sorting process increases the chance of a mismatch between gene trees and species tree (64, 71, 74-76). Such a risk of gene tree – species tree discordance is smaller for the mitochondrial genome, because lineage sorting is realized faster compared to the nuclear genome (given the fourfold smaller effective population size of the mitochondrial genome due to haploid and uniparental inheritance (17, 77)).

We do not claim that our current attempt resolves the crested newt species tree once and for all; studying a much larger battery of nuclear DNA markers than previously used is required to further home in on the crested newt species tree (75). However, considering the data currently available, we suggest that the Bayesian mitogenomic phylogeny as yet provides the most reliable estimation of the crested newt species tree. We here employ the new phylogeny to explore the potential causes underlying the splits between the crested newt morphotypes.

The potential of paleogeography to explain crested newt speciation

Based on temporal estimates associated with the crested newt splits (Table 2), potential vicariant events can be identified by consulting paleogeographic reconstructions. We here concentrate on the three splits which gave rise to the four crested newt morphotypes (i.e. nodes I-III in Fig. 3); for vicariant events underlying the three splits within morphotypes (i.e. nodes c-e in Fig. 3), see (65, 66). An earlier attempt to reconstruct the historical biogeography of crested newts assumed a ‘hard’ polytomous relationship for the four morphotypes (66). In effect, a temporal estimate was only provided for the crown of the crested newts and proposed vicariant events were derived from this date.

The present study has resolved the relationships among the morphotypes (i.e. the polytomy in (66) turned out to be 'soft' after all). In line with the increased phylogenetic resolution, more recent dates are appointed to the newly resolved nodes and their morphotype lineages. The crested newt crown, i.e. the split between the *T. karelinii* group and the remaining crested newts (node I in Fig. 3), is dated at ca. 10.4 Ma. The origin of the Aegean Sea at 12-9 Ma (78), which separated the Balkan Peninsula from Anatolia, is a likely underlying vicariant event (sensu 66). No obvious vicariant events can be associated with the two splits that gave rise to the three remaining morphotypes (79): the separation of *T. carnifex* – *T. macedonicus* versus *T. cristatus* and *T. dobrogicus* (node II) at approximately 9.3 Ma and the split between *T. cristatus* and *T. dobrogicus* (node III) around 8.8 Ma (contra 66).

No comprehensive paleogeographical reconstructions are as yet available for the Balkan Peninsula in the period between 11 and 8.5 Ma (79). It is feasible that vicariant events relevant to the crested newt case have yet to be discovered. As a way forward, we suggest that more taxa with Balkan distributions should be surveyed in a historical biogeographical context (19, 66). By uncovering congruent spatio-temporal signatures, such studies should assist in paleogeographical reconstruction of the Balkan Peninsula. This strategy might not be so straightforward; genetic structuring in the two other groups of newts that occur on the Balkan Peninsula (*Ichthyosaura* and *Lissotriton*), though relatively old, originated considerably more recent than that in the crested newts (80, 81).

Could ecological divergence have played a role in crested newt speciation?

The role of ecological divergence in historical biogeography is often regarded as passive; external factors such as geology and climate are considered to be responsible for the actual dividing of ancestral stocks and potential ecological divergence occurs at a later point (82). However, ecology can play an active role in the speciation process: disruptive selection along an ecological gradient can result in restrictions to gene flow, in the absence of geographical isolation (82-85). Could such a parapatric mode of speciation apply to the crested newt case?

The crested newt morphotypes do show ecological differentiation in the time they annually spend in the water. The duration of the annual aquatic period is three months in the *T. karelinii* group, four in *T. carnifex*, five in *T. cristatus* and six in *T. dobrogicus* (63). Crested newts thus show a correlation between phenotype and phenology: sturdy bodies and a low NRBV count are associated with a more terrestrial way of life and slender bodies and a high NRBV count with a more aquatic life style (63).

This notion of a terrestrial versus aquatic trade-off associated with body shape is further supported by the even more robust marbled newt *T. marmoratus*, whose two-month aquatic phase is the shortest of the *Triturus* newts (66).

The body shape differentiation in crested newts occurred over a brief timespan (Fig. 3 and Table 2): at least two of the three NRBV additions during crested newt evolution are associated with short internal branches. Under the assumption that today's phenology-phenotype correlation has been valid through time, the ecological divergence of the crested newt morphotypes must have similarly taken place over a short period. Considering the fundamental role water bodies play in amphibian reproduction (86), it is reasonable to suggest that differences in the availability of standing water would present different adaptive peaks. The time frame of the crested newt radiation corresponds to a period of increased seasonality in Eurasia during the Late Miocene (11.6-5.3 Ma), associated with the uplift of the Tibetan Plateau, which led to a more heterogeneous landscape in terms of humidity (87).

With a clear speciation scenario involving vicariance lacking, we, as an alternative hypothesis, suggest that the crested newts' body shape differentiation reflects a rapid adaptive radiation to different water regimes. It should be noted that these two hypotheses are not necessarily mutually exclusive.

Reflections on NRBV and its adaptive value in Triturus

Salamanders have become a model group to understand patterns of morphological evolution (88). Variation of salamander body shape has been accomplished by modifying the vertebral column, by either altering the length of the individual vertebrae or by changing the total number of vertebrae (89). Interestingly, the intrageneric range in NRBV count shown by *Triturus* is unprecedented in Salamandridae (see Additional file 1), suggesting body shape plasticity played a prominent role during crested newt evolution. Work on the genetic pathways underlying the evolutionary development of the different *Triturus* morphotypes will provide more insight into this phenomenon (J.M. Ziermann et al., in prep.).

What could be the adaptive value of the crested newt NRBV radiation? The dualism of an amphibian lifestyle poses conflicting demands on body shape. The rapid adaptive radiation scenario we propose for the crested newts, suggests that the balance struck for this trade-off differs among the morphotypes, due to the different ecological background each of them experiences. What do we currently understand about the differential performance of the morphotypes in the aquatic and the terrestrial environment?

Although (90) found that *Triturus* stockiness is positively correlated with running speed, this is not so for slenderness and swimming speed. What could be the reason for this partially unexpected result? Maybe 'speed' is not the most suitable way to characterize terrestrial or aquatic specialization? Perhaps body elongation benefits more aquatic *Triturus* newts some other way, e.g. by increasing maneuverability or by providing more space for egg production (90)? More research is required to elucidate the adaptive value of the different *Triturus* body shapes against distinct ecological backgrounds.

Conclusion

Although it has proven difficult to resolve the rapid radiation of crested newts, by employing full mitochondrial DNA sequence data we now have a precise estimate of the chronology of branching events. The relationship among the four crested newt morphotypes found agrees with a maximally parsimonious interpretation of NRBV evolution, increasing our confidence in the accuracy of the branching order. The basal dichotomy sorting out the crested newt morphotypes can be associated with a major vicariant event, but we cannot pinpoint drivers for the other two splits sorting out the morphotypes. We propose that (as yet) undiscovered vicariant events and/or ecological divergence (reflected by body shape differentiation) resulted in a disruption of gene flow. Crested newts are a suitable model to study eco-evo-devo in a rapid radiation and the new phylogenetic framework presented here serves as a baseline for future research.

Methods

Samples

We included seven crested newts (see Additional file 2), representing all recognized species, as well as three distinct mitochondrial DNA clades that constitute the *T. karelinii* group (cf. 65). We follow (65) in awaiting a taxonomic revision of the *T. karelinii* group before applying specific names to the three constituent mitochondrial DNA clades (the name *T. karelinii* sensu stricto would apply to the 'eastern clade' and *T. arntzeni* has been applied to the 'western clade'; no name has as yet been proposed for the 'central clade'). We also sequenced the two marbled newts (*T. marmoratus* and *T. pygmaeus*), the remaining members of the genus *Triturus*, to function as outgroup taxa. Additionally, we added a sequence of *Calotriton asper*, sister to the genus *Triturus*, available from (91) (GenBank accession number EU880307).

Sequences

The complete mitogenomes of the nine *Triturus* newts were sequenced in fifteen overlapping parts. We followed the laboratory protocol of (91) and designed more specific and/or internal primers where required (detailed in Additional file 3). Cycle sequencing was done commercially through Macrogen Inc. Forward and reverse sequences were checked by eye and consensus sequences were compiled with Sequencher 4.5 (Gene Codes Corporation). The fifteen fragments per individual were manually aligned and merged in MacClade 4.08 (92). The length of the resulting sequences ranged from 16,424 to 16,649 bp. The *Triturus* mitogenomes are composed of thirteen protein-coding genes, twenty-two transfer RNA genes, two ribosomal RNA genes, the D-loop, and a non-coding region (which is highly variable in length) and gene order is identical to that found in the rest of the family Salamandridae (cf. 91). The newly produced mitogenomic sequences have been submitted to GenBank (accession numbers are noted in Additional file 2). The 15420 bp data matrix used for phylogenetic analyses, comprising the ribosomal RNA, transfer RNA and protein-coding genes, is available from TreeBASE (study ID S11081).

Data partitioning

We compared four different partitioning strategies for organizing the mitochondrial sequence data (cf. 93). Each partitioning strategy treated the two ribosomal RNA genes and the concatenated transfer RNA genes as separate partitions. Differences among the partitioning strategies are based on the treatment of the protein-coding genes, dividing the protein-coding data according to: first, second and third codon position (6 partitions in total), each gene (16 partitions); first plus second and third codon position for each gene (29 partitions); and first, second and third codon position for each gene (42 partitions). The most appropriate model of sequence evolution for each data partition was determined with MrModeltest 2.2 (94), based on the Akaike Information Criterion (see Additional file 4). The optimal partitioning scheme was selected based on the differences in the harmonic mean of the $-\ln$ likelihood scores resulting from the Bayesian phylogenetic inference. The $2 \ln$ Bayes factors were calculated for each partitioning strategy by subtracting the score resulting from simpler partitioning strategies and multiplying the outcome by -2 (95, 96). A value for $2 \ln$ Bayes factor exceeding 10 was used as a threshold for preferring the more complex model (97).

Phylogenetic analyses

Mixed-model Bayesian phylogenetic inference was carried out with MrBayes 3.1.2 (98). For each data partition the rate of sequence evolution and parameters were unlinked. Two simultaneous four chain runs proceeded for one hundred million generations, with a sampling frequency of 0.001 and a heating parameter of 0.05. The first half of the sampled trees was discarded as burn-in and the phylogenetic inference was drawn from the remaining 'forest'. Tracer (99) was used to check for stabilization of overall likelihood within and convergence between runs. Partitioned Maximum Likelihood phylogenetic inference was carried out with RAxML 7.2.7 (100). Robustness of the tree was tested via 100 bootstrap replicates. All phylogenetic analyses were carried out via the CIPRES Science Gateway(101).

Temporal calibration

We used two independent calibration points for molecular dating, one fossil-based and one geology-based (cf. 65). A fossil dated at 24 Ma was interpreted as a minimum estimate for the most recent common ancestor of the genus *Triturus* (cf. 102) and the origin of the Adriatic Sea at 5.33 Ma, at the end of the Messinian Salinity Crisis, was interpreted as the vicariant event causing the *T. carnifex* – *T. macedonicus* split (cf. 66). Divergence times were estimated with r8s 1.71 (103) and BEAST 1.5.3 (104). In r8s we used the penalized-likelihood approach in combination with the truncated-Newton algorithm. *Calotriton asper* was pruned from the dataset, while keeping the root position, to avoid performing the time estimation on a basal trichotomy. The optimal smoothing parameter ($S=1$) was determined by a cross-validation procedure, using the Bayesian consensus tree as input. Mean temporal estimates and 95% confidence intervals were determined by profiling the last thousand sampled Bayesian topologies. In BEAST, we applied the uncorrelated lognormal relaxed clock model and a Yule speciation model. The fixed calibration point was appointed a normally distributed prior with a small standard deviation (0.001) and the minimum estimate a lognormally distributed prior with the default standard deviation (1.0). The tree resulting from the Bayesian analysis was used as starting topology. Each data partition was allowed its own model of sequence evolution, as previously determined with MrModeltest. Divergence times were estimated based on two independent 100 million generation runs, sampled every 1000 generations, after discarding the first half of generations as burn-in. Tracer (99) was used to check whether effective sample sizes were at least 200.

Supplementary data

Supplementary data associated with this article can be found, in the online version of this paper at <http://www.biomedcentral.com/1471-2148/11/162>.

- Additional file 1: NRBV tracing for the Salamandridae.
- Additional file 2: Sampling details.
- Additional file 3: Primer information.
- Additional file 4: Models of sequence evolution.

Acknowledgements

G.P. Wallis and two reviewers provided valuable comments on an earlier version of this manuscript.

Chapter 2: Cryptic crested newt diversity at the Eurasian transition: The mitochondrial DNA phylogeography of Near Eastern *Triturus* newts

This chapter is based on: Wielstra B, Espregueira Themudo G, Güçlü Ö, Olgun K, Poyarkov NA, Arntzen JW (2010) Cryptic crested newt diversity at the Eurasian transition: The mitochondrial DNA phylogeography of Near Eastern *Triturus* newts. *Molecular Phylogenetics and Evolution* 56: 888-896

Abstract

Crested newts of the *Triturus karelinii* group occur in a phylogeographically understudied region: the Near East. Controversy surrounds the systematic position of these newts within the complete crested newt assemblage (the *Triturus cristatus* superspecies). We explore the situation using mitochondrial sequence data (ND2 and ND4, ≈ 1.7 kb) and employing different methods of phylogenetic inference (Bayesian inference and Maximum Likelihood using mixed models) and molecular dating (r8s and BEAST). The *T. karelinii* group is monophyletic and constitutes one of four main lineages in the *T. cristatus* superspecies. The separation of the *T. karelinii* group from the remaining crested newts around 9 Ma is related to the formation of the Mid-Aegean Trench, which separated the Balkan and Anatolian landmasses. The *T. karelinii* group comprises three geographically structured clades (eastern, central and western). The genetic divergence shown by these clades is comparable to that among recognized crested newt species. We suggest the uplift of the Armenian Plateau to be responsible for the separation of the eastern clade around 7 Ma, and the re-establishment of a marine connection between the Black Sea and the Mediterranean at the end of the Messinian Salinity Crisis to have caused the split between the central and western clade around 5.5 Ma. Genetic structuring within the three clades dates to the Quaternary Ice Age (< 2.59 Ma) and is associated with alternating periods of isolation and reconnection caused by periodic changes in sea level and surface runoff.

Introduction

Historical biogeography seeks to understand the processes governing the spatio-temporal distribution of biodiversity. Patterns in biodiversity can be established objectively by exploring the genotype (10, 105). Phylogeography refers to the section of historical biogeography that aims to uncover the geographical distribution of genealogical lineages within (groups of related) species (12). Present-day distribution patterns are the result of past processes and, aided by gene geography, factors responsible for former vicariance and dispersal can be inferred.

Although each species will have had unique evolutionary responses, similarities in genetic patterns are expected to be present among the components of a region's contemporary biodiversity (10, 19). The phylogeographic approach provides the foundation for formulating biogeographical hypotheses, initially for individual model species and ultimately for entire communities. It can be seen as a tool for reconstructing paleogeological scenario's, analogous to, for example, paleontology and palynology (105).

The Mediterranean region serves as a natural laboratory for phylogeographically oriented studies. The area has experienced a turbulent geological and climatological history, resulting from the continental collision of Eurasia and Africa-Arabia (e.g. 79, 106, 107). This dynamic past is reflected by the rich biodiversity characterizing the region today (108, 109). The accumulation of phylogeographical information enables the extraction of prevailing biogeographical patterns in the Mediterranean region. However, phylogeographic research has been biased towards the southern European peninsulas (e.g. 110).

Amphibians provide an excellent model system for phylogeographical studies (10, 111). The crested newt *Triturus cristatus* superspecies is distributed in a large segment of the Mediterranean region (e.g. 63). Crested newts have been subjected to previous phylogeographic analyses, but the emphasis lay on the Balkan Peninsula (e.g. 66, 69). The range of the crested newts traditionally referred to as '*T. karelinii*' encompasses, next to an isolated Serbian enclave and Thrace on the Balkan Peninsula, the regions Anatolia, Caucasia, Crimea, and the southern shore of the Caspian Sea (Fig. 1).

Wallis and Arntzen (69), based on limited sampling, already hinted at the presence of substantial genetic variation in '*T. karelinii*'. Subsequently, Steinfartz et al. (102) suggested that '*T. karelinii*' actually constitutes a paraphyletic grouping. Recently, Espregueira Themudo et al. (70) uncovered two distinct clades in '*T. karelinii*', which were postulated to represent two distinct species (elevating the subspecies *arntzeni* to species level). The phylogenetic scope of these studies – reflected in geographically restricted, low density sampling – hinders the translation of taxonomical interpretation to geographical population; firstly, it is not settled how many distinct forms are included, and secondly, it is not clear how these forms would be distributed (cf. 112). For ease of communication, we refer to the '*T. karelinii*' crested newts as the *T. karelinii* group throughout this paper.

We present a range-wide phylogeographic analysis for the *T. karelinii* group, based on mitochondrial DNA sequence data. We (1) investigate the phylogenetic position of the *T. karelinii* group in the genus *Triturus*, (2) explore the distribution and structuring of genetic variation within the *T. karelinii* group and (3) formulate a hypothesis on the biogeographical history of the *T. karelinii* group, based on a qualitative comparison of gene geography and paleo-reconstructions.

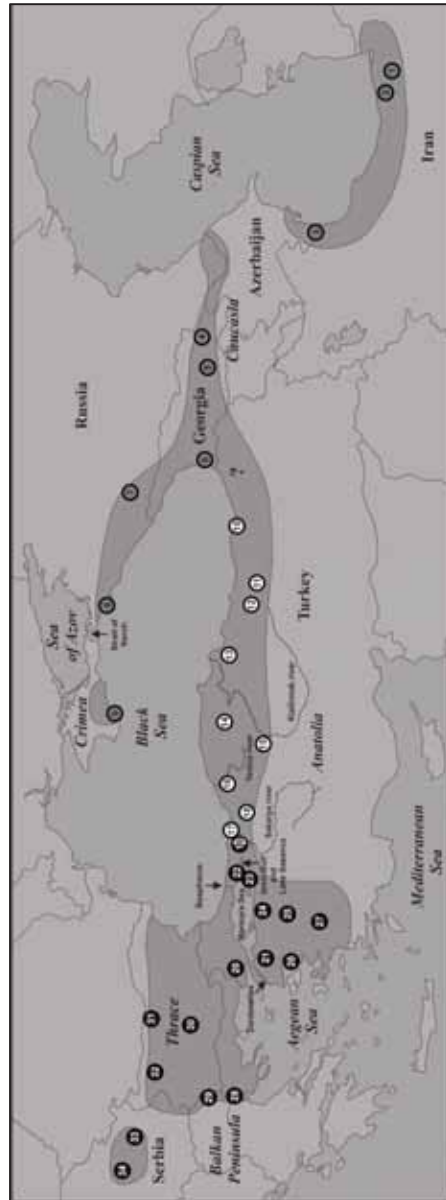


Figure 1 Approximate distribution of crested newts belonging to the *T. karelinii* group (modified from 63). Sampled populations are numbered and correspond to Table 1. Localities belonging to the eastern, central or western clade are shown in grey, white or black (cf. Fig. 2). Crested newt presence could not be established in the area indicated with a question mark; distribution could be discontinuous here (see discussion).

Methods

Sampling strategy

Sampling covers the entire distribution range of the *T. karelinii* group and includes 144 individuals from 34 georeferenced localities (Table 1, Fig. 1 and Supplementary data Appendix 1). Representatives of the other *Triturus* species – the four remaining crested newt species (*T. carnifex*, *T. cristatus*, *T. dobrogicus* and *T. macedonicus*) and the two marbled newt species (*T. marmoratus* and *T. pygmaeus*) – are included (Supplementary data Appendix 1). The Pyrenean brook newt *Calotriton asper*, being the closest living relative of *Triturus* (e.g. 91), serves as an outgroup.

Laboratory methods

Total genomic DNA was extracted from a small amount of tissue, using the DNeasy Tissue Kit (Qiagen). Two mitochondrial protein coding genes were amplified by PCR: the complete subunit 2 (ND2) and a segment of subunit 4 (ND4) of the NADH dehydrogenase gene complex. For details on primers see Table 2. Reaction conditions were initial denaturation for 180 s at 94 °C, 35 cycles composed of 30 s denaturation at 94 °C, 30 s annealing at 58 °C and 60 s extension at 72 °C, and a 240 s final extension step at 72 °C. PCR products were purified with the Wizard SV Gel and PCR Clean-up System (Promega). Cycle sequencing of both forward and reverse strands was done commercially through Macrogen, Inc.

Phylogenetic analysis

The forward and reverse sequences were checked by eye and a consensus sequence was compiled with Sequencher 4.5 (Gene Codes Corporation). Sequences were aligned manually in MacClade 4.08 (92). The two mitochondrial fragments were collated and identical sequences were merged into haplotypes.

We tested four data partitioning strategies: a single partition (all data), two partitions (per gene), three partitions (per codon position) and six partitions (per gene and codon position). For each data partition, the most appropriate model of sequence evolution was determined with MrModeltest 2.2 (94), based on the Akaike Information Criterion.

The data was analyzed under Bayesian inference with MrBayes 3.1.2 (98) for each partitioning strategy. Four Metropolis Coupled Monte Carlo Markov Chains were ran, one cold and three incrementally heated, starting from a random topology. The heating parameter was set to 0.01, to facilitate mixing between chains.

Table 1 Populations of the *T. karelinii* group sampled in this study, with details on the distribution of haplotypes (if more than one copy is present in a population the frequency is stated in parentheses). Population numbers correspond to Fig. 1. See Supplementary data Appendix 1 for coordinates and the division of individuals in haplotypes.

No.	Country and Locality	Haplotypes
1	Iran: Alandan	TkarA05 (3)
2	Iran: Qu'Am Shahr	TkarA03, TkarA04
3	Azerbaijan: Avyarud	TkarA01 (2), TkarA02, TkarA06, TkarA07
4	Georgia: Telavi	TkarA08 (2), TkarA09 (3)
5	Georgia: Tsodoreti	TkarA09 (4)
6	Georgia: Kobuleti	TkarA10 (5)
7	Russia: Psebay	TkarA11 (3), TkarA12, TkarA13
8	Russia: Cape Malyi Utrish	TkarA14 (4), TkarA15
9	Ukraine: Nikita	TkarA16 (4), TkarA17
10	Turkey: Yomra	TkarB01
11	Turkey: Şebinkarahisar	TkarB02 (4), TkarB03
12	Turkey: Reşadiye	TkarB04 (3), TkarB05, TkarB06
13	Turkey: Kavak	TkarB07, TkarB08 (3), TkarB09
14	Turkey: Cebeci	TkarB10 (5)
15	Turkey: Kalecik	TkarB11 (5)
16	Turkey: Bartın	TkarB12 (3), TkarB13 (2)
17	Turkey: Karasu	TkarB14 (2)
18	Turkey: Abanta Gölü	TkarB15 (2)
19	Turkey: Adapazarı	TkarB16 (2), TkarC02, TkarC05 (3)
20	Turkey: Keşan	TkarC01 (4), TkarC19
21	Turkey: Çan	TkarC03 (2), TkarC04, TkarC12, TkarC13
22	Turkey: Gebze	TkarC08 (2), TkarC09, TkarC10, TkarC11
23	Turkey: Orhangazi	TkarC06 (2), TkarC07
24	Turkey: Mustafa Kemalpaşa	TkarC14 (3), TkarC15 (2)
25	Turkey: Bigadiç	TkarC18 (3)
26	Turkey: Dikili	TkarC16 (4), TkarC17
27	Turkey: Bozdağ	TkarC18 (5)
28	Greece: Dafnochori	TkarC19 (3)
29	Macedonia: Mitrašinci	TkarC19 (3), TkarC20 (2)
30	Bulgaria: Rakovski	TkarC20 (4)
31	Bulgaria: Levski	TkarC20 (2), TkarC21 (3)
32	Bulgaria: Lilyache	TkarC20 (2)
33	Serbia: Sicevac	TkarC22, TkarC23, TkarC24, TkarC25
34	Serbia: Arandelovac	TkarC20 (2), TkarC26, TkarC27, TkarC28

Table 2 Primers used for PCR amplification and sequencing of the ND2 and ND4 mitochondrial protein coding genes.

Primer	Sequence (5'-3')	Reference
	ND2 fragment	
L3780	TCGAACCTACCCTGAGGAGAT	(80)
H5018	TCTGGGTTGCATTGAGAAGA	(80)
	ND4 fragment	
	Ingroup:	
KARF4	AGCGCCTGTCGCCGGTCAATA	(66)
KARR1	AACTCTTCTGGTGCCTAG	(66)
	Outgroup:	
ND4	CACCTATGACTACCAAAGCTCATGTAGAAGC	(113)
Leu	CATTACTTTTACTTGGATTGCACCA	(113)

Two separate runs of twenty million generations were conducted simultaneously and for each run the cold chain was sampled every 1000 generations. When using more than one data partition, parameters for each were unlinked and rates were allowed to vary independently. Tracer 1.5 (99) was used to check for stabilization of overall likelihood within and convergence between runs. The first quarter of sampled trees was discarded as burn-in and the inference was drawn from the remaining 'forest'.

The optimal partitioning scheme was selected based on the differences in the harmonic mean of the $-\ln$ likelihood scores resulting from the Bayesian inferences for the four partitioning schemes (excluding the burn-in). By subtracting the score of the next simpler model and multiplying the outcome by -2 , the $2 \ln$ Bayes factor was calculated for each partitioning scheme (95, 96). A value for $2 \ln$ Bayes factor exceeding 10 was used as a threshold for preferring the more complex model (97).

We expanded upon the phylogenetic analyses by conducting a partitioned Maximum Likelihood analysis with RAxML 7.0.3 (100). We conducted this analysis for the sixfold (per gene and codon position) data partitioning scheme only, applying independent GTR+G+I substitution models for each partition. Clade robustness was assessed by 1000 rapid bootstrap replicates.

Molecular dating

Divergence times were estimated with the programs BEAST 1.5.3 (104) and r8s 1.71 (103). In BEAST, we applied the uncorrelated lognormal relaxed clock model and a coalescent model assuming constant size. The data was analyzed under the sixfold partitioning scheme (per gene and codon position) and each partition was allowed its own model of sequence evolution (as previously determined with MrModeltest).

The tree resulting from the Bayesian analysis (based on the sixfold partitioning scheme) was used as starting topology. Divergence times were estimated based on two independent 100 million generation runs, sampled every 1000 generations, after discarding the first quarter of generations as burn-in.

In r8s we used the penalized-likelihood approach in combination with the truncated-Newton algorithm. The outgroup *C. asper* was pruned from the dataset, while keeping the root position, to avoid performing the time estimation on a basal polytomy. The optimal smoothing parameter ($S=1$) was first determined by a cross-validation procedure, using the Bayesian consensus tree as input. Mean temporal estimates and 95% confidence intervals were subsequently determined by profiling the last thousand sampled Bayesian topologies for each of the two runs resulting from the inference using the sixfold partitioning scheme.

We used two independent calibration points, one fossil-based and one geology-based. A *Triturus* fossil dated at 24 Ma was interpreted as approximating the crown of the genus *Triturus*. This treatment is derived from a comprehensive study on divergence times within the family Salamandridae, using multiple fossils and applying cross-validation with paleogeological data (102). The origin of the Adriatic Sea at 5.33 Ma, at the end of the Messinian Salinity Crisis, was interpreted as the vicariant event which separated the *T. carnifex*–*T. macedonicus* species pair (sensu 66).

In r8s the two calibration points used were set as fixed. In BEAST the calibration points were effectively fixed by appointing them a normally distributed prior with a small (0.001) standard deviation. We used the calibration points both separately and in conjunction. This means we conducted a total of six dating analyses: two different dating methods with three calibration strategies each.

Results

The 144 *T. karelinii* group individuals comprise 61 haplotypes, the other *Triturus* samples and the *C. asper* outgroup each represent unique haplotypes (for details and GenBank Accession Numbers see Supplementary data Appendices 1 and 2). Sequences could be unambiguously aligned; the only length variation is observed at the 3' end of ND2, with a one or two triplet deletion in the crested newts, relative to the marbled newts and the outgroup *C. asper*. The total alignment comprises 1699 bp (1035-1041 for ND2 and 658 for ND4). The corresponding data matrix has been submitted to TreeBASE (study ID S10317).

Models of sequence evolution for each tested partition are noted in Table 3. The Bayes factor analysis, comparing the results of the Bayesian inference under different partitioning schemes, suggests that treating each codon position for each mitochondrial fragment separately is preferred over the three tested alternatives (Table 4). We only present the Bayesian phylogenetic tree obtained using this data partitioning model (Fig. 2). The outcome of the partitioned Maximum Likelihood analysis is congruent with the Bayesian inference (Fig. 2).

Table 3 List of the partitioning schemes tested, with the number of characters present in each partition and the models selected per partition based on MrModeltest.

Partitioning scheme	# characters	Model
all data:		
ND2+ND4	1699	GTR+I+G
per gene:		
ND2	1041	GTR+G
ND4	658	GTR+I+G
per codon position:		
ND2+ND4 1st pos	567	GTR+I+G
ND2+ND4 2nd pos	566	HKY+I+G
ND2+ND4 3rd pos	566	GTR+G
per gene and codon position:		
ND2 1st pos	347	GTR+G
ND2 2nd pos	347	HKY+I+G
ND2 3rd pos	347	GTR+G
ND4 1st pos	220	GTR+G
ND4 2nd pos	219	HKY+I+G
ND4 3rd pos	219	GTR+I+G

Table 4 Evaluation of the optimal partitioning scheme for the mitochondrial sequence data based on Bayes factor analysis. N.a. = not applicable, i.e. a simpler model for Bayes factor comparison is unavailable.

Partition scheme	Harmonic mean (-ln)	2ln Bayes factor
all data	8657.29	N.a.
per gene	8851.68	-388.78
per codon position	8308.15	1087.05
per gene and codon position	8270.46	75.37

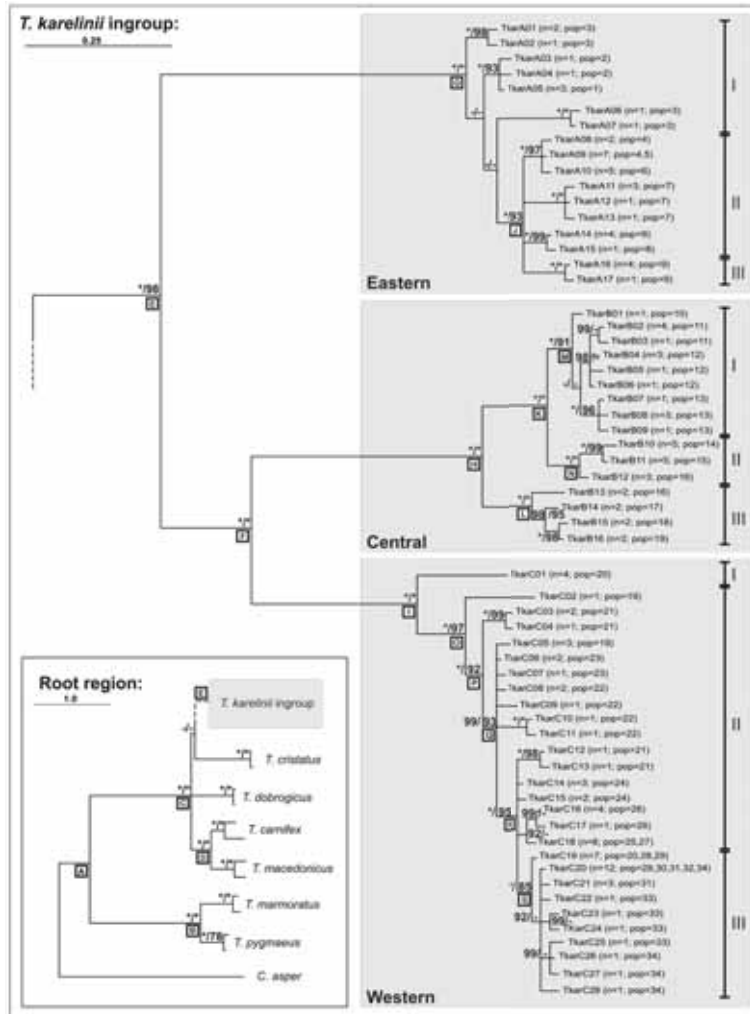


Figure 2 Majority rule consensus phylogenetic tree resulting from the Bayesian inference. Focus lays on the *T. karelinii* group; the inset shows the root region of the tree on a different scale. Three major clades identified in the *T. karelinii* group are labeled eastern, central and western, and subdivided into three groups each, labeled I, II and III (see text for details). Tips are labeled with haplotype identifiers, for which the frequency (n) and the populations (pop) where they are found are stated in parentheses (cf. Fig.1, Table 1 and Supplementary data Appendices 1 and 2). Scale bars denote expected changes per site. Node support is indicated as Bayesian posterior probability before and Maximum Likelihood bootstrap after the slash. Both are presented as percentages, with a 100 percent denoted with an asterisk and 75 percent or less with a vertical bar. For those nodes accompanied by a boxed letter, temporal estimates are presented in Table 5.

The *T. karelinii* group forms a monophyletic assemblage, separated from the other crested newts with statistically significant support. Three unambiguously supported, geographically coherent clades are present in the group, which are from here on designated as 'eastern', 'central' and 'western', in line with their distributions. The eastern clade encompasses Caucasia, Crimea, and the southern Caspian Seashore, the central clade is distributed in northern Turkey, along the southern shore of the Black Sea, and the western clade comprises western Asiatic Turkey and the Balkan Peninsula. The eastern clade is the first to split off and the central and western clade are sister groups. The central and western clades are parapatrically distributed (occurring in syntopy at locality 19), whereas no geographical overlap was found for the eastern and central clades.

The eastern, central and western clades show substantial genetic substructuring. We divided each clade into three (not necessarily monophyletic) groups of haplotypes (Fig. 2). The relatively homogenous groups from Caucasia (eastern II) and Crimea (eastern III) are nested within the genetically diverse southern Caspian Seashore group (eastern I). The central clade shows three reciprocally monophyletic groups (central I-III), with representatives of central II and central III observed in syntopy at locality 16. In the western clade, a basal haplotype is found in European Turkey (western I), whereas haplotypes from Asiatic Turkey (western II) are paraphyletic with respect to the remaining European ones (western III).

Temporal estimates for significantly supported splits among *Triturus* species and within the *T. karelinii* group are provided in Table 5. Dates are similar across methods and using different calibration strategies.

Discussion

Systematic position

The *T. karelinii* group composes one of four mitochondrial DNA lineages (the others being *T. carnifex* plus *T. macedonicus*, *T. cristatus* and *T. dobrogicus*) that form a basal polytomy in the *Triturus cristatus* superspecies (Fig. 2; 66). This means that either the mitochondrial data analyzed here contain too little information to resolve the order of speciation events (a soft polytomy), or that the four lineages truly split simultaneously (a hard polytomy). Espregueira Themudo et al. (70), using a suite of nuclear markers, managed to recover more detailed crested newt relationships (clustering *T. dobrogicus* with the *T. carnifex* and *T. macedonicus* lineage) despite cladogenesis having occurred in close temporal proximity. This implies that the basal polytomy we found is, at least in part, a soft one.

Table 5 Divergence time estimates among *Triturus* species and within the *T. karelinii* group (in Ma). Nodes are coded according to Fig. 2. For each of the two programs used (r8s and BEAST), three calibration strategies are applied: 1 = the *Triturus* crown fixed at 24 Ma; 2 = the *T. carnifex* – *T. macedonicus* split fixed at 5.33 Ma; and 3 = both calibration points together (see text for rationale). When nodes were used as calibration point they are marked with an asterisk. 95% confidence intervals are stated in parentheses.

r8s Node	1	2	3
A	24*	25.7 (19.4-32.1)	24*
B	5.3 (4.1-6.5)	5.7 (3.8-7.6)	5.3 (4.1-6.5)
C	9.3 (8.0-10.7)	9.9 (7.7-12)	9.4 (8.2-10.6)
D	5.2 (4.1-6.4)	5.33*	5.33*
E	6.8 (5.4-8.2)	7.2 (5.2-9.1)	6.8 (5.5-8.2)
F	5.4 (4.2-6.5)	5.7 (4.1-7.2)	5.4 (4.3-6.5)
G	1.3 (1.0-1.7)	1.4 (1.0-1.9)	1.3 (1.0-1.7)
H	1.8 (1.3-2.3)	1.9 (1.3-2.6)	1.8 (1.3-2.3)
I	2.1 (1.5-2.7)	2.2 (1.5-2.9)	2.1 (1.5-2.7)
J	0.8 (0.5-1.0)	0.8 (0.5-1.1)	0.8 (0.5-1.0)
K	0.9 (0.6-1.2)	0.9 (0.6-1.3)	0.9 (0.6-1.2)
L	0.7 (0.3-1.0)	0.7 (0.3-1.0)	0.7 (0.3-1.0)
M	0.5 (0.3-0.7)	0.5 (0.3-0.8)	0.5 (0.3-0.7)
N	0.4 (0.2-0.6)	0.4 (0.2-0.7)	0.4 (0.2-0.6)
O	1.3 (0.9-1.6)	1.3 (0.8-1.8)	1.3 (0.9-1.6)
P	0.9 (0.6-1.2)	1.0 (0.6-1.3)	0.9 (0.6-1.2)
Q	0.7 (0.5-0.9)	0.7 (0.5-1.0)	0.7 (0.5-0.9)
R	0.4 (0.3-0.6)	0.5 (0.3-0.7)	0.5 (0.3-0.6)
S	0.3 (0.2-0.4)	0.3 (0.2-0.5)	0.3 (0.2-0.4)

The initial split of the ancestor of the *T. karelinii* group from the remaining crested newts is estimated to have occurred around 9 Ma (Fig. 2 and Table 5). In the Early through Middle Miocene (23.03-11.61 Ma), the ancestral crested newt distribution presumably encompassed the continuous Balkan-Anatolian landmass (Fig. 3A; 114). During the late Middle and early Late Miocene (ca. 12-9 Ma), the formation of the Mid-Aegean Trench caused a divide between the Balkan and Anatolian landmasses and initiated a long-lived marine communication between the Mediterranean and the Paratethys (Fig 3B; 78, 107). We propose that the formation of this barrier severed the ancestor of the *T. karelinii* group from the remaining crested newts. For a reconstruction of the historical biogeography of the other crested newt species, see (66).

Table 5 continued

BEAST Node	1	2	3
A	24*	29.0 (20.8-37.7)	24*
B	4.5 (3.1-5.9)	5.4 (3.5-7.3)	4.8 (3.5-6.3)
C	8.6 (6.8-10.5)	10.4 (8.1-12.8)	9.4 (7.9-11.1)
D	4.4 (3.2-5.7)	5.33*	5.33*
E	6.7 (5.1-8.4)	8.1 (5.8-10.5)	7.2 (5.6-8.9)
F	5.1 (3.8-6.5)	6.2 (4.4-8.1)	5.5 (4.2-6.9)
G	1.1 (0.7-1.5)	1.3 (0.9-1.8)	1.2 (0.8-1.6)
H	1.6 (1.1-2.2)	1.9 (1.3-2.6)	1.7 (1.1-2.3)
I	1.8 (1.2-2.5)	2.2 (1.4-3.0)	2.0 (1.3-2.6)
J	0.6 (0.4-0.9)	0.7 (0.4-1.1)	0.7 (0.4-1.1)
K	0.7 (0.4-1.0)	0.9 (0.5-1.3)	0.9 (0.5-1.3)
L	0.5 (0.2-0.7)	0.6 (0.3-0.9)	0.6 (0.3-0.9)
M	0.3 (0.2-0.5)	0.4 (0.2-0.6)	0.4 (0.2-0.6)
N	0.3 (0.1-0.5)	0.3 (0.1-0.6)	0.3 (0.1-0.6)
O	1.0 (0.7-1.4)	1.2 (0.8-1.7)	1.2 (0.8-1.7)
P	0.7 (0.4-1.0)	0.8 (0.5-1.2)	0.8 (0.5-1.2)
Q	0.5 (0.4-0.8)	0.7 (0.4-0.9)	0.7 (0.4-0.9)
R	0.3 (0.2-0.5)	0.4 (0.2-0.6)	0.4 (0.2-0.6)
S	0.2 (0.1-0.3)	0.2 (0.1-0.4)	0.2 (0.1-0.4)

The origin of the eastern, central and western clades

We uncovered three distinct, geographically structured mitochondrial DNA clades in the *T. karelinii* group (Fig. 2). The basal split that gave rise to the eastern clade is placed around 7 Ma (Fig. 2 and Table 5). Temporally and geographically, this split is congruent with the uplift of the Armenian Plateau (10-5 Ma), caused by the Arabia-Eurasia collision (Fig 3B; 106, 115). We propose this orogeny isolated ancestral eastern clade crested newts in what is now Iran. This vicariance event might have been reinforced by episodic marine connections between the Mediterranean and the Paratethys via the Turkish-Iranian region (115, 116). Remaining land currently inhabited by the eastern clade was probably not yet accessible; Caucasia, which would eventually divide the Paratethys into the current Black and Caspian Seas and constitute a terrestrial passageway to southern Russia, was still an archipelago at the time (107).

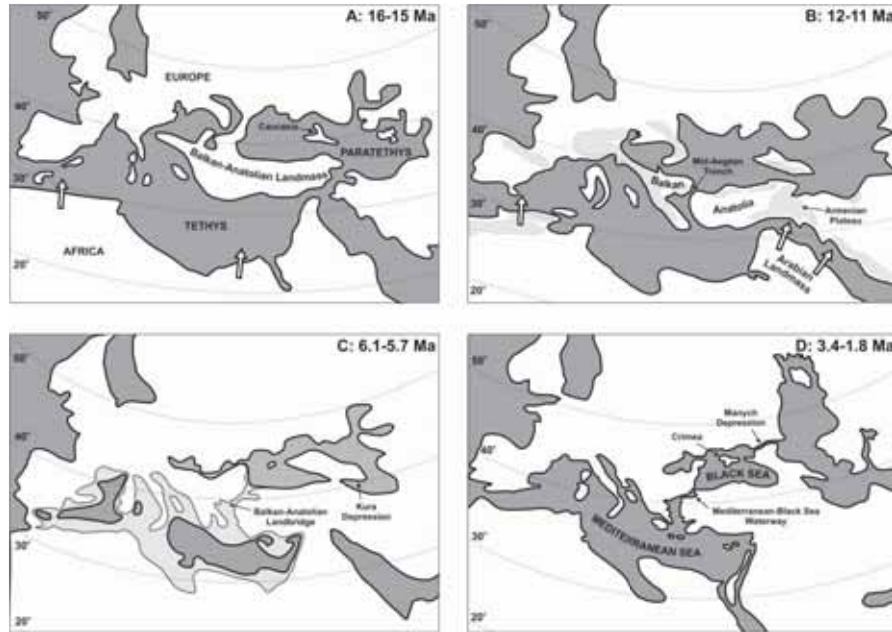


Figure 3 Paleogeological reconstructions for the Mediterranean region, showing stages relevant for the *T. karelinii* group (adapted from 79). A: A continuous Balkan-Anatolian landmass allows a continuous distribution for a proto crested newt. B: The origin of the Mid-Aegean Trench splits of the *T. karelinii* group in Anatolia from the Balkan crested newts. Extensive orogenesis (shaded light grey) due to the movement of Africa towards Europe leads to the uplift of the Armenian Plateau, which isolates the eastern clade. C: The desiccation of the Mediterranean during the Messinian Salinity Crisis exposes part of the sea bed (shaded light grey), including a land bridge between the Balkans and Anatolia, allowing crested newts to colonize Europe from Asia. Caucasia gradually becomes connected to the Asian mainland, but there is still marine embayment via the Kura Depression. D: After the conclusion of the Mediterranean Salinity Crisis, a marine connection between the Mediterranean and the Black Sea is re-established, causing the split between the central and western clades. The Manych Depression starts to close, making Caucasia a land bridge between Asia and Europe. Crimea is gradually moving towards the mainland. Periodical drops in global sea level during the Pleistocene cause occasional terrestrial connections between the Balkans and Anatolian and the Russian mainland and Crimea.

The split of the central and western clades in the *T. karelinii* group is dated around 5.5 Ma (Fig. 2 and Table 5). This coincides with the conclusion of the Messinian Salinity Crisis, an event which comprised the temporary desiccation of the Mediterranean. Isolation of the Mediterranean from the Atlantic was established at 5.59 Ma by the tectonically induced closing of the Betic and Rifian corridors (117).

Subsequent evaporation resulted in a dramatic drop in sea level and created opportunity for crested newts to move between Anatolia and the Balkan Peninsula via terrestrial connections (Fig 3C; 118, 119). At 5.33 Ma, the barrier cutting of the Mediterranean from the Atlantic gave way as the Strait of Gibraltar was formed (117). During the resulting 'Zanclean flood', the Mediterranean abruptly re-filled and sea water from the Atlantic penetrated, via the Aegean Sea, into the Black Sea (e.g. 119, 120, 121). We propose the resulting Mediterranean-Black Sea Waterway bisected a continuously distributed crested newt stock into an Anatolian and a Balkan component, corresponding to the central and western clades (Fig 3D).

Structuring within the three clades

The phylogeographical pattern of the eastern clade suggests a center of origin along the southern shore of the Caspian Sea and colonization of the Caucasus and Crimea at a later point. During the Messinian (7.25-5.33 Ma), soon after the initial split of the eastern clade from the remaining members of the *T. karelinii* group, the first land based connection with the Greater Caucasus landmass would appear (Fig 3C; 115). However, an extensive marine embayment by the Black and Caspian Seas and recurring communication between the two via the Kura and Manych Depressions (situated south and north of the Greater Caucasus ridge) will have seriously hampered northward expansion (Fig 3C and D; 115, 122). On the other hand, the periodical drop in global sea level during the Quaternary Ice Age may have reduced the impact of this dispersal barrier (123). The distribution of the eastern I and eastern II groups is presently discontinuous; central Azerbaijan appears to be devoid of crested newts (Fig. 1; personal observation; 63). Crimea originated as an island in the Eastern Paratethys and became peninsular at the Plio-Pleistocene boundary at 2.59 Ma (Fig 3D; 115, 124). The Strait of Kerch, which connects the Sea of Azov to the Black Sea (Fig. 1), currently separates the Crimean newts (eastern III) from the remainder of the range (eastern I-II). During Quaternary glaciations, however, lowering of the sea level caused land-based connections to emerge (122).

The central clade shows three distinct groups of haplotypes. A basal split separates samples from either side of the Yenice river valley, with the exception of Bartın (locality 16), where they co-occur (Figs. 1 and 2). A subsequent bifurcation separates samples from either side of the river Kızılırmak, with no syntopy detected. Rivers are sometimes considered a driving force for generating phylogeographical structuring in amphibians, but spatial coincidences may also be formed at a later point (125, 126). Denser sampling is required to distinguish between these competing hypotheses.

The phylogeographical pattern observed in the western clade suggests a Balkan origin, subsequent expansion into Anatolia, and eventual secondary colonization of the Balkan Peninsula, where new colonizers came into contact with newts already present. Currently, the Bosphorus, the Marmara Sea and the Dardanelles separate the Balkan Peninsula and Anatolia (Fig. 1). The Dardanelles already came in place during the Pliocene (5.33-2.59 Ma) (118). On the other hand, the outflow of the Marmara Sea into the Black Sea has since been re-ordered due to tectonic movements. The Bosphorus originated during the Holocene (11.7 Ka to present); before that time, the Istanbul Peninsula was directly accessible from the Balkan Peninsula via a terrestrial route (127). Throughout the Pleistocene (2.59 Ma–11.7 Ka), the Marmara and Black Seas were connected via the İzmit Gulf – Lake Sapanca – Sakarya Valley waterway (Fig. 1; 121). This geological history explains the presence of the western clade on either side of the Bosphorus, but not the long term presence in western Anatolia or the recently derived haplotypes in the Balkan Peninsula. However, global sea level fluctuations corresponding to the Quaternary climatic oscillations likely caused periodical emergence of the shallow sea straits separating Europe and Asia (123).

Taxonomic considerations and perspectives for further research

We applied a dense intraspecific sampling regime and found that the *T. karelinii* group, from a mitochondrial perspective, constitutes a monophyletic assemblage. This contradicts the notion of paraphyly proposed by Steinfartz et al. (102). We identified three mitochondrial DNA clades within the *T. karelinii* group, which show genetic differentiation comparable to that among recognized *Triturus* species (Fig. 2). Espregueira Themudo et al. (70) suggest that the *T. karelinii* group comprises two species: *T. karelinii sensu stricto* and *T. arntzeni*. The former name would apply to the eastern clade and the latter to the western clade. We identified a third assemblage, the central clade, for which no name appears to be available. Whereas the European *Triturus* species can be distinguished on morphological grounds (67), a range-wide study on the morphology of the *T. karelinii* group is as yet lacking.

Mitochondrial DNA divergence in itself does not provide conclusive evidence for evolutionary independence (e.g. 128). Permeability of mitochondrial DNA phylogeographic breaks for nuclear DNA indicates ongoing gene flow. Congruent patterns between both genomes could suggest either true genetic incompatibility or long term spatial isolation of clades. We intend to assess the structuring of nuclear DNA by exploring nuclear DNA markers. Contact zones are suitable places to study the presence and extent of gene flow in the *T. karelinii* group.

The central and western clades occur in syntopy at the Sakarya Valley (locality 19 in Fig. 1), suggesting secondary contact after the recent closing (11.7 Ka) of the İzmit Gulf – Lake Sapanca – Sakarya Valley waterway. Whether the eastern and central clades are in contact is unclear; historical records (reviewed in 63) exist from the intervening area between Kobuleti in Georgia (locality 6) and Yomra in Turkey (locality 10), but no recent observations could be made (personal observation; M. Sparreboom, in lit.).

The Mediterranean region is a biodiversity hotspot but is also experiencing intense anthropogenic pressure (108, 109). We hope our case study contributes to a better understanding of the biogeographical history of the region. This is not as straightforward as it may seem. The ranges of *Ommatotriton* and the *Lissotriton vulgaris* group largely overlap with that of the *T. karelinii* group and representatives of these three newt genera can often be found occurring in syntopy. Yet intriguing differences remain. The range occupied by the central *T. karelinii* group clade is practically devoid of *Lissotriton*, leaving a Caucasian clade isolated from the rest of the *Lissotriton* range. *Ommatotriton* is mostly absent from the range of the western *T. karelinii* group clade and does not share the distribution of the eastern clade in Iran. Its distribution does however encompass part of the Middle East. The evolutionary history of the *L. vulgaris* group appears to have unfolded itself over a more recent time span than that of the *T. karelinii* group (80). For *Ommatotriton* a detailed phylogeographic study is as yet lacking. Despite their ecological similarities, these three groups of newts already show incongruent scenarios. To distil a prevailing biogeographical pattern for the Near East, a wider array of species should be investigated and compared. Knowledge on Near Eastern phylogeographical patterns is rapidly accumulating and the time is ripe for a thorough review. The data available so far suggest the Near East to be a cradle for biodiversity, on a par with the southern European peninsulas.

Supplementary data

Supplementary data associated with this article can be found in the online version at doi:10.1016/j.ympev.2010.04.030.

- Appendix 1: Division of individual newts into haplotypes.
- Appendix 2: GenBank Accession Numbers.

Acknowledgements

B.W. thanks the 'J.J. ter Pelkwijk fund' for support. G.E.T. was financed through a PhD grant from the Fundação para a Ciência e a Tecnologia, Lisbon, Portugal (SFRH/BD/16894/2004).

N.A.P. was supported by a Naturalis 'Martin fellowship' and by a grant from the 'Pieter Langerhuizen Lambertuszoon Fonds', allocated by the 'Koninklijke Hollandsche Maatschappij der Wetenschappen'. Permits for Turkey were made available by TÜBİTAK. The authors thank W. Babik, J. Badridze, S. Carranza, D. Cogălniceanu, E. Galoyan, H. Gholi Kami, A. Kidov, N. Moin, I. Serbinova, D. Tarkhnishvili and N. Üzüm for help with collecting. A. K. Skidmore and G. P. Wallis provided comments on an earlier version of the manuscript.

Chapter 3: Corresponding mitochondrial DNA and niche divergence for cryptic crested newt species

This chapter is based on: Wielstra B, Beukema W, Arntzen JW, Skidmore AK, Toxopeus AG, Raes N (in press) Corresponding mitochondrial DNA and niche divergence for cryptic crested newt species. *PLoS ONE*

Abstract

Genetic divergence of mitochondrial DNA does not necessarily correspond to reproductive isolation. However, if mitochondrial DNA lineages occupy separate segments of environmental space, this supports the notion of their evolutionary independence. We explore niche differentiation among three candidate species of crested newt (characterized by distinct mitochondrial DNA lineages) and interpret the results in the light of differences observed for recognized crested newt species. We use a recently proposed framework (129) to quantify niche differences among all crested newt (candidate) species and test hypotheses regarding niche evolution, employing the two best performing techniques (PCA-env and ENFA). All (candidate) species occupy significantly different segments of environmental space. Niche overlap values for the three candidate species are not significantly higher than those for the recognized species. The three candidate crested newt species are, not only in terms of mitochondrial DNA genetic divergence, but also ecologically speaking, as diverged as the recognized crested newt species. Our findings support the hypothesis that they represent cryptic species.

Introduction

Phylogeography has yielded a wealth of information by documenting geographical genetic variation (12). One key finding is the frequent presence of extensive mitochondrial DNA variation within taxa, not matched by morphological differentiation (105). Simply translating such 'cryptic diversity' to species status would explicitly interpret mitochondrial DNA divergence as reflecting evolutionary independence. However, the evolutionary signal encrypted in mitochondrial DNA is not necessarily a suitable proxy for nuclear gene flow (17, 77). On the other hand, ecological divergence acts as a barrier to gene flow and can promote reproductive isolation and thus speciation (82-85, 130). If geographical populations characterized by distinct mitochondrial DNA lineages (hereafter referred to as 'candidate species') also occur under different ecological conditions, this increases support for their treatment as distinct species.

The crested newt *Triturus cristatus* superspecies consists of five parapatric groups (Fig. 1a). Four of these, *T. carnifex*, *T. macedonicus*, *T. cristatus* and *T. dobrogicus*, are recognized as distinct species. The systematics of the fifth group, traditionally referred to as *T. karelinii*, is more complex. In a previous phylogeographic study (65), we uncovered three geographically structured mitochondrial DNA lineages in the *T. karelinii* group (Fig. 1b), which show a level of genetic divergence comparable to that among the recognized crested newt species (131).

The recognized species are morphologically distinct (63) and represent discrete nuclear gene pools (132). There are currently no morphological grounds for distinguishing the three *T. karelinii* candidate species (63, 133) and information on nuclear gene flow is as yet lacking. This raises the question whether the three mitochondrial DNA lineages comprising the *T. karelinii* group should be recognized as a single or as several species.

We explore the use of niche divergence as a criterion for assigning species status to candidate species identified with mitochondrial DNA. To this aim, we use a statistical framework recently proposed by Broennimann et al. (129), which quantifies niche differences and tests hypotheses regarding niche evolution. We determine niche differences among the three crested newt candidate species and interpret these differences by treating niche divergence among recognized species of crested newt as a benchmark.

Methods

Distribution and environmental data

We composed a dataset of 2404 crested newt occurrences covering all recognized species and partitioned those for the *T. karelinii* group into three classes according to mitochondrial DNA: 120 *T. carnifex*, 1698 *T. cristatus*, 136 *T. dobrogicus*, 139 *T. macedonicus*, 135 *T. karelinii*, 32 *T. karelinii* central and 144 *T. karelinii* east (see Appendix S1 in Supporting Information for details). For ecological data layers, we used bioclimatic variables at 2.5 arcminute resolution (c. 5 x 5 km) available from the WorldClim database 1.4 (134; <http://www.worldclim.org>). It is recommended to focus on data layers that are deemed biologically meaningful based on life history knowledge of the model system (9, 135). Considering that the recognized crested newt species differ in their requirements concerning the availability of water bodies for breeding (63), we selected a set of layers that encompasses seasonal variation in evaporation and precipitation, in casu bio10 = mean temperature of warmest quarter, bio11 = mean temperature of coldest quarter, bio15 = precipitation seasonality, bio16 = precipitation of wettest quarter, and bio17 = precipitation of driest quarter. To set our study area we drew a buffer around all crested newt localities (136). We used a 200 km radius following (137).

Quantifying and interpreting niche overlap

In order to calibrate niches, measure niche overlap and test hypotheses regarding niche evolution, we applied a recently presented framework (129) implemented in R (138).

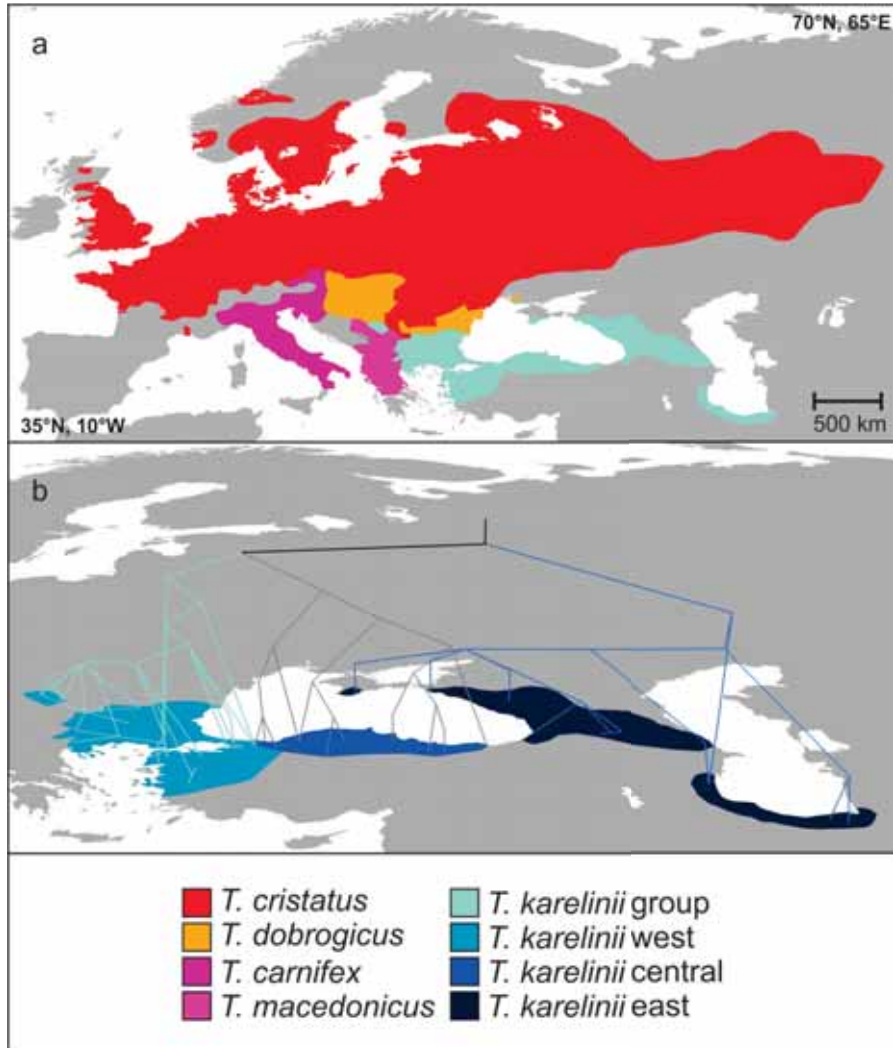


Figure 1 The distribution of the crested newt *Triturus cristatus* superspecies. Fig. 1a shows the distribution of the four recognized crested newt species and the *Triturus karelinii* group. Fig. 1b shows the distribution of the distinct eastern, central and western mitochondrial DNA lineages comprising the *Triturus karelinii* group (sensu 65), with a geophylogeny superimposed (created with GeoPhyloBuilder; 26).

We used the two best performing niche calibration techniques in Broennimann et al. (129): Principal Component Analysis calibrated on the entire environmental space of the study area – PCA-env (129) and Ecological Niche Factor Analysis – ENFA (33). In PCA-env, a PCA is conducted to transform the climate layers into a reduced number of linearly uncorrelated variables, i.e. principal components (129). The first component accounts for as much of the variability in the original variables as possible and each following component accounts for as much of the remaining variability. In PCA-env the PCA is calibrated on the entire study area (including species occurrences). Differences in the position of (candidate) species along the principal components reflect their environmental differences. ENFA similarly is an ordination technique. It compares the environmental conditions experienced by a (candidate) species' distribution to that present in the entire study area (33, 129). The principal components in ENFA have a direct ecological interpretation. The first component reflects the marginality: the ecological distance between the (candidate) species' optimum and the mean conditions of the study area. The second component reflects specialization: the ratio of the ecological variance in the study area to that observed for the (candidate) species.

Application of the framework involves three steps. Firstly, the niche and occurrence density are calibrated. Environmental space is defined by the first two axes in which the chosen ordination technique summarizes the environmental conditions in the study area. This environmental space is divided into a grid of $r \times r$ cells (we use $r = 100$ as in 129) bounded by the minimum and maximum values occurring in the study area. Each cell in environmental space represents a unique combination of environmental conditions present in one or more of the grid cells in geographical space. To correct for potential sampling bias, a smoothed occurrence density for each (candidate) species in each grid cell is estimated using a kernel density function (129). Secondly, niche overlap for pairs of (candidate) species is calculated using Schoener's D (139). This metric ranges from 0, which means niches are completely dissimilar, to 1, which signifies that niches completely overlap (129). To test whether pairwise niche overlap values for candidate species differed from those for recognized species, we conducted a t -test using IBM SPSS 20.

Thirdly, the framework tests hypotheses regarding niche evolution (as in 39). The niche equivalency test explores whether niches of two (candidate) species are identical. The occurrences for a pair of (candidate) species are pooled, two random sets of occurrences with the same original sample sizes are extracted, and the overlap scores are determined.

By repeating this procedure (here a hundred times), a null distribution of overlap scores is obtained, to which the actual overlap score for the two (candidate) species is compared. If the actual niche overlap is significantly smaller, this means the (candidate) species occupy distinct segments of environmental space. The niche similarity test explores whether the niche overlap between (candidate) species is larger than expected by chance, based on the different environmental conditions they encounter. We defined this 'background' for each (candidate) species by drawing a 200 km buffer around its occurrences. The niche similarity test determines niche overlap of one (candidate) species with a random model based on the background of the other (using as much random samples as there are occurrences for the other), and the reciprocal. This is repeated (here a hundred times), resulting in two null distributions, one for each (candidate) species, to which the actual niche overlap between the two (candidate) species is subsequently compared. A statistically significantly higher niche overlap value indicates that the niches of the two (candidate) species are more similar than expected by chance.

Results

The environmental space occupied by each (candidate) species as determined by PCA-env is shown in Fig. 2 and results from ENFA can be found in Appendix S2. Both the recognized and the candidate species differ in their position in environmental space. The distribution of *T. dobrogicus* in environmental space is relatively narrow. Niche overlap values calculated with PCA-env and ENFA can be found in table 1. The *t*-test shows that niche overlap among the three candidate species is not significantly larger from that among the recognized species, based on both PCA-env ($p = 0.338$) and ENFA ($p = 0.165$). Among recognized species, the overlap of *T. dobrogicus* with the other (candidate) species is significantly lower based on ENFA only ($p = 0.025$). All the niche equivalency tests produced non-significant results. Part of the similarity tests are significant (Table 1); this is relatively more often the case for candidate species (4 and 3 out of 6 tests based on based on PCA-env and ENFA) than for recognized species (5 and 2 out of 12 tests).

Discussion

The three candidate species comprising the *T. karelinii* group are, not only in terms of mitochondrial DNA genetic divergence, but also ecologically speaking as diverged as the recognized crested newt species: niche overlap among them is not significantly higher than that among recognized crested newt species. The niche equivalency tests reveal that all (candidate) species occupy different climatic corners of environmental space (Fig. 2, Appendix S2).

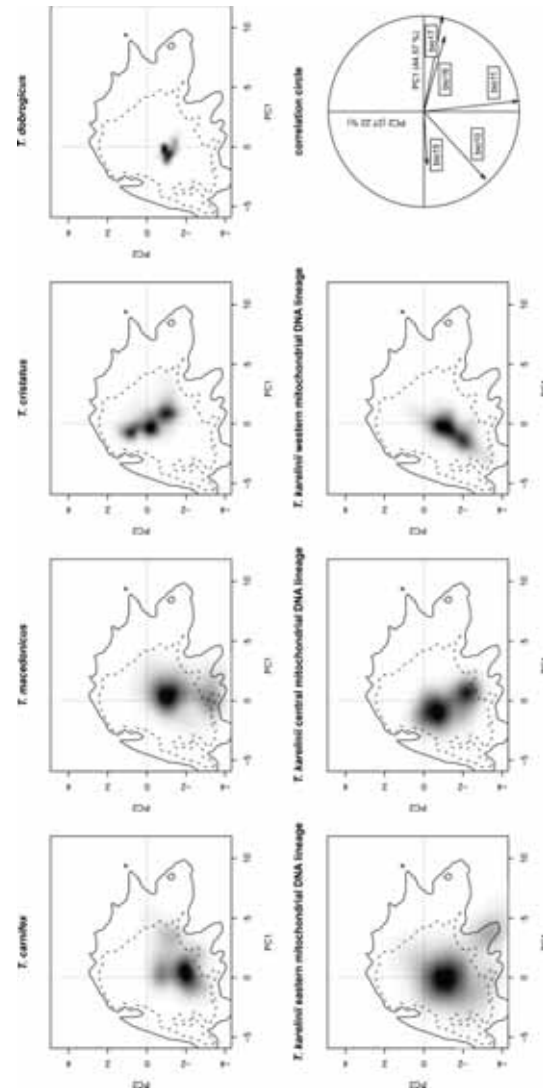


Figure 2 Niches of the different crested newt (candidate) species based on PCA-env. Each (candidate) species' niche is displayed on the same referential: a multi-dimensional scale represented by the first two axes of a principal component analyses summarizing the entire study area. Grey shading reflects the density of the occurrences of each (candidate) species in each cell. The solid and dashes contour lines illustrate 100% and 50% of the available environment in the study area. The correlation circle (bottom left) shows the contribution of the climatic variables on the two axes of the PCA and the percentage of inertia explained by the two axes.

Table 1 Niche overlap values and results of similarity tests for each pair of crested newt candidate species (the three *Triturus karelinii*'s) and recognized species as determined with PCA-env (below diagonal) and ENFA (above diagonal).

	1: <i>T. karelinii</i> east	2: <i>T. karelinii</i> central	3: <i>T. karelinii</i> west	4: <i>T. carnifex</i>	5: <i>T. macedonicus</i>	6: <i>T. cristatus</i>	7: <i>T. dobrogicus</i>
1	-	0.244 ^{ns/*}	0.559	0.366 ^{*/ns}	0.456 ^{ns/*}	0.347	0.060
2	0.329 ^{*/*}	-	0.422 ^{*/*}	0.345	0.450	0.254	0.252
3	0.209	0.281 ^{*/*}	-	0.325	0.411 ^{*/*}	0.399	0.318
4	0.408 ^{*/*}	0.498 ^{ns/*}	0.239 ^{*/ns}	-	0.309	0.446	0.182 ^{*/*}
5	0.485 ^{*/*}	0.391 ^{ns/*}	0.162	0.448 ^{ns/*}	-	0.319	0.135
6	0.128 ^{*/*}	0.124 ^{ns/*}	0.182	0.253 ^{*/ns}	0.120 ^{*/*}	-	0.224
7	0.041	0.090	0.188	0.055 ^{*/ns}	0.040	0.142	-

Similarity tests compare one (candidate) species with the background of the other and the reverse. If one or both comparisons are significant, results for the comparison of (candidate) species listed from top to bottom with the background of the one listed from left to right are noted before the slash; after the slash the reverse combination is noted. * = significantly larger ($p < 0.05$) and ns = non-significant.

Although the niche overlap values among candidate species are not significantly higher than those among recognized species, the niche similarity tests show that candidate species relatively more often show a higher degree of overlap than would be expected based on the differentiation of their ecological backgrounds. This would suggest the candidate species occupy relatively diverged backgrounds. Compared to other crested newt (candidate) species, *T. dobrogicus* is ecologically specialized. It has a comparatively limited spread in environmental space, which is reflected by significantly lower niche overlap values for those pairwise comparisons involving *T. dobrogicus*. Morphologically speaking, *T. dobrogicus* is the most derived crested newt species: whereas the ancestral body shape in crested newts is relatively stocky, *T. dobrogicus* has a comparatively slender build (131, 140). It has been suggested that body elongation in crested newts was associated with niche shifts (63, 140, 141).

Indeed, *T. dobrogicus* shows habitat specialization: it strictly inhabits riverine floodplains. It is also the most aquatic crested newt species, spending half of the year in the water (63).

The environmental conditions where candidate species are observed to occur should not be confused with those where they could occur (142). The potential niche envelopes those environmental conditions that exists in nature, under which a candidate species could persist and reproduce. The realized niche comprises the portion of the potential niche that is actually occupied, given that historical and biotic factors pose further restriction on a candidate species' distribution (142). It follows that although candidate species may differ in their realized niche, they might still possess the same potential niche. Differences among candidate species' realized niches could reflect niche evolution, in other words, an actual change in the potential niche (and a mechanism resulting in ecological isolation). However, these differences could also reflect niche plasticity, with candidate species possessing the same potential niche despite expressing a different realized niche. Controlled field experiments are required to distinguish niche plasticity from niche evolution. In the meantime, an approximation of the significance of the observed differences can be made by treating the degree of niche divergence between recognized congeneric species as a minimum threshold that candidate species should express to qualify for species status.

The detailed knowledge regarding morphological and genetic differentiation that has become available for other crested newts led to their recognition as distinct species (63, 132, 143, 144). Such information is as yet inconclusive (morphology) or lacking (nuclear genome) for the *T. karelinii* group. However, next to the previously found mitochondrial DNA divergence among candidate species, there is now another line of evidence suggesting the presence of three morphologically cryptic species: niche divergence. A multimarker nuclear DNA phylogeography is required to further test the prediction of an explicit barrier to nuclear gene flow.

The integration of spatial ecological methods in mitochondrial DNA phylogeographical surveys provides a powerful tool, aiding the delineation of cryptic species (145, 146). Using phylogenetically informed partitioning of occurrence data is facilitated by the rapid increase in the availability of both sequence data (especially via mitochondrial DNA barcoding initiatives) and occurrence data (147). The approach outlined in this paper will aid systematicists and conservationists alike in assessing the potential species status of distinct mitochondrial DNA lineages, in relatively little time and at low cost.

Acknowledgements

D.M. Kidd provided advice on creating the GeoPhylogeny.

Supplementary data

The supplementary data associated with this chapter can be found at <http://science.naturalis.nl/media/333560/ch3suppdata.zip>.

- Appendix S1: Occurrence data for crested newt (candidate) species.
- Appendix S2: ENFA results for each pairwise comparison of (candidate) species.

Chapter 4: Tracing glacial refugia of *Triturus* newts based on mitochondrial DNA phylogeography and species distribution modeling

This chapter is based on: Wielstra B, Crnobrnja-Isailović J, Litvinchuk SN, Reijnen B, Skidmore AK, Sotiropoulos K, Toxopeus AG, Tzankov N, Vukov T, Arntzen JW (submitted) Tracing glacial refugia of *Triturus* newts based on mitochondrial DNA phylogeography and species distribution modeling

Abstract

The major climatic oscillations during the Quaternary Ice Age heavily influenced the distribution of species and left their mark on intraspecific genetic diversity. Past range shifts can be reconstructed with the aid of species distribution modeling and phylogeographical analyses. We test the response of *Triturus* newts as the climate shifted from the previous glacial period (the Last Glacial Maximum, ~21Ka) to the current interglacial. We present the results of a dense mitochondrial DNA phylogeography (visualizing genetic diversity within and divergence among populations) and species distribution modeling (using two different climate simulations) for the nine *Triturus* species on composite maps. The two independent techniques provide insight in the glacial reduction and postglacial expansion of *Triturus*. *Triturus* newts generally conform to the 'southern richness and northern purity' paradigm. The pattern is most dramatic in *T. cristatus*, which colonized most of temperate Europe after the Last Glacial Maximum. For most species we manage to deduce the position of glacial refugia, the only exception being *T. dobrogicus*. This species, according to mitochondrial DNA, went through a severe bottleneck. We provide a detailed treatment for each *Triturus* species. Introgression of mitochondrial DNA is mostly restricted to contact zones between the species, but involves a large geographical range in the case of the asymmetrical introgression of *T. marmoratus* mitochondrial DNA into *T. pygmaeus* and western *T. karelinii* mitochondrial DNA lineage into *T. macedonicus*. The species distribution models support a scenario of postglacial species displacement in both cases. The combined use of species distribution modeling and mitochondrial phylogeography provides a more complete understanding of the historical biogeography of *Triturus* than both approaches would on their own.

Introduction

The Quaternary Ice Age (~2.59Ma-present) is associated with large climatic oscillations (148-151). Long, cold and dry glacial cycles are alternated by relatively short, warm and wet interglacials. The transition between the two takes place in a geological blink of an eye (152, 153). The climatic oscillations have a major impact on species distribution patterns (148). Generally, impacts of glacial cycles are more extreme, further away from the equator (and at higher elevations): areas at a higher latitude (and elevation) become inhospitable, whereas climate at a lower latitude (and elevation) remains habitable (148, 154). Populations at higher latitude may cope with climate change *in situ*, through adaptation or phenotypic plasticity, or alternatively they may track suitable habitat (153, 155). However, a more likely outcome is that such populations go extinct (155-157).

At lower latitudes, populations can endure glacial periods relatively unimpaired, in so called glacial refugia (149, 157, 158). During interglacial, repressed species can reclaim their former distribution again, by rapidly recolonizing the large tracts of still uninhabited, but again habitable land from glacial refugia (148).

The fluctuating climate during the Quaternary left its mark on patterns of genetic diversity (148-150, 152, 159). Populations persisting in glacial refugia have a relatively long and stable demographical history compared to those in areas claimed postglacially. As a result, populations in glacial refugia are characterized by high levels of genetic diversity, whereas populations established after the most recent glacial cycle typically show little genetic variation. This is the concept – devised from a northern hemisphere perspective – of ‘southern richness and northern purity’ (148). Furthermore, species displacement after postglacial secondary contact regularly coincides with introgression of genetic material (especially of cytoplasmic DNA) (159, 160). By uncovering the spatial structuring of genetic lineages between glacial refugia and along recolonization routes, and by detecting mismatches between genetic markers and species boundaries, phylogeographical surveys provide insights in past distribution rearrangement (156).

Independent from genetics, species distribution modeling can be applied to answer historical biogeographical questions (161). Species distribution modeling involves the approximation of the ecological requirements of a species, based on the range of environmental conditions experienced at known localities (30). The constructed model can then be extrapolated on current climate layers, to determine the species’ potential distribution. Similarly, the model can be projected on climatological reconstructions of the past. Niches evolve over time, questioning the validity of predicting past distributions based on present day models. However, considering the relatively short time period spanning the shift from the last glacial cycle to the present day, niche conservatism is a realistic assumption (38, 162). Comparison of present and past potential distribution provides information on range shifts.

The distribution of amphibians is tightly linked to environmental conditions and thus has to follow suit in the face of rapid climate change (163-166). The marbled and crested newts (genus *Triturus*) (63, 167, 168) are a group of nine closely related lineages, hereafter referred to as species (Table 1). *Triturus* newts are distributed across most of Europe and adjacent Asia (Fig. 1). They are found in regions generally regarded as important glacial refugia, such as the Iberian, Italian and Balkan Peninsulas, Anatolia, Caucasia and the southern Caspian basin (150, 156, 157).

On the other hand, *Triturus* newts occupy large tracts of land which would have been uninhabitable during glacial periods, particularly temperate Eurasia (169). Thus, within this single model system, we expect to observe varying responses to glaciation.

We first conduct a dense phylogeographical survey: employing mitochondrial DNA, we determine geographical genetic structuring (i.e. diversity within and divergence among populations) for each of the different *Triturus* species. Subsequently, we approximate the distributions of the different *Triturus* species at the Last Glacial Maximum (~21Ka) using species distribution modeling. The outcome of the two independent approaches is visualized on composite maps, which show the nine different species the side by side. By comparing the signatures of past distribution dynamics as inferred from mitochondrial DNA phylogeography and species distribution modeling, we show that both methods support a general scenario, but the two techniques also show some interesting differences.

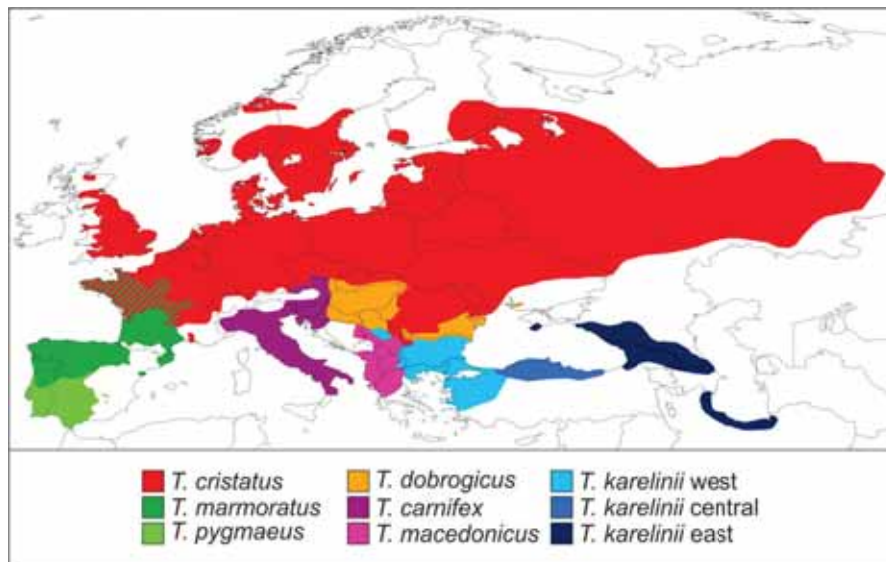


Figure 1 The distribution of the genus *Triturus*. Species mostly meet at parapatric contact zones, but note the area of sympatry of *T. marmoratus* and *T. cristatus* in western and central France. This map is adapted from (131).

Table 1 Systematics of the genus *Triturus*

Marbled newts
<i>Triturus marmoratus</i> (Latreille, 1800)
<i>Triturus pygmaeus</i> (Wolterstorff, 1905)
Crested newts
<i>Triturus cristatus</i> (Laurenti, 1768)
<i>Triturus carnifex</i> (Laurenti, 1768)
<i>Triturus macedonicus</i> (Karaman, 1922)
<i>Triturus dobrogicus</i> (Kiritzescu, 1903)
<i>Triturus karelinii</i> (Strauch, 1870)*
Eastern mitochondrial DNA lineage
Central mitochondrial DNA lineage
Western mitochondrial DNA lineage

*The taxon traditionally referred to as *T. karelinii* actually comprises three distinct mitochondrial DNA lineages (65). These are referred to as western, central and eastern. The three mitochondrial DNA lineages may well warrant species status and we treat them as such throughout this paper.

Methods

Genetic approach

We included genetic data (658 bp of subunit 4 of the NADH dehydrogenase gene complex; ND4) for 2354 *Triturus* newts, representing 457 populations (Fig. 2 and Dataset S1). A large segment of these individuals (n=1795) were taken from previous studies (published (65, 131) or submitted (132, 133, 170-172); see Dataset S1 for details). The remainder (n=559) was newly sequenced for the current paper, using the primers in Table 2 and following the protocol outlined in (66). Sequences were manually aligned and identical ones merged into haplotypes using MacClade 4.08 (92). All (new) haplotypes are available via GenBank (see Dataset S3 for GenBank accession numbers). Our purpose was not to infer phylogenetic relationships among the *Triturus* species (cf. 131), but 1) to detect mitochondrial DNA introgression between species, and 2) to infer the spatial genetic variation within each species. To detect which individuals retain their 'original' mitochondrial DNA and which possess introgressed mitochondrial DNA (derived from one of the other lineages), we first assigned mitochondrial DNA haplotypes to species by conducting a Neighbor Joining analysis in MEGA 5.05 (173). *Calotriton asper* was used as outgroup (taken from (65); GenBank accession number: GU982378).

To infer interspecific geographical structuring, we first excluded introgressed mitochondrial DNA (as it does not properly reflect the evolutionary history of either 'host' or 'donor'). Subsequently, we determined – for each species – 1) the genetic diversity within populations and 2) the genetic distance among populations.

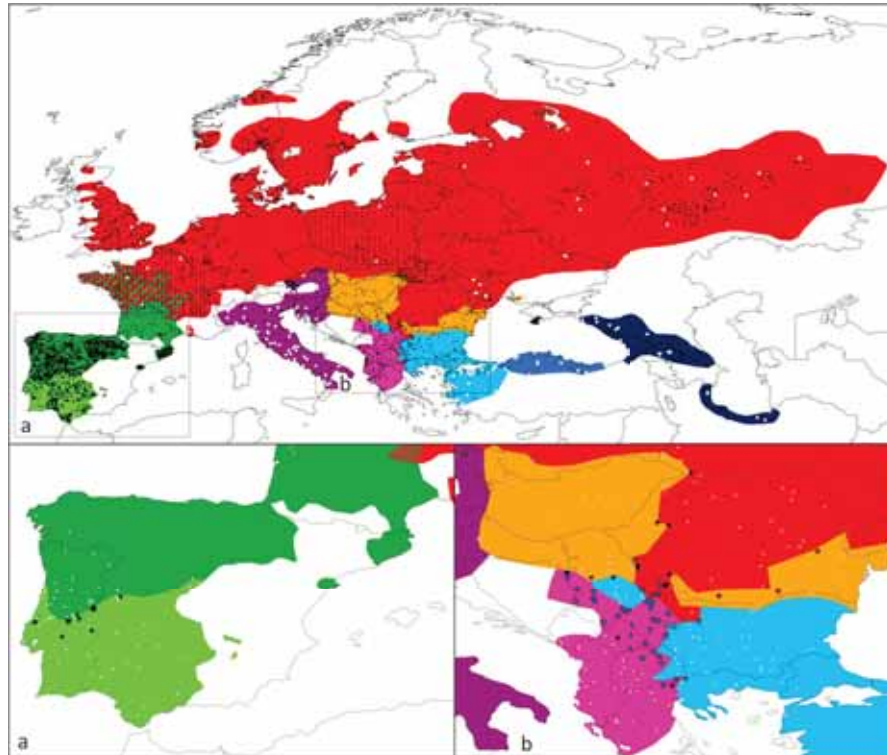


Figure 2 Maps showing the *Triturus* localities used for the mitochondrial DNA phylogeography and species distribution modeling. The inset shows part of the localities used in the genetic analyses (white circles) and the additional ones used for species distribution modeling (black circles). Two cut-outs (A and B) show more details on introgressed mitochondrial DNA: populations containing foreign mitochondrial DNA are labeled with a colored star (with the color denoting the 'donor' species) and populations containing two mitochondrial DNA types (of which one mostly, but not exclusively, is of the original species) as a black star; populations containing original mitochondrial DNA are again labeled with white circles. The colors used correspond to Fig. 1. Details on localities can be found in Dataset S1 and S2.

The mean number of pairwise differences among haplotypes (π), as determined with Arlequin 3.5 (174), was used as a measure of genetic diversity within populations. We only included populations for which more than one sequence was available (π will always be zero for populations with only one sequence). To determine the genetic distance among populations we used Alleles in Space 1.0 (175). Alleles in Space connects the populations in a network, based on Delaunay triangulation.

Subsequently, the program produces values of average genetic distance among the populations that are connected by the network (the proportion of mismatched nucleotide sites; Z_i). These values are positioned at the midpoints of the connections in the network.

We interpolated the values for π and Z_i across geographical space using inverse distance weighting in the spatial analyst extension of ArcGIS (www.esri.com) (cf. 176). The output for each species was cropped according to its distribution range (cf. Fig. 1). For both π and Z_i , we compiled a single composite map from the nine crops (i.e. one for each *Triturus* species). We used a color scheme running from blue to red to reflect low to high values of π and Z_i . Using a single scale for all *Triturus* species facilitates comparison among them, but runs the risk that variation in genetically poor species is overshadowed by that of genetically rich species. We additionally apply a species specific scale to better express intraspecific structuring. This way we managed to visualize 1) regions of relatively high and low intraspecific genetic diversity and 2) the relative genetic divergence among populations within species.

Table 2 Primers used for amplification and sequencing of the ND4 mitochondrial DNA fragment

Species or groups of species with their forward and reverse primers	Source
<i>T. marmoratus</i>	
MARF1: CACCTGTGATTACCTAAAGCTCATGTAGAAGC	This study
ND4R2: CCCTGAAATAAGAGAGGGTTTAA	(66)
<i>T. pygmaeus</i>	
PYGF1: CACCTCTGATTGCCTAAAGCCACGTAGAGGC	This study
ND4R2: CCCTGAAATAAGAGAGGGTTTAA	(66)
<i>T. karelinii</i> group crested newts	
KARF4: AGCGCCTGTCGCCGGGTCAATA	(66)
KARR1: AACTCTTCTGGTGCCTAG	(66)
Other crested newts	
KARF4: AGCGCCTGTCGCCGGGTCAATA	(66)
DOBR2: GTGTTTCATAACTCTTCTGGT	(66)

Species distribution modeling approach

We composed a dataset of 4493 *Triturus* localities (incorporating the 457 populations included in the genetic analysis; see Fig. 2 and Dataset S2). We used the bioclimatic variables available at a 2.5 arcminute resolution (c. 5 x 5 km) from the WorldClim database version 1.4 (134) to calibrate our species distribution models.

In order to prevent model overfitting, which would negatively influence transferability (162), we minimized multicollinearity among data layers by selecting a subset that showed a Pearson's correlation of $r < 0.7$. Furthermore, focusing on climate layers that are deemed biologically meaningful based on life history knowledge of the model system yields the most appropriate species distribution models (cf. 177). Variation in the availability of standing water during the breeding season appears to have driven the ecological radiation among *Triturus* newts (131). Therefore, we included a set of layers that encompasses seasonal variation in evaporation and precipitation, in casu bio10 = mean temperature of warmest quarter, bio11 = mean temperature of coldest quarter, bio15 = precipitation seasonality, bio16 = precipitation of wettest quarter, and bio17 = precipitation of driest quarter. Bioclimatic variables are also available from the WorldClim database for the Last Glacial Maximum (~21Ka) These data are derived from the Paleoclimate Modelling Intercomparison Project phase 2 (178; <http://pmip2.lsce.ipsl.fr/>) and based on two climate simulations: the Model for Interdisciplinary Research on Climate version 3.2 (MIROC) [<http://www.ccsr.u-tokyo.ac.jp/kyosei/hasumi/MIROC/techrepo.pdf>] and the Community Climate System Model version 3 (CCSM) (179).

Species distribution models were created with Maxent 3.3.3k (180). We restricted the feature type to hinge features as this produces smoother model fits, so forcing models to be focused on key trends rather than potential idiosyncrasy in the data. This approach facilitates extrapolation to a different time (or place) (181). The environmental range covered by the pseudo-absence data, used to discriminate presence data from background, should neither be too narrow or too broad (137, 182, 183). Too narrow a range results in complex models that do not generalize well, whereas too broad a range results in too simple models that focus on coarse-scale and neglect fine-scale variation. A practical solution is to focus on area that is potentially accessible to the species of interest if it were not for abiotic factors, i.e. an area where spread would not be hampered by major physical barriers. However, competition could lead to further exclusion of the target species, even though the area would be suited in the absence of such biotic interactions (184). Taking these considerations into account, we restricted the area from which pseudo-absence was drawn to the distribution of the entire genus *Triturus*. This area was broadly defined as a 200 km buffer zone (cf. 137) around known *Triturus* localities (Dataset S2).

The species distribution models were tested for statistical significance against a null model derived from random localities (185). For each tested species distribution model, we created a null distribution of 99 AUC values. These AUC values were derived from species distribution models, based on as many random localities as used for the tested species distribution model. The AUC value of the tested species distribution model was treated as a 100th value and deemed statistically significant if it ranked higher than the 95th value (i.e. above the 95% confidence interval). Random point data were created with ENMTools 1.3 (136; <http://enmtools.blogspot.com/>). The null model approach prevents interpreting model quality based on an arbitrary AUC threshold and precludes the requirement to set aside part of the localities for model testing (185).

The species distribution models were projected on the Last Glacial Maximum climate layers and composite maps were created for each set of climate layers. Maxent provides predicted probability values between zero and one and we used a color scheme running from blue to red to reflect these values.

Results

The 2354 *Triturus* sequenced newts comprise 302 haplotypes (see Dataset S1 for details and Dataset S3 for GenBank accession numbers). The Neighbor Joining phylogeny shows that haplotypes group in nine reciprocally monophyletic lineages, corresponding to species (Fig. 3). A large number of individuals ($n=342$; c. 14.5%) that belong to one species, possess mitochondrial DNA characteristic of another (Fig. 2 and Dataset S1). This mitochondrial DNA introgression is mostly restricted to near the contact zones; only *T. pygmaeus* and *T. macedonicus* have extended ranges in which foreign mitochondrial DNA is present (derived from *T. marmoratus* and the western *T. karelinii* mitochondrial DNA lineage).

Measures of genetic diversity within (π) and genetic divergence among (Z) populations can be found in Dataset S1 and S4. Composite maps visualizing this genetic structuring in each species are depicted in Fig. 4 and 5. Because Alleles in Space places the values for genetic divergence among populations at the midpoint of the network connecting the populations, information falling outside the current range is lost in Fig. 5 (e.g. in the case of two allopatric populations). Uncropped maps for each species, showing a more comprehensive picture per species but at the cost of conciseness, can be found in Figure S1.

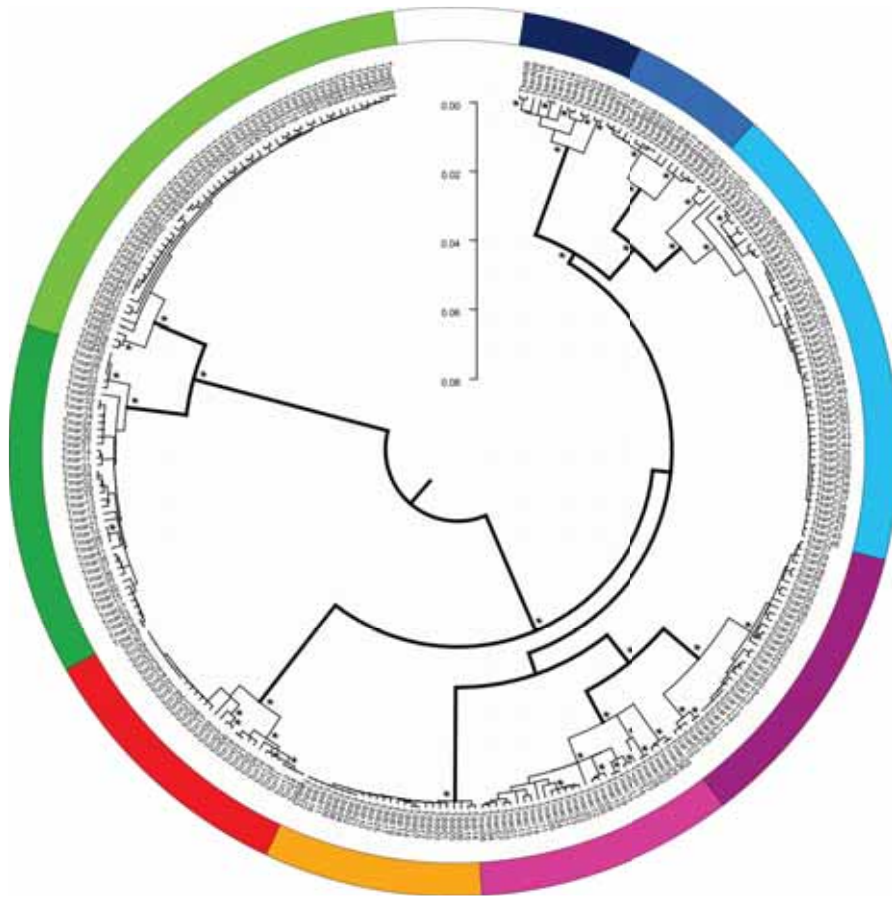


Figure 3 A Neighbor Joining phylogeny for the *Triturus* ND4 haplotypes. The *Triturus* haplotypes cluster into nine monophyletic mitochondrial DNA lineages, corresponding to species and colored as in Fig. 1. Significantly supported branches ($\geq 80\%$, based on a thousand bootstrap replicates) are denoted with an asterisk. The *Calotriton asper* outgroup used to root the phylogeny is not shown.

Species distribution models perform statistically significantly better than random expectation (Dataset S5). Composite maps depicting the predicted suitability of each species' distribution range at the Last Glacial Maximum, based on the two different climate simulations (MIROC and CCSM), are provided in Fig. 6 and 7. As species were not necessarily bound to their current ranges through time, projections for each species on a wider area (roughly the distribution of the entire genus *Triturus*) are provided in Figure S2.

The ranges of all *Triturus* species are predicted to have been restricted at the Last Glacial Maximum. A composite map showing species distribution models projected on present day climate layers is provided in Fig. 8. Predicted suitability of the distribution range of each species under current conditions shows a considerable overlap with the sketched outlines of their ranges (cf. Fig. 1).

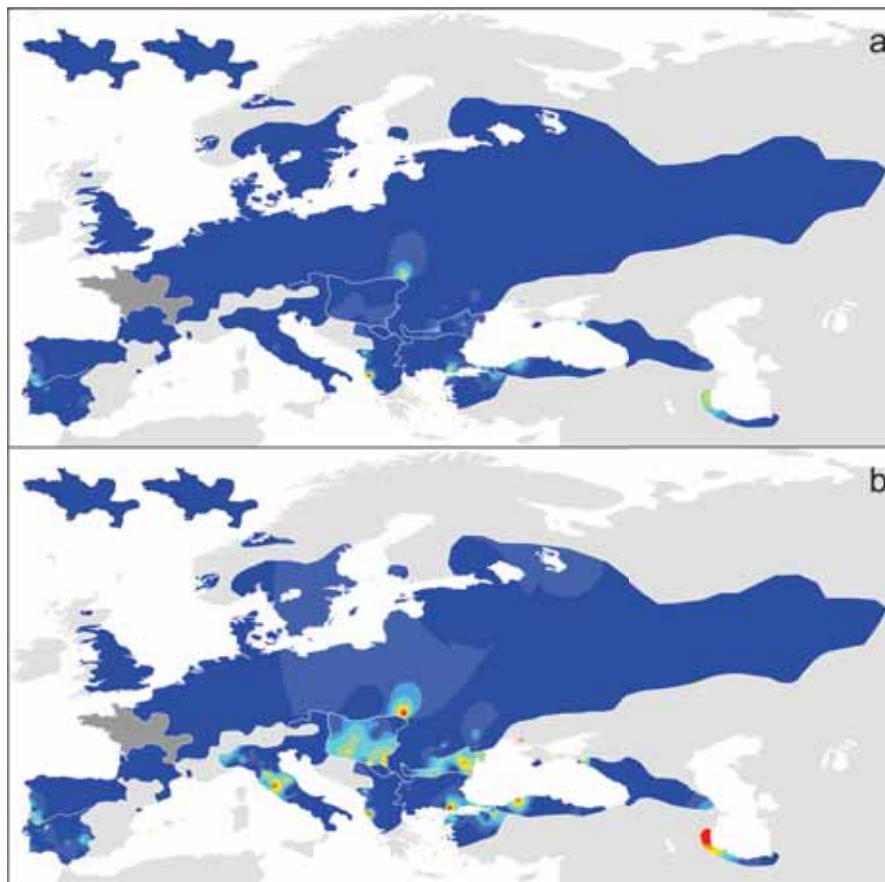


Figure 4 The geographical distribution of genetic variation for the different *Triturus* species. These are composite maps for all nine *Triturus* species. For each species, the genetic variation within each population (π) was determined and subsequently interpolated across its distribution range. In Fig. 4a we use a single scale for all *Triturus* species (allowing direct comparison among species) whereas in Fig. 4b we use a species specific scale (better expressing genetic structure in genetically relatively poor species). Warmer colors refer to a higher genetic diversity. The insets show the situation for *T. cristatus* (left) and *T. marmoratus* (right) in their area of sympatry (shown in dark gray on the main maps).

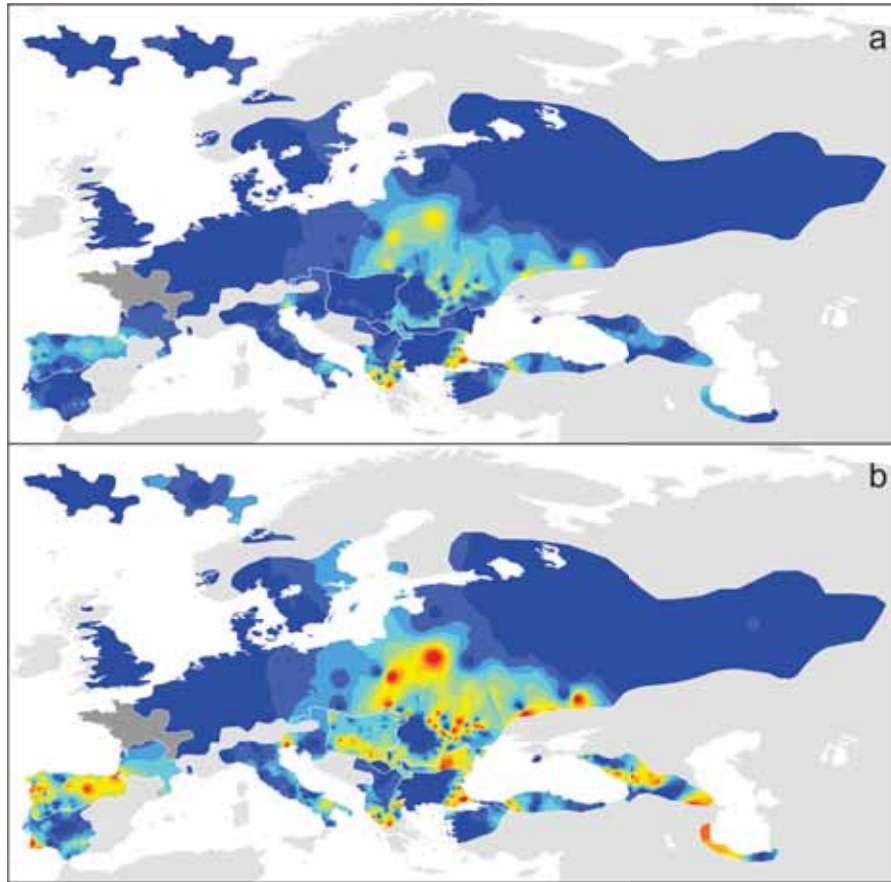


Figure 5 The genetic (dis)similarity among populations within the different *Triturus* species. These are composite maps for all nine *Triturus* species. For each species, the genetic divergence among populations (Z) was determined and subsequently interpolated across its distribution range. In Fig. 5a we use a single scale for all *Triturus* species (allowing direct comparison among species) whereas in Fig. 5b we use a species specific scale (better expressing genetic structure in genetically relatively poor species). Warmer colors refer to a higher genetic divergence. The insets show the situation for *T. cristatus* (left) and *T. marmoratus* (right) in their area of sympatry (shown in dark gray on the main maps).

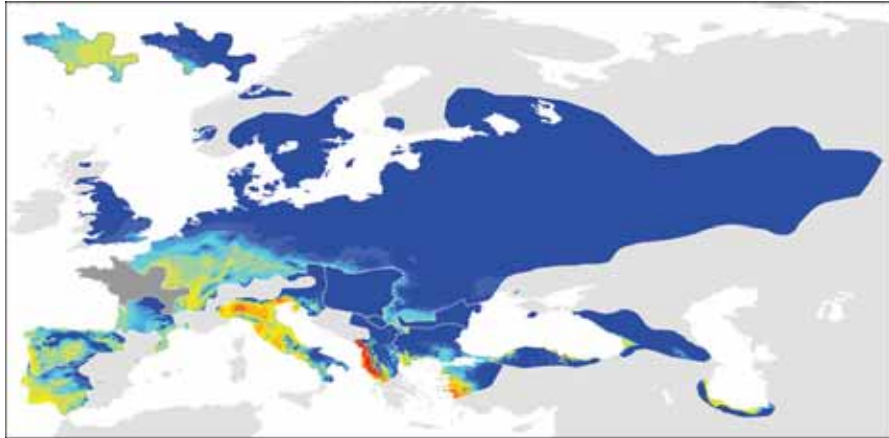


Figure 6 The predicted suitability of each *Triturus* species' range at the Last Glacial Maximum (MIROC model). This is a composite map for all nine *Triturus* species. For each species, its species distribution model was projected on Last Glacial Maximum climate layers (based on the MIROC model) for its current distribution range. Warmer colors refer to a higher predicted suitability. The insets show the situation for *T. cristatus* (left) and *T. marmoratus* (right) in their area of sympatry (shown in dark gray on the main map).

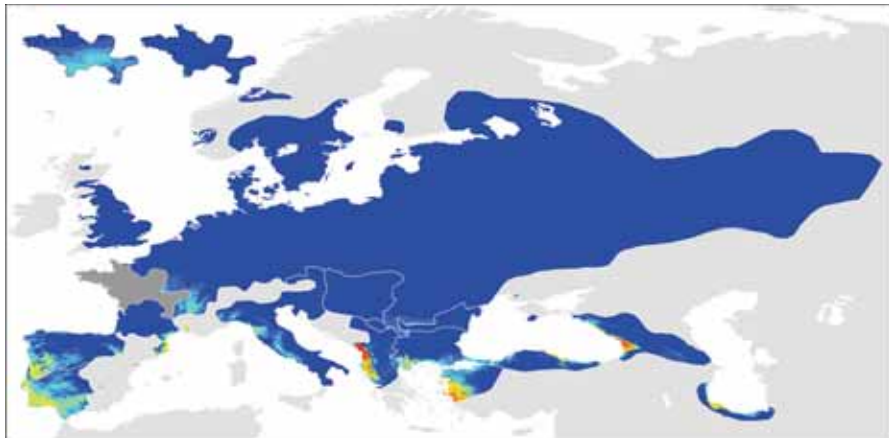


Figure 7 The predicted suitability of each *Triturus* species' range at the Last Glacial Maximum (CCSM model). This is a composite map for all nine *Triturus* species. For each species, its species distribution model was projected on Last Glacial Maximum climate layers (based on the CCSM model) for its current distribution range. Warmer colors refer to a higher predicted suitability. The insets show the situation for *T. cristatus* (left) and *T. marmoratus* (right) in their area of sympatry (shown in dark gray on the main map).

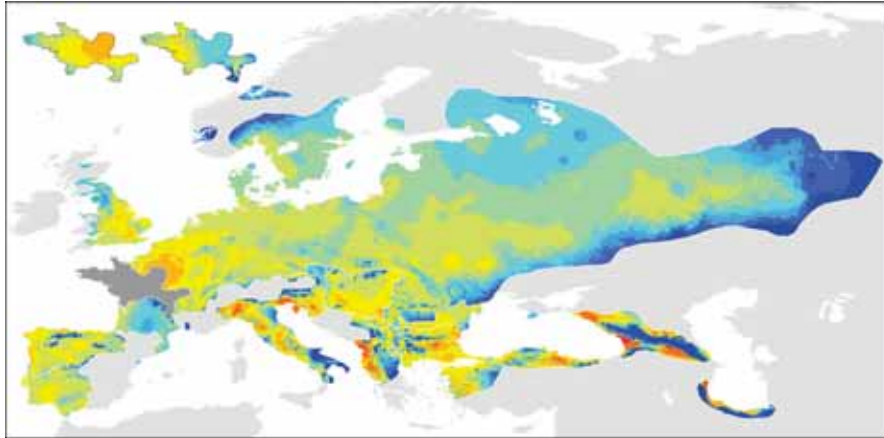


Figure 8 The predicted suitability of each *Triturus* species' range under current climate conditions. This is a composite map for all nine *Triturus* species. For each species, its species distribution model was projected on current climate layers for its current distribution range. Warmer colors refer to a higher predicted suitability. The insets show the situation for *T. cristatus* (left) and *T. marmoratus* (right) in their area of sympatry (shown in dark gray on the map).

Discussion

The combination of phylogeography and species distribution modeling aids the locating of glacial refugia (40, 57, 186-188). The two approaches to visualize intraspecific geographical genetic structuring together provide a picture of which areas are genetically rich and thus suspected to reflect long term inhabited area and which areas are genetically poor and thus probably only recently became habitable (Figs. 4 and 5). Independently, the two reconstructions of potential distribution at the Last Glacial Maximum (based on the MIROC and CCSM climate simulations) provide an indication of which areas were habitable at the time and which were unsuitable for *Triturus* (Figs. 6 and 7). Our results conform to the general pattern of the three European appendages, the Iberian, Italian and Balkan Peninsulas, having functioned as a glacial refugium. Furthermore, several regions that are getting more and more appreciated as having acted as glacial refugia (e.g. 61, 189) are also identified as such for *Triturus*: Anatolia, the southern Caspian basin and Colchis (western Georgia). Similarly, areas typically identified as having been postglacially colonized from glacial refugia stand out for *Triturus*: *T. marmoratus*, *T. carnifex*, *T. dobrogicus* and 'eastern *T. karelinii*' protruded into temperate Europe from their southerly positioned refugia, but such postglacial expansion is best exemplified by *T. cristatus*.

The contemporary range of *T. cristatus* encompasses, next to its glacial refugium in the Carpathian region in Romania (suggested suitable based on species distribution models and genetic diversity), a huge (c. 4.75 million km²) postglacially acquired area, stretching all the way from western Europe to Scandinavia and central Russia (unsuitable according to the species distribution models and genetically depleted). This gives an indication of the rapidness with which postglacial colonization can be accomplished.

Triturus species generally show considerable spatial variation in their genetic composition (reflected by 'warm' and 'cold' areas in Figs. 4 and 5). A high value for genetic diversity within populations (Fig. 4) can result from two distinct processes: long term presence *in situ* and secondary contact from distinct source populations. (Although new haplotypes typically evolve during a population expansion, these will also be rare and very similar to haplotypes already presents, thus not leading to a major increase in genetic diversity (159)). To separate these two processes, phylogenetic relationship among haplotypes should be consulted. For example, the obvious 'hot spot' found in *T. cristatus* (Fig. 4; SW Ukraine) reflects the postglacial comingling of haplotypes belonging to the two distinct clades present in this species (Fig. 3). On the other hand, the 'hot spot' found in eastern *T. karelinii* (Fig. 4; SE Azerbaijan) represents genetic variation built up in a climatically stable and long term inhabited region. Maps showing genetic divergence among populations (Fig. 5) reflect a different aspect of geographical genetic structuring. On the one hand, areas with a high genetic overturn among populations (e.g. the southern part of the range of *T. macedonicus*) show many hotspots. In some cases clear barriers to gene flow stand out, such as the Greater Caucasus mountain range separating eastern *T. karelinii* on its northern and southern side. On the other hand, genetically homogenous areas, due to high levels of gene flow and/or demographic expansion stand out as cold areas (e.g. both of these processes likely determine the lack of genetic structuring among *T. dobrogicus* populations, cf. Fig. 4a). The visualization of genetic divergence among populations is relatively sensitive to sampling density: the higher the sampling density, the better the map. In *T. cristatus*, for example, the transition between a genetically rich and a genetically poor region is positioned relatively outward of its hypothesized glacial refugium, because of a lack of samples from nearby postglacially acquired area. Maps showing the genetic variation within and the genetic divergence among populations complement each other and their combined use is recommended.

Triturus ranges are mostly parapatric; they exclude each other geographically (63). This suggests that the different species are ecologically too similar to co-exist, suggesting a tension at contact zones. The current contact zones are the result of secondary contact: whereas at the Last Glacial Maximum the species ranges were restricted (Fig. 6 and 7), after glacial conditions were alleviated, species expanded their ranges and as a consequence came into contact with others (Fig. 8). Ecological differences likely determine which species fares best against which ecological background (131). However, this is not the complete story. Species can be blocked during postglacial expansion by geophysical barriers (150). Furthermore, species can cut each other off during postglacial expansion and the presence of one prevents the spread of the other by high density blocking (6). Such a first come, first served process rivals the role of competitive exclusion: instead of the species best suited to a particular area, another may occur there. Species distribution models projected on climate layers for the present, outside of species' current distribution areas (Figure S2) give an indication. An example is provided by *T. carnifex*. The Alps present a barrier and there where *T. carnifex* would be able to pass them, *T. cristatus* is present. The species distribution model suggests areas beyond the Alps would be suitable for *T. carnifex*. 'Luckily' *T. carnifex* has been anthropogenically aided in colonizing areas that would normally be out of reach, providing an independent test from the species distribution models. In several locations where *T. carnifex* has been introduced into the range of *T. cristatus*, it manages to survive among, and even locally outcompete, *T. cristatus* (190-194). Three introduction localities (Surrey, England, Munich, Germany and Geneva, France / Switzerland) are indeed predicted suitable. A fourth (Veluwe, The Netherlands), however, is not. An explanation for this could be that the realized niche of *T. carnifex* from which localities are drawn to calibrate the species distribution model deviates from the potential niche (142).

Asymmetrically introgressed mitochondrial DNA provides a source of insight for interspecific interaction after secondary contact (160). For *Triturus* newts, introgression is mostly restricted to their contact zones, suggesting minor range rearrangement after secondary contact. However, in the case of *T. marmoratus* – *T. pygmaeus* and *T. karelinii* west – *T. macedonicus*, an extensive area is covered, suggestive of past interspecific competition (Fig. 2). The similarity of the introgressed mitochondrial DNA to that present in the 'donor' species suggest a recent (postglacial) transference across the species boundary. Given the climatic oscillations during the Quaternary Ice Age, the *Triturus* newt species are presumed to have been in periodic contact through time. However, we did not identify ancient mitochondrial DNA introgression events (as in e.g. (195-197)).

A potential explanation is that introgressed mitochondrial DNA was limited to areas of postglacial expansion and never penetrated those areas that repeatedly acted as glacial refugia. In effect, any mitochondrial DNA that became introgressed during an interglacial would be erased by the next glacial period.

Below we discuss our results in more detail, addressing each *Triturus* species separately. We focus on similarities and distinctions between the two different sources of information - geographical mitochondrial DNA structuring and predicted distribution at the Last Glacial Maximum - and present a scenario for glacial regression and postglacial expansion for each *Triturus* species.

Marbled newts

The two marbled newts illustrate the different effect of glaciations on species with a relatively southern and relatively northern distribution. The extent that *T. marmoratus* is predicted to have withdrawn its range at the Last Glacial Maximum is extensive (especially according to the CCSM climate simulation; Fig. 7), whereas it is minimal for *T. pygmaeus*. In *T. marmoratus* genetic structuring is highest in the south of its range, but for *T. pygmaeus* this is not the case (Fig. 4 and 5). The presence of *T. marmoratus* mitochondrial DNA in the northern part of the range of *T. pygmaeus* suggests that in this area the former was replaced by the latter (cf. 171, 198, 199). This is confirmed by the distribution models projected on Last Glacial Maximum climate data outside of the current species ranges (Figure S2): at the time, area predicted suitable for *T. marmoratus* (but not for *T. pygmaeus*) was present in the northern part of the area currently occupied by *T. pygmaeus*. Striking is that both *T. marmoratus* and *T. pygmaeus* mitochondrial DNA occurs throughout this area (Fig. 2). Although a species will often simply show foreign mitochondrial DNA where it replaced another (160), there are exceptions, similar to the *T. marmoratus*-*T. pygmaeus* case (200). The genetic divergence among *T. pygmaeus* populations within the region of displacement is generally low, corresponding with postglacial expansion.

The marbled and crested newt contact

The ranges of the marbled newt *T. marmoratus* and the crested newt *T. cristatus* widely overlap in western and central France (cf. Fig. 1). The appearance of sympatry is partially a matter of scale: zoomed in the distribution of the two species is more mosaic like, suggesting competitive exclusion. However, segregation is not complete and the two species still do widely occur in syntopy.

Although there is no niche partitioning in the aquatic environment (201), there is so in the terrestrial habitat, with *T. marmoratus* preferring a relatively higher degree of forestation and relief than *T. cristatus* (202, 203). As a consequence, outcompeting of *T. marmoratus* by *T. cristatus* (202-204) or the reverse (though as yet not studied in detail) takes place on a local scale. In one region where *T. cristatus* is displacing *T. marmoratus*, minor nuclear genetic leakage from *T. marmoratus* into *T. cristatus* has been documented (202, 205). This would suggest the possibility of introgression of *T. marmoratus* mitochondrial DNA into *T. cristatus*. However, despite a relatively large sample size, we did not detect this. This observation can be partially explained by a striking asymmetry in hybrid survival, showing a relatively strong selection against *T. marmoratus* mothered hybrids (which would be required for mitochondrial DNA introgression to occur as *T. cristatus* is the invader in this case) (205). Perhaps a setting where *T. marmoratus* outcompetes *T. cristatus*, not included in the present study, could reveal mitochondrial DNA exchange between the species.

How did the two species meet up in France? The zone of sympatry was unsuitable for *T. marmoratus* at the Last Glacial Maximum (Figs. 6 and 7). The mitochondrial DNA data suggest a postglacial colonization from the Iberian Peninsula, where the majority of France haplotypes are found (and to which the one unique France haplotype is very similar). The zone is predicted to have been suitable for *T. cristatus* based on the MIROC climate simulation (Fig. 6), but there is only minor support for this based on the CCSM climate simulation (Fig. 7). Furthermore, the mitochondrial DNA data strongly suggest a postglacial colonization from the Balkans for *T. cristatus* (more details below). Clearly, the two species established secondary contact after postglacially colonizing their current zone of sympatry. It should be noted that fossils ascribed to *T. marmoratus* dated to the Quaternary are known from e.g. Germany (206), suggesting the contact zone in the current interglacial might be very different from that during previous ones.

Crested newts: *T. cristatus*, *T. carnifex*, *T. dobrogicus* and *T. macedonicus*
The mitochondrial DNA data suggest that *T. cristatus* dramatically expanded its range postglacially, colonizing temperate Eurasia. Haplotypes outside of the Balkans are very similar and the same haplotype can be found at the western and eastern extremes of its range (separated by a distance of c. 3500 km). Such extreme genetic homogeneity is in line with leading edge expansion from a single source population (159). In general, the species distribution modeling approach supports this pattern: at the Last Glacial Maximum most of the current range of *T. cristatus* was unsuitable. However, the MIROC simulation suggests extensive suitable area in France and Germany.

This is unsupported by the CCSM simulation and genetic data. Only in the Carpatho-Balkan part of its range does *T. cristatus* show genetic differentiation among populations (Fig. 5), although variation within populations is low (Fig. 4). The MIROC climate simulation, although it overpredicts elsewhere, suggests suitable area here, whereas the CCSM climate simulation shows a more restricted suitable surface (Fig. 6 and 7). It seems plausible that *T. cristatus* distribution at the Last Glacial Maximum extended into the range currently occupied by *T. dobrogicus* (cf. Figure S2). The presence of *T. cristatus* mitochondrial DNA in *T. dobrogicus* (Fig. 2) supports this scenario, but sampling along the contact zone of the two newt species is limited (especially the addition of *T. dobrogicus* samples from western Romania would be illuminating). The Carpathian region, even though situated relatively northerly, is more and more appreciated as having acted as a refugium for a suite of other species (150). Even though *T. cristatus* extended its range slightly further southwards at the expense of the western *T. karelinii* mitochondrial DNA lineage (as deduced from asymmetric mitochondrial DNA introgression), the presence of several relatively old *T. cristatus* mitochondrial DNA lineages in Serbia and Bulgaria suggest a long-term presence south of the Danube River. *Triturus cristatus* is the only crested newt species for which no comprehensive phylogeography has yet been conducted (for all other species these are published, submitted or in preparation). The high genetic variation revealed here encourages further exploration, requiring a more detailed sampling in Romania, particularly the southwest.

For *T. carnifex* there is a discrepancy between the two climate simulations, with the Last Glacial Maximum predicted distribution according to MIROC showing a high correspondence with the current range, whereas CCSM shows a considerable reduction, with little suitable area predicted in the Italian Peninsula and none at all in the current northern Balkan range (Figs. 6 and 7). The mitochondrial DNA data better corresponds to the modeled distribution based on the MIROC simulation, as it shows distinct genetic clusters distributed on both sides of the Adriatic Sea and high genetic diversity in Italy (Figs. 3-5), supporting long term presence in the Balkans and a stable population in Italy. Both climate simulations agree that *T. carnifex* colonized the part of its range east and north of the Alps postglacially. The *T. carnifex* mitochondrial DNA introgressed into *T. cristatus* where the two species meet (cf. 194) suggest that Balkan *T. carnifex* were involved in this range expansion (in line with nuclear genetic data; 190). The presence of *T. dobrogicus* mitochondrial DNA at the eastern edge of the *T. carnifex* range (Fig. 2) provides further support for *T. carnifex* expansion. See (170) for a detailed treatment on *T. carnifex* phylogeography.

Strikingly, the entire current distribution area of *T. dobrogicus* is predicted to have been unsuitable at the Last Glacial Maximum, based on both climate simulations (Figs. 6 and 7). Also, a refugia positioned outside the current range (e.g. in currently submerged land) is not supported (Figure S2). Considering the specialization of this species on river floodplains, such a shift in distribution would not be feasible anyway (63, 141, 207). The mitochondrial DNA data support a major reduction of the distribution of *T. dobrogicus* as there is very low genetic diversity (note the shallow branches in comparison to the other *Triturus* species in Fig. 3 and the homogenous genetic structuring in Fig. 4 and 5). Furthermore, the large number of very similar but mostly low frequency haplotypes (i.e. a starburst phylogeny) is consistent with a rapid demographical expansion of a strongly bottlenecked population. A relatively high genetic diversity in allozyme data does suggest *T. dobrogicus* must have survived the last glaciation in multiple refugia (208). There is no genetic divergence between the populations from the Dobrogean and Pannonian Plains, situated on both sides of the southern spur of the *T. cristatus* range (Fig. 1), suggesting gene flow through *T. cristatus* territory (most likely along the Danube River at the Iron Gates, cf. (63)). Similarly, the allopatric population in the Dnepr delta is genetically similar to the main range (sharing two of three haplotypes). Past lowering of the Black Sea sea level, not only during the Last Glacial Maximum but also afterwards during the Holocene (cf. 209), joined the Danube and Dnepr rivers together in a 'paleodelta' (still visible on Google Earth at approximately 43° 50' N and 30° 26' E). This joined river system formed a route that would have facilitated recent genetic exchange. Asymmetrical introgression of *T. dobrogicus* mitochondrial DNA into four other species (*T. carnifex*, *T. cristatus*, *T. karelinii* western mitochondrial DNA lineage and *T. macedonicus*) shows that these pushed *T. dobrogicus* out of part of its former range. A detailed multimarker phylogeography of *T. dobrogicus* is in preparation (210).

The western part of the current range of *T. macedonicus* is predicted to have been suitable during the Last Glacial Maximum (Fig. 6 and 7). This does not fully correspond to mitochondrial DNA data, which shows structuring in the southern part of the range, including the southeast, but not in the northwest (Figs. 4 and 5). Genetic variation in *T. macedonicus* is the highest of all *Triturus* newts (Fig. 3). A distinct clade occurs on Corfu, which is currently disconnected from mainland Greece, but was connected during glaciations due to the accompanied drop in sea level (211).

In a large part of its range, *T. macedonicus* possesses western *T. karelinii* mitochondrial DNA (Fig. 2). This can be explained by *T. macedonicus* displacing the western *T. karelinii* mitochondrial DNA lineage there after the Last Glacial Maximum. The species distribution modeling approach suggests that this area indeed only became unsuitable for *T. macedonicus* after the Last Glacial Maximum (see (172) for a more detailed analysis).

Crested newts: the three T. karelinii mitochondrial DNA lineages

In the western *T. karelinii* mitochondrial DNA lineage, a basal split separates a clade occurring in European Turkey and extreme southeastern Bulgaria (Fig. 3). The species distribution modeling approach suggests suitable area was present here during the Last Glacial Maximum (Fig. 6 and 7). The genetic distinction of this clade is expressed by the 'barrier' in Fig. 5 surrounding the populations in which it is represented. The reciprocal clade shows extensive structuring in Asiatic Turkey. A single sub-clade derived from (i.e. nested within) Asiatic Turkey has recently colonized most of the Balkan part of the range; it shows a starburst phylogeny (Fig. 3), in line with demographic growth during a range expansion (159). In Asiatic Turkey, genetic diversity is highest in the extreme northwest, suggesting it acted as a refugium, but the species distribution modeling approach suggests that the western coast was particularly suitable at the Last Glacial Maximum. A scenario of postglacial expansion into the Balkan Peninsula agrees with the species distribution modeling approach, which demonstrates that the area only became hospitable after the Last Glacial Maximum. As noted above, the western *T. karelinii* mitochondrial DNA lineage was outcompeted out of part of the post-glacially acquired Balkan range by *T. macedonicus* (see (172) for a more detailed analysis).

The central *T. karelinii* mitochondrial DNA lineage shows a fragmented distribution at the Last Glacial Maximum (Fig. 6 and 7). This is reflected by an east west divide (the 'barrier' in Fig. 5) between two distinct clades separated by a basal split (cf. Fig. 3), which are currently in secondary contact (the 'warm' spot in Fig. 4). It should be noted that for the three mitochondrial DNA lineages found in *T. karelinii*, there are as yet no other criteria to classify individuals as species except mitochondrial DNA (65), meaning we currently cannot recognize potential mitochondrial DNA introgression between these lineages. Mitochondrial DNA introgression may apply to the central and western mitochondrial DNA lineages as the two are found in syntopy in northwestern Asiatic Turkey (cf. Dataset S1). However, as the eastern and central mitochondrial DNA lineages appear to be allopatrically distributed, mitochondrial DNA introgression is not expected to be an issue for these two lineages (65).

For the eastern *T. karelinii* mitochondrial DNA lineage, the southern Caspian basin and western Georgia (Colchis) are suggested to have harbored suitable area at the Last Glacial Maximum (Fig. 6 and 7). Genetic diversity is particularly high along the southern Caspian Sea shore (Fig. 3-5). Relatively recently a single clade colonized the Caucasus and Crimea from the Caspian part of the range (cf. 65). However, this clade is still relatively distinct (reflected by a deep coalescence; see Fig. 3), suggesting that colonization happened during a previous interglacial and thus that the clade persisted here in a glacial refugia during one or several glacial cycles. Indeed, marine intrusion in central Azerbaijan due to the higher water level of the Caspian Sea at the Last Glacial Maximum would have hampered colonization at the time (212) and the region is still suggested to be unsuitable at present (Figure S2). Periodic exposure of the sea strait currently separating the Crimea (cf. 209) would have facilitated the colonization of the current Crimean range from the Caucasus region.

Acknowledgements

D. Canestrelli generously shared unpublished sequence data. M.P. Miller provided advice on the use of Alleles in Space. J. van Alphen, W. Babik, W. Beukema, S. Bogaerts, S. Branković, Henrik Bringsøe, D. Canestrelli, D. Cogălniceanu, A. Crottini, G. Džukić, G. Espregueira Themudo, E. Froufe, A. Geraldes, Ö. Güclü, I. Haxhiu, M. Kalezić, H.G. Kami, A. Loureiro, A. Maletzky, Đ. Milošević, N. Moin, O. Mozaffari, P. Mikulíček, B. Naumov, K. Olgun, N.A. Poyarkov, B. Safaei, J.F. Schmidtler, A. Urošević, N. Üzüm, J. Vörös and B. Vrenosi aided with the collection of samples and locality data. The PMIP 2 Data Archive is supported by CEA, CNRS and the Programme National d'Etude de la Dynamique du Climat (PNEDC). We acknowledge the international modeling groups for providing their data for analysis and the Laboratoire des Sciences du Climat et de l'Environnement (LSCE) for collecting and archiving the model data.

Supplementary data

The supplementary data associated with this chapter can be found at science.naturalis.nl/media/333564/ch4suppdata.zip.

- Dataset S1: Details on the *Triturus* populations included in the genetic analysis.
- Dataset S2: Details on the *Triturus* populations used for species distribution modeling.
- Dataset S3: A list of ND4 haplotypes with their GenBank accession numbers.
- Dataset S4: Values of average genetic distance among populations (Z) within each *Triturus* species.

- Dataset S5: The AUC values for the species distribution models of each *Triturus* species, tested against null models.
- Figure S1: The genetic (dis)similarity among populations within the different *Triturus* species, not cut according to the current species ranges.
- Figure S2: The species distribution model of each *Triturus* species projected for Last Glacial Maximum and current climate conditions, not cut according to the current species ranges.

Chapter 5: Postglacial species displacement in *Triturus* newts deduced from asymmetrically introgressed mitochondrial DNA and ecological niche models

This chapter is based on: Wielstra B, Arntzen JW (2012) Postglacial species displacement in *Triturus* newts deduced from asymmetrically introgressed mitochondrial DNA and ecological niche models. *BMC Evolutionary Biology* 12: 161

Abstract

If the geographical displacement of one species by another is accompanied by hybridization, mitochondrial DNA can introgress asymmetrically, from the outcompeted species into the invading species, over a large geographical extent. This phenomenon is shown by the two crested newt species *Triturus macedonicus* and *T. karelinii*, on the Balkan Peninsula in south-eastern Europe. We first delimit a ca. 54,000 km² area in which *T. macedonicus* contains *T. karelinii* mitochondrial DNA. This introgression zone bisects the range of *T. karelinii*. Similarity of the introgressed mitochondrial DNA haplotypes suggests a recent transfer across the species boundary. We then use ecological niche modeling to explore the suitability of the introgression zone under current and Last Glacial Maximum conditions. The introgression zone was inhospitable during the Last Glacial Maximum for either species, but has since that time become suitable. The extraordinary spatial setting of this study, in which the advance of *T. macedonicus* created an enclave of *T. karelinii*, provides insight into the particular process causing asymmetric mitochondrial DNA: *T. macedonicus* invaded *T. karelinii* territory and thus moved into an area where 'foreign' mitochondrial DNA was present; mitochondrial DNA was not pulled into the *T. macedonicus* range by natural selection. The presence of the enclave suggest *T. karelinii* was the first to colonize the eastern part of the introgression zone after the Last Glacial Maximum. Subsequently, it was outcompeted by *T. macedonicus*, which captured *T. karelinii* mitochondrial DNA via introgressive hybridization in the process. The western part of the zone was probably never inhabited by *T. karelinii* itself, but *T. karelinii* mitochondrial DNA could spread there through the bodies of *T. macedonicus*.

Introduction

When reproductive isolating mechanisms have become of sufficient strength to prevent two diverging gene pools from merging, speciation has been reached (82). If, however, low frequency hybridization still occurs, the stage is set for the interspecific transference of mitochondrial DNA (159, 160, 213, 214). Mitochondrial DNA is transmitted clonally (matrilineally) in the majority of eukaryotes and, as a consequence, does not dilute via recombination (215). Through an initial hybridization event and subsequent backcrossing of female progeny with the paternal species, mitochondrial DNA can become fixed on the 'wrong' species background (Fig. 1a).

In parapatric species, mitochondrial DNA introgression can be asymmetric, with one species showing mitochondrial DNA typical of the other over a significant part of its range (reviewed in ref. 160). This can be explained by the former displacing the latter (159, 160, 214).

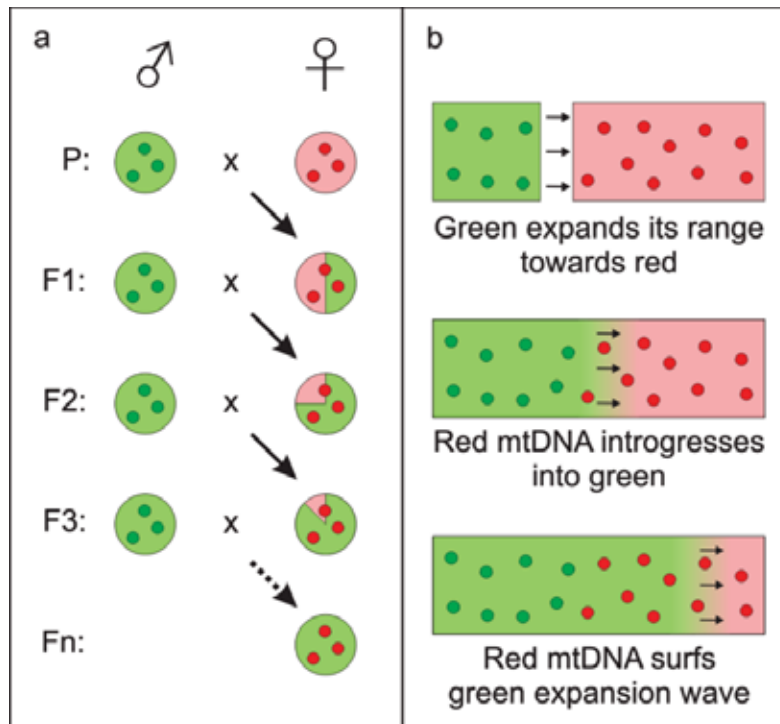


Figure 1 A schematic representation of asymmetric mitochondrial DNA introgression via hybridization and species displacement. Fig. 1a depicts the transference of mitochondrial DNA across the species boundary via introgressive hybridization. Large circles reflect the nuclear DNA composition of individuals, small ones their mitochondrial DNA type. There is an initial hybridization between the members of two species, a red female and a green male. The F1 offspring contain a mix of red and green nuclear DNA, but only red mitochondrial DNA (due to mitochondrial DNA's matrilineal transmission). Subsequent backcrossing of admixed females with green males over the generations dilutes the red nuclear DNA out, in effect leading back to the green species. However, all subsequent generations contain red mitochondrial DNA (ensured by mitochondrial DNA's clonal transmission). Fig. 1b shows how the outcompeting of one species by another can result in asymmetric mitochondrial DNA introgression. Small circles now reflect the spatial distribution of mitochondrial DNA type and the background the geographical nuclear DNA composition of the population. At the top, the ranges of a red and a green species are in allopatry, but green expands its range towards red. In the middle, green and red have become parapatric. The species hybridize at the contact zone, where red mitochondrial DNA introgresses into the green species (as in Fig. 1a). At the bottom, green shifts its distribution further to the right, at the expense of red. As the members of the green species leading the expansion contain red instead of green mitochondrial DNA, only red mitochondrial DNA spreads in the region where the green species displaces the red species. This figure is based on (159, 214).

The rationale is as follows: mitochondrial DNA of a common, native ‘donor’ species is captured by an initially rare invader, through introgressive hybridization. As the invader expands its range at the expense of the native species, its population increases and introgressed mitochondrial DNA is co-amplified. Consequently, the introgressed mitochondrial DNA surfs the wave of advance and is left in its wake (Fig. 1b). The initial mitochondrial DNA introgression does not have to occur at a high frequency to result in a mismatch between species and mitochondrial DNA type spanning an extensive area. A likely driver causing the necessary geographical displacement of closely related species is the rearrangement of distributions in response to climate oscillations related to glacial/interglacial cycles (159, 160).

On the Balkan Peninsula in southern Europe, the two parapatrically distributed crested newts *Triturus macedonicus* and *T. karelinii* show the preconditions for asymmetric mitochondrial DNA introgression. *Triturus karelinii* comprises three distinct mitochondrial DNA lineages, which might better be regarded as different species (65, 131). Therefore, throughout the current paper, we only consider the lineage that occurs in the Balkans and western Turkey, in parapatry with *T. macedonicus*, when we refer to *T. karelinii*. *Triturus macedonicus* and *T. karelinii* can be distinguished on morphological grounds – meristic, morphometric and qualitative (63, 67). Analysis of a suite of allozyme markers has shown the nuclear gene pools of these newts to have remained isolated, although limited genetic admixture occurs at the contact zone (112, 132, 190). Furthermore, *T. macedonicus* contains mitochondrial DNA typical of *T. karelinii* at localities removed from the current contact zone (66, 69). Finally, geographical displacement by *T. macedonicus* has been invoked to explain an apparent enclave of *T. karelinii*, cut-off from the main distribution range (67).

Here we further explore the *T. macedonicus* – *T. karelinii* case. We first delimit the zone of *T. karelinii* mitochondrial DNA asymmetrically introgressed into *T. macedonicus* through a phylogeographical survey. We then built ecological niche models for both species and project these on current and Last Glacial Maximum climate layers. Inferred distribution shifts across the zone of asymmetric mitochondrial DNA introgression suggest that *T. macedonicus* displaced *T. karelinii* postglacially.

Results

As *T. macedonicus* and *T. karelinii* mitochondrial DNA differ considerably ($D_{XY} = 0.091$), sequenced individuals could be unambiguously assigned to mitochondrial DNA type (details in Additional file 1).

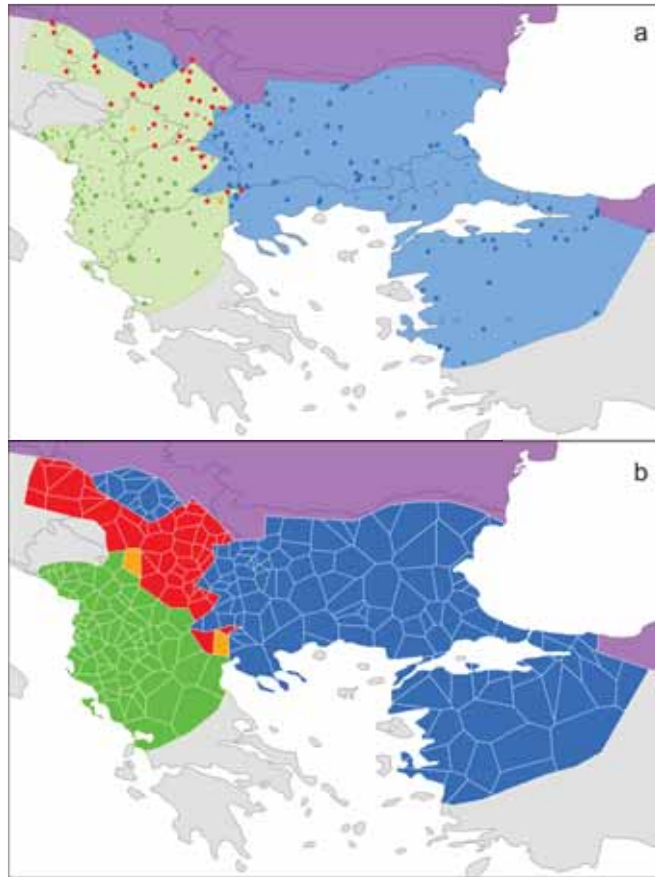


Figure 2 Distribution and sampling of *Triturus macedonicus* and *T. karelinii* and the zone of asymmetric introgression of *T. karelinii* mitochondrial DNA. Fig. 2a shows the distribution of *T. macedonicus* (shaded green) and *T. karelinii* (blue), as deduced from morphology and allozyme data (see Methods for details). Note that the north-western part of the range of *T. karelinii* is disconnected from the main range (i.e. an enclave). Ranges are limited by sea (white), uninhabited land (grey) and other *Triturus* taxa (purple). Green dots represent *T. macedonicus* populations containing original *T. macedonicus* mitochondrial DNA, blue dots *T. karelinii* populations containing *T. karelinii* mitochondrial DNA, red dots *T. macedonicus* populations containing *T. karelinii* mitochondrial DNA and two orange dots *T. macedonicus* populations containing both original and introgressed mitochondrial DNA. Large dots represent populations for which mitochondrial DNA was sequenced and small dots additional localities included in ecological niche modeling. Fig. 2b shows the geographical distribution of mitochondrial DNA based on Thiessen polygons, where each polygon covers the area that is closer to its corresponding population than to another one. Color codes are the same as in Fig. 2a. The red and orange polygons were combined to delimit the zone of asymmetric mitochondrial DNA introgression.

Out of 71 of the *T. macedonicus* populations for which sequence data are available, 35 contain only original *T. macedonicus* mitochondrial DNA, 34 contain only *T. karelinii* mitochondrial DNA and in two populations syntopy of both mitochondrial DNA types was established (Fig. 2a). There is no *T. macedonicus* mitochondrial DNA found in any of the 86 *T. karelinii* populations for which sequence data is available. The clear-cut geographical distribution of mitochondrial DNA allows us to safely interpret 16 of the 68 *T. macedonicus* populations and all 49 *T. karelinii* populations for which no sequence data is available as containing *T. karelinii* mitochondrial DNA. By employing Thiessen polygons, we delimit an extensive (ca. 54,000 km²) area of asymmetric mitochondrial DNA introgression, in which *T. macedonicus* contains *T. karelinii* mitochondrial DNA (Fig. 2b).

The *T. karelinii* mitochondrial DNA shows extensive structuring and comprises three spatio-temporal groups (Fig. 3). A 'Balkan basal' clade, restricted to the extreme south-east Balkan Peninsula, is distinct from the remaining *T. karelinii* haplotypes ($D_{xy} = 0.035$). A genetically relatively diverse group of haplotypes is distributed in western 'Asiatic Turkey' (Fig. 3). A 'Balkan recent' clade is nested within, and closely related to, the 'Asiatic Turkey' haplotypes (separated by a single substitution). The 'Balkan recent' haplotypes show a starburst pattern: they are genetically similar, comprising a few common and a large number of rare ones (Fig. 3). For the *T. karelinii* mitochondrial DNA, only the 'Balkan recent' clade shows signs of demographic expansion (Fig. 4).

The original *T. macedonicus* mitochondrial DNA is genetically diverse (Additional file 2) and does not indicate demographic growth (Fig. 4). All introgressed *T. karelinii* mitochondrial DNA belongs to the 'Balkan recent' clade (Fig. 3). The low level of diversification of the 'Balkan recent' clade renders it difficult to distinguish multiple introgression events from the evolution of new haplotypes within *T. macedonicus*, derived from a single introgressed *T. karelinii* haplotype. However, it is likely that the three *T. karelinii* haplotypes shared between *T. karelinii* and *T. macedonicus* (of which two represent the most frequent haplotypes found in either species) reflect independent introgression events rather than convergent evolution.

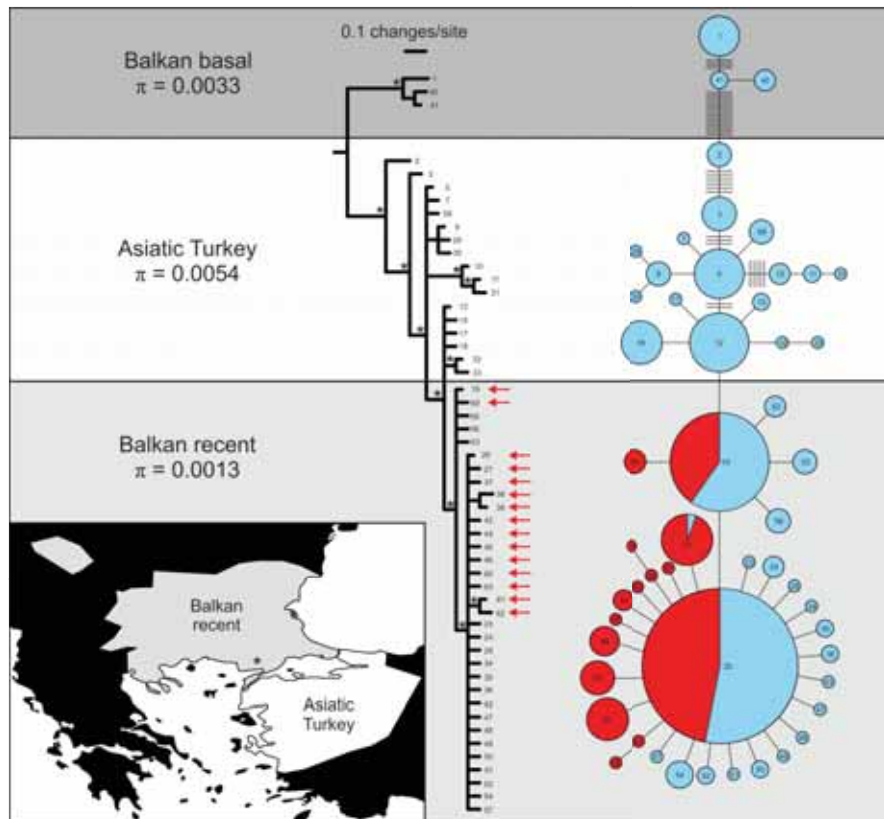


Figure 3. The genetic structuring of *Triturus karelinii* mitochondrial DNA, including that introgressed into *T. macedonicus*. Three spatio-temporal groups of haplotypes are recognized: 'Balkan basal', 'Asiatic Turkey' and 'Balkan recent'. The inset shows the geographical range of each group: 'Asiatic Turkey' in white and 'Balkan recent' in light grey (note the enclave); populations in which 'Balkan basal' haplotypes are found are marked with dark grey stars (see Additional file 1 for details on haplotype distribution). For each group the nucleotide diversity (π) is determined. In the phylogenetic tree, red arrows signify haplotypes that are (also) found as introgressed mitochondrial DNA in *T. macedonicus*. Statistically significantly supported clades (meaning a Bayesian posterior probability of 0.95 or higher) are denoted with an asterisk (*). In the haplotype network, pie diameter expresses haplotype frequency (cf. Additional file 5) and bars the number of mutations along a branch if more than one. Blue pies reflect *T. karelinii* mitochondrial DNA found in *T. karelinii* and red pies *T. karelinii* mitochondrial DNA present in *T. macedonicus*. If *T. karelinii* haplotypes are shared between *T. karelinii* and *T. macedonicus*, frequencies are reflected by the size of the slices. The numbers in the phylogeny and haplotype network refer to *T. karelinii* mitochondrial DNA haplotypes as coded in Additional file 5.

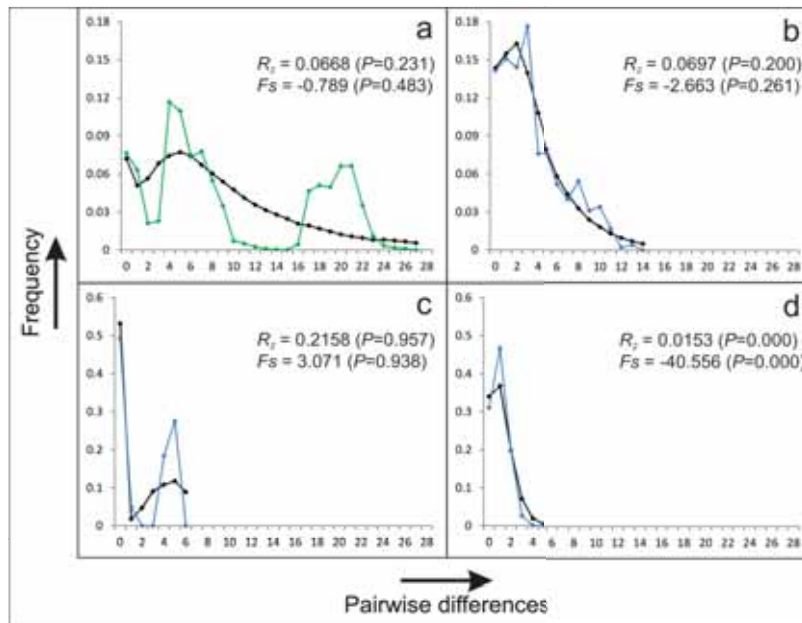


Figure 4 The mismatch distribution and Ramos-Onsins and Rozas' R_2 and Fu's F_s statistics for different groups of haplotypes. Groups of haplotypes are: *T. macedonicus* (a), *T. karelinii* Asiatic Turkey (b), *T. karelinii* Balkan basal (c) and *T. karelinii* Balkan recent (d). The colored curves (green for *T. macedonicus* and blue for the three groups of *T. karelinii* haplotypes) show the observed frequency distribution of pairwise differences and the black curves that expected for an expanding population. Based on the R_2 and F_s statistics, the null hypothesis of a constant population size is only rejected for *T. karelinii* Balkan recent. This agrees with the shape of the mismatch distributions. A unimodal and smooth distribution is indicative of demographic expansion, whereas a multimodal and ragged distribution suggests demographic stability.

The ecological niche models of both crested newt species perform statistically significantly better than expected by random chance (Additional file 3). When hindcasted on Last Glacial Maximum data layers, the models suggest that the ranges of both crested newt species were contracted at the time (Fig. 5). To link this shift in suitability to the observed mitochondrial DNA introgression, we zoom in on the introgression zone (Fig. 6). The introgression zone is predicted to be much more suitable at present than it was at the Last Glacial Maximum, although the western half is predicted to still be unsuitable for *T. karelinii*. The ecological niche models are most affected by the mean temperature of the coldest quarter in both species and precipitation in the wettest quarter plays an important additional role in *T. macedonicus* (Additional file 4).

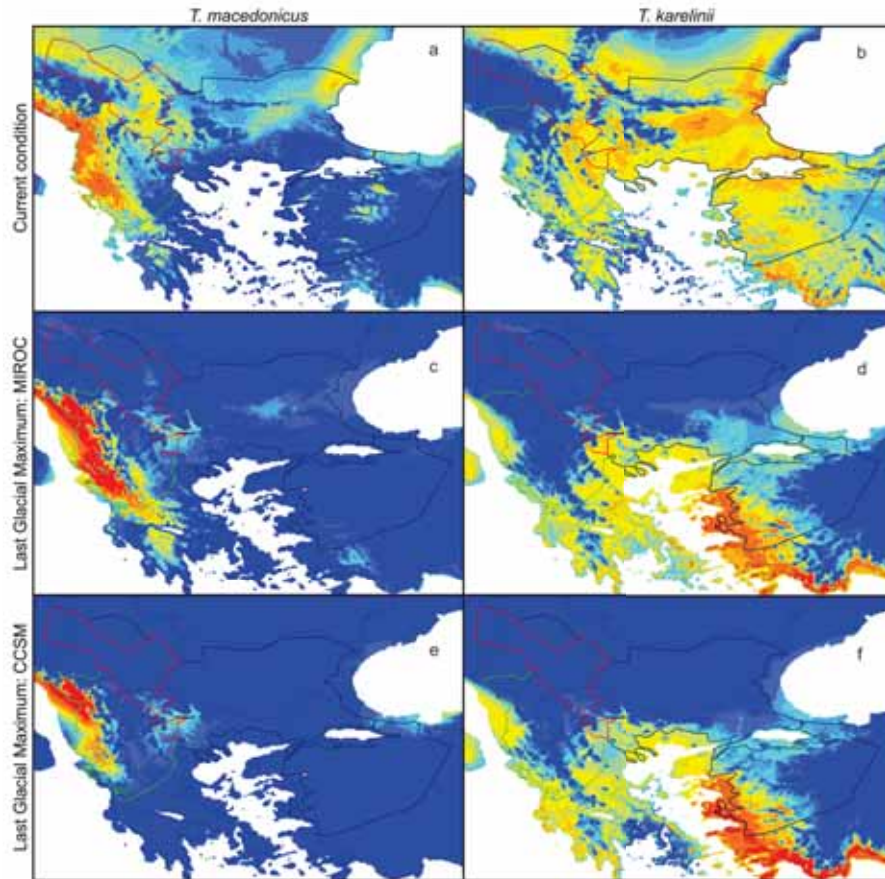


Figure 5 The predicted distribution for *T. macedonicus* and *T. karelinii* under current and Last Glacial Maximum conditions based on ecological niche modeling. The ecological niche models projected on current and MIROC and CCSM Last Glacial Maximum climate layers for *T. macedonicus* are shown on the left (a, c, e) and those for *T. karelinii* on the right (b, d, f). The warmer a grid cell's color, the higher its predicted suitability (see the legend of Fig. 6 for suitability scores). The current range of *T. karelinii* is outlined in blue and that of *T. macedonicus* in green, with the zone of asymmetric mitochondrial DNA introgression outlined in red. Political boundaries are overlaid in black.

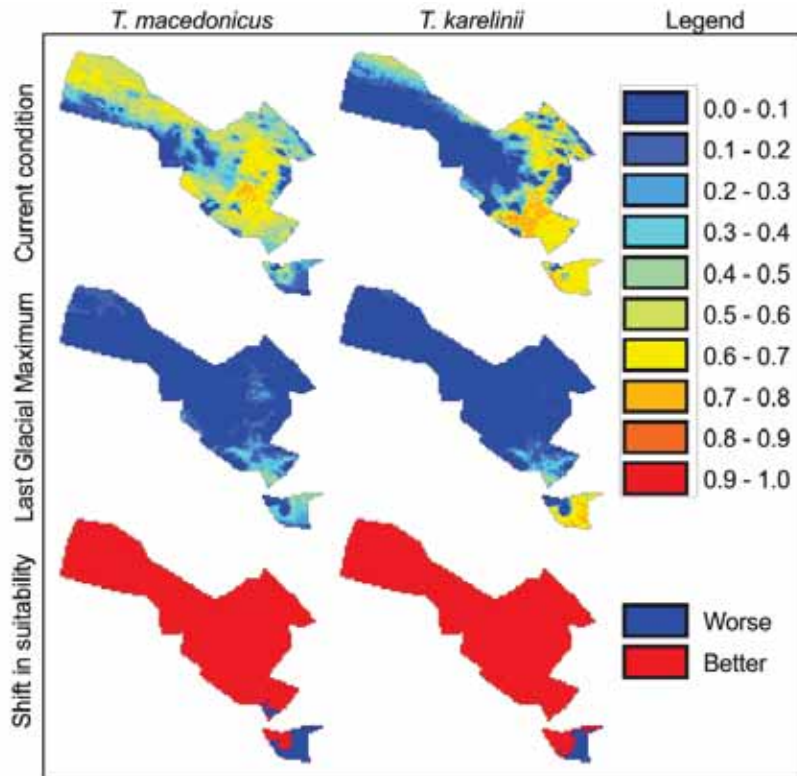


Figure 6 The suitability of the zone of asymmetric mitochondrial DNA introgression as predicted by ecological niche modeling. The situation for *T. macedonicus* is shown on the left and for *T. karelinii* on the right. The top row shows the suitability of the zone of asymmetric mitochondrial DNA introgression under current conditions and the middle row at the Last Glacial Maximum (based on the MIROC model, results using the CCSM model are highly similar, cf. Fig. 5). The bottom row shows the area that currently has a better or worse predicted suitability than at the Last Glacial Maximum.

Discussion

A scenario of species displacement

We confirm that the range of *T. karelinii* is bisected by *T. macedonicus* (Fig. 2a), corroborating a previously hypothesized *T. karelinii* enclave (cf. 67). Considering that crested newts are surface-bound and have limited dispersal capabilities, the presence of the *T. karelinii* enclave is best explained by it having been cut off from the main *T. karelinii* range by an expanding *T. macedonicus* (the enclave having been cut from the north by another *Triturus* species (*T. cristatus*), as one might expect based on Fig. 2, is not supported by a mitochondrial DNA phylogeography (216)).

However, the mitochondrial DNA data suggest that a considerably larger area is involved in the geographical displacement of *T. karelinii* by *T. macedonicus* than that required to explain the enclave (Fig. 2b). How was this introgression zone established? The structuring of the mitochondrial DNA of the two crested newt species and their predicted distributions based on ecological niche modeling provide the necessary insight.

The ranges of both crested newt species were reduced at the Last Glacial Maximum (Fig. 5). For *T. karelinii*, the south-western margin of its current Balkan range (extending into land currently occupied by *T. macedonicus*) was hospitable. However, the mitochondrial DNA data suggest that the 'Balkan basal' clade was likely restricted to the south-east, whereas the 'Balkan recent' clade originates from a recent colonization from Asiatic Turkey (Fig. 3). Indeed, Turkey's west coast was also suitable at the Last Glacial Maximum and mitochondrial DNA indicates a stable demographical history here (Fig. 5). Furthermore, the 'Balkan recent' clade shows the signature of demographic growth, in line with a range expansion (Fig. 4). The west side of the current range of *T. macedonicus* was also suitable at the Last Glacial Maximum, corresponding to long-lasting presence *in situ* as suggested by the mitochondrial DNA data (Fig. 4).

The introgression zone was uninhabitable for either crested newt species at the Last Glacial Maximum and their secondary contact was established after glacial conditions had alleviated (Fig. 6). In accordance to this, the *T. karelinii* haplotypes introgressed into *T. macedonicus* are similar or identical to those found in *T. karelinii* itself, suggesting that introgression happened recently (195, 196, 217). For *T. karelinii*, the western part of the introgression zone is predicted to be unsuitable still. We suggest that, even if this part was never colonized by *T. karelinii* itself, the *T. karelinii* mitochondrial DNA could still have reached this region via the *T. macedonicus* host. We summarize the invoked distribution dynamics of the two crested newt species in Fig. 7.

Ecologically driven displacement

The outcompeting of *T. karelinii* by *T. macedonicus* across the introgression zone must have been facilitated by some kind of advantage of *T. macedonicus*. A striking example of geographical displacement linked to natural selection, that could be deduced because it was 'documented' by mitochondrial DNA capture, is provided by *Salamandra* salamanders (218).

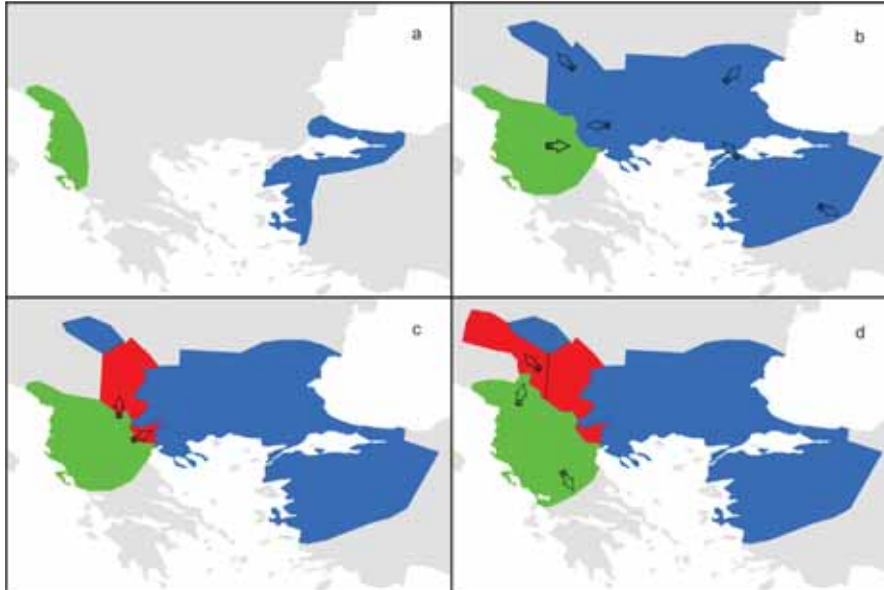


Figure 7 A historical biogeographical scenario explaining the presence of *Triturus karelinii* mitochondrial DNA in *T. macedonicus*. The ranges of *T. karelinii* and *T. macedonicus* are shown in blue and green and the region where *T. macedonicus* contains *T. karelinii* mitochondrial DNA is shown in red. During the last glaciation, both species' ranges were repressed (a). After glacial conditions alleviated, *T. karelinii* derived from Turkey colonized a considerable part of the Balkan Peninsula and *T. macedonicus* expanded its range and came into contact with *T. karelinii* (b). Subsequently, *T. macedonicus* displaced *T. karelinii* over part of its range and in the process cut off a *T. karelinii* enclave; due to mitochondrial DNA introgression, *T. macedonicus* possessed *T. karelinii* mitochondrial DNA, there where it displaced *T. karelinii* (c). Finally, *T. macedonicus* expanded its range further and, as part of the source population contained *T. karelinii* mitochondrial DNA, this mitochondrial DNA spread, via the bodies of *T. macedonicus*, into an area not inhabited by *T. karelinii* itself (beyond the interrupted line) (d).

On the northern edge of the Iberian Peninsula, after a shift in climate, a *Salamandra* taxon using a viviparous reproduction mode (giving birth to terrestrial juveniles) became favored over one using an ovoviviparous reproduction mode (giving birth to aquatic larvae). Although not showing such obvious life history differences as in the *Salamandra* situation, the two crested newt species do appear to differ in the time annually allocated to an aquatic and a terrestrial life style, with adult *T. macedonicus* presumed to spend one more month in the water than *T. karelinii* (63, 131).

Bioclimatic variable contribution to the ecological niche models is at least partially in line with the hypothesis that *T. macedonicus* is adapted to relatively wetter conditions, as its occurrence correlates with a higher precipitation than is found for *T. karelinii* (Additional file 4). Future research is required to further study if *T. macedonicus* has an adaptive advantage over *T. karelinii* at the introgression zone. It would also be interesting to study whether the two species are currently in spatial equilibrium or whether the contact zone is still moving.

What tipped the balance in the introgression zone in favor of *T. macedonicus*? The reconstructed distributions of the two crested newt species make clear that colonization of the introgression zone could only occur during the Holocene (i.e. the current interglacial), after the last glacial cycle came to an end. An increased evaporation due to the relatively higher temperature (though similar precipitation) in Europe at the mid-Holocene (178) might have benefitted the more terrestrial *T. karelinii*, so allowing it to colonize (at least part of) the introgression zone at the time. Indeed the shifting climate of the Holocene in itself impacted species distributions (161). However, species' distribution dynamics were probably not straightforward, as Holocene climate fluctuated considerably (219-221). The climatic drive behind the *T. macedonicus* – *T. karelinii* overturn can be further tested once a detailed time series of Holocene climate reconstructions has become available.

Reinforcement of asymmetric mitochondrial DNA transmission

The demographical inequality that accompanies geographical displacement is in itself sufficient to explain the presence of mitochondrial DNA of the originally common in the initially rare species (160). However, the asymmetry could be strengthened by factors favoring the relative frequency (prezygotic factors) or viability (postzygotic factors) of one hybrid class over the other (159, 160, 213).

Examples of pre- and postzygotic selection are known in nature: in the tree frogs *Hyla cinerea* and *H. gratiosa*, differences in behavior (courting at the edge versus inside the breeding pond and presence versus absence of satellite mating behavior) cause *H. cinerea* males to more often intercept *H. gratiosa* females than vice versa, resulting in biased mitochondrial DNA transmission (222). The uneven viability of hybrids between the crested newt *T. cristatus* and the marbled newt *T. marmoratus* causes the frequency of *T. marmoratus*-mothered hybrids to drop from fifty percent in embryo's to ten percent in adults, resulting from an incompatibility between the *T. cristatus* X chromosome and *T. marmoratus* cytoplasm (205).

A higher frequency or reproductive success of *T. karelinii*-mothered hybrids over *T. macedonicus*-mothered hybrids would have acted like a filter, hampering the spread of *T. macedonicus* mitochondrial DNA into the introgression zone. Perhaps, *T. macedonicus* males were more likely to mate with *T. karelinii* females than the reverse when *T. macedonicus* invaded the *T. karelinii* range (e.g. due to male-biased dispersal or biased disassortative mating). Furthermore, hybrids mothered by *T. macedonicus* might experience stronger negative selection than those mothered by *T. karelinii*. Research into the presence of such asymmetries in *T. macedonicus* – *T. karelinii* hybridization is a prospect for future research.

What about positive selection?

Asymmetric mitochondrial DNA introgression due to the positive selection of ‘foreign’ mitochondrial DNA (17, 215, 223) would have experienced a distinctly different geographical spread than when it was caused by species displacement: instead of the contact zone between two species moving across their mitochondrial DNA boundary, which is the case with geographical displacement (cf. Fig. 1b), positive selection would result in mitochondrial DNA of one species being ‘pulled’ into the range of the other. A selective sweep, where ‘foreign’ mitochondrial DNA replaces the original mitochondrial DNA, has been demonstrated experimentally in *Drosophila* flies (224).

Positive selection has also been suggested to cause asymmetric mitochondrial DNA introgression in nature (225, 226). However, when encountering asymmetric mitochondrial DNA introgression, it might be difficult to choose between the two scenarios. For example, in *Lissotriton newts*, the original mitochondrial DNA of *L. montandoni* has been fully replaced by that of *L. vulgaris* (80). However, this exchange of mitochondrial DNA did not have a single origin but involved multiple, independent introgression events of well differentiated *L. vulgaris* mitochondrial DNA. Does this pattern reflect repeated geographical replacement during multiple interglacials, when the more mountainous *L. montandoni* shifted its range to a lower elevation or several uptakes of ‘foreign’ mitochondrial DNA that subsequently spread in *L. montandoni*?

Why do we in the present case favor the geographical displacement scenario over the positive selection scenario? ‘Foreign’ *T. karelinii* mitochondrial DNA is only present in *T. macedonicus* in postglacially colonized area, but in the case of positive selection causing the asymmetric mitochondrial DNA introgression, it should have been able, but did not, to also penetrate into the region that acted as a glacial refugium for *T. macedonicus*.

Furthermore, the bisecting of the *T. karelinii* range by *T. macedonicus* (plus *T. macedonicus* having spread *T. karelinii* mitochondrial DNA into a region where we infer *T. karelinii* was never present) provides positive evidence in favor of *T. macedonicus* expanding its range at the expense of *T. karelinii*.

Conclusion

Given the extraordinary spatial setting, the *T. macedonicus* – *T. karelinii* case provides a unique insight into asymmetric mitochondrial DNA introgression. The system shows an introgression zone varying in width, from narrow in the south to broad in the north. Furthermore, the fact that *T. macedonicus* bisects the range of *T. karelinii* provides a clear indication of directionality: *T. macedonicus* likely invaded *T. karelinii* territory, not the other way around. Future approaches employing genomic data will focus on the shape of clines for individual nuclear DNA markers across the contact zone and in particular the variation among them. In the current paper, based on a combination of phylogeography and ecological niche modeling, we suggest that the asymmetric introgression of mitochondrial DNA from *T. karelinii* into *T. macedonicus* is due to postglacial species displacement (see the summarized scenario in Fig. 7). As these crested newt species expanded their ranges in response to climate change after the conclusion of the Last Glacial Maximum, they came into spatial contact. Subsequently, the newly established hybrid zone between the two moved across the landscape, as *T. macedonicus* outcompeted *T. karelinii*. However, the former distribution of *T. karelinii*, before *T. macedonicus* started to invade its range, could be recovered thanks to the asymmetrically introgressed *T. karelinii* mitochondrial DNA. In conclusion, a mismatch between mitochondrial DNA and morphology is not necessarily a nuisance but can provide key insights into historical biogeography.

Methods

Distribution and genetic data

We gathered 139 *T. macedonicus* and 135 *T. karelinii* localities (Fig. 2 and Additional file 1). Species identity was primarily based on morphological characters (throat pattern and body build); for a subset (conveniently arranged along transects across the contact zone) diagnostic allozyme markers have been published (112, 132, 190). Note that at five localities the species are found in syntopy. We obtained a 658 bp segment of ND4 for 600 newts (70 previously published in, and 530 newly sequenced following the protocol of (65)) from 71 of the *T. macedonicus* and 86 of the *T. karelinii* populations (Fig. 2 and Additional file 1).

Among them, the sequenced individuals contained 83 haplotypes (Additional file 5). We delimited the zone of asymmetrically introgressed mitochondrial DNA by Thiessen polygons (as in 202).

Genetic analyses

Phylogenetic trees were constructed with MrBayes 3.1.2 (98), employing two, four chain, twenty million generation runs, with a sampling frequency of 0.001 and a heating parameter of 0.1. MrModeltest (94) identified GTR+I, HKY+I+G and HKY+G as the most suitable models of sequence evolution for codon positions 1, 2 and 3. Rate and parameters for these data partitions were unlinked. The first quarter of the sampled trees was discarded as burn-in after analysis of the output in Tracer 1.5 (99). Minimum spanning haplotype networks were created with HapStar 0.5 (227), based on distance matrices produced with Arlequin 3.5 (174). DnaSP5 (228) was used to determine the nucleotide diversity (π) within and the average number of nucleotide substitutions (D_{xy}) between groups of haplotypes. To test for signals of demographic expansion, we compared the observed mismatch distribution with that expected under population expansion (229). We interpreted the differences based on the Ramos-Onsins and Rozas' R_2 and Fu's F_s statistics (230), for which statistical significance was obtained based on 1,000 coalescent simulations in DNAsp.

Environmental data

For climate layers we used bioclimatic variables at 2.5 arcminute resolution, available from WorldClim 1.4 (134). To obtain realistic and transferable models, it is recommended to mirror the physiological limitations of the study species and minimize the effects of multicollinearity among data layers (177). Therefore we included a subset of bioclimatic values encompassing seasonal variation in temperature and rainfall and showing a Pearson correlation < 0.7 : bio10 = mean temperature of warmest quarter, bio11 = mean temperature of coldest quarter, bio15 = precipitation seasonality, bio16 = precipitation of wettest quarter, and bio17 = precipitation of driest quarter. Bioclimatic variables are also available from WorldClim for the Last Glacial Maximum, being derived from the Paleoclimate Modelling Intercomparison Project phase 2 (178; <http://pmip2.lsce.ipsl.fr/>), based on simulations using the Model for Interdisciplinary Research on Climate version 3.2 (MIROC) (231) and the Community Climate System Model version 3 (CCSM) (179).

Ecological niche modeling

Ecological niche models were created using Maxent 3.3.3e (180). We restricted the feature type to hinge features as this produces smoother model fits, so forcing models to be more focused on key trends rather than potential idiosyncrasy in the data, which would hamper extrapolation to a different time or place (181). An important consideration is the environmental range covered by the pseudo-absence data used to discriminate presence data from background (137, 182, 183). Too narrow a range results in too complex models that do not generalize well, whereas too broad a range results in too simple models that focus on coarse-scale and neglect fine-scale variation. A practical solution is to focus on area that is potentially accessible to the species of interest as its spread would not be hampered by major physical barriers, meaning that it would be abiotic features that determine its distribution inside the area (184). However, competition could lead to further exclusion of the target species, even though the area would be suited in the absence of such biotic interactions (184). Considering these issues, we restricted the area from which pseudo-absence was drawn to the distribution of the entire crested newt *T. cristatus* superspecies. This area was broadly defined as a 200 km buffer zone (cf. 137) around known crested newt localities (Additional file 1 and 6). The ecological niche models were tested for statistical significance against a null model, to test whether they perform better than expected by random chance (185). Models were projected on the current and Last Glacial Maximum climate layers. We explored variable importance and response curves and conducted a jackknife test to determine how ecological niche models of the two species differed.

Acknowledgements

W. Beukema, A.K. Skidmore and A.G. Toxopeus provided comments on an earlier version of this paper. J. van Alphen, W. Babik, W. Beukema, S. Bogaerts, S. Branković, Henrik Bringsøe, D. Canestrelli, D. Cogălniceanu, J. Crnobrnja-Isailović, A. Crottini, G. Džukić, Ö. Güclü, I. Haxhiu, M. Kalezić, H.G. Kami, S. Litvinchuk, A. Maletzky, Đ. Milošević, N. Moin, O. Mozaffari, P. Mikulíček, B. Naumov, K. Olgun, N.A. Poyarkov, B. Safaei, J.F. Schmidtler, K. Sotiropoulos, N. Tzankov, A. Urošević, N. Üzüm, J. Vörös, B. Vrenosi, and T. Vukov aided with the collection of samples and locality data. The PMIP 2 Data Archive is supported by CEA, CNRS and the Programme National d'Etude de la Dynamique du Climat (PNEDC). We acknowledge the international modeling groups for providing their data for analysis and the Laboratoire des Sciences du Climat et de l'Environnement (LSCE) for collecting and archiving the model data.

Supplementary data

The supplementary data associated with this chapter can be found at <http://science.naturalis.nl/media/333569/ch5suppdata.zip>.

- Additional file 1: Sampling. *Triturus karelinii* and *T. macedonicus* localities included in the genetic analysis (a subset) and in ecological niche modelling (all).
- Additional file 2: *Triturus macedonicus* mitochondrial DNA structuring. A phylogenetic tree and haplotype network for *T. macedonicus*.
- Additional file 3: Ecological niche modeling performance. The ecological niche models for *T. macedonicus* and *T. karelinii* tested against a null model.
- Additional file 4: Contribution of bioclimatic variables to the ecological niche models. Response curves, contribution and permutation importance and results of a jackknife test for the bioclimatic variables.
- Additional file 5: list of mitochondrial DNA haplotypes. For each mitochondrial DNA haplotype, its GenBank accession number and its frequency of occurrence in both *T. macedonicus* and *T. karelinii* is provided.
- Additional file 6: Localities of additional crested newt species. Additional localities, used to determine the distribution of the entire crested newt *Triturus cristatus* superspecies

Chapter 6: A multimarker phylogeography of crested newts (*Triturus cristatus* superspecies) reveals cryptic species

This chapter is based on: Wielstra B, Baird AB, Arntzen JW (submitted) A multimarker phylogeography of crested newts (*Triturus cristatus* superspecies) reveals cryptic species

Abstract

Mitochondrial DNA represents just a single gene tree and, ideally, multiple nuclear DNA markers should be included in phylogeographical studies to distill the true evolutionary history. The crested newt *Triturus cristatus* superspecies is composed of five recognized species. One of these, *T. karelinii* sensu lato, comprises three geographically structured mitochondrial DNA lineages. Genetic divergence among these lineages is comparable to that among recognized crested newt species, but morphologically they are as yet indistinguishable. We conduct a multimarker phylogeography to explore the evolutionary independence of these mitochondrial DNA lineages and include representatives of the other species to guide our interpretation of the results. All markers show distinct patterns when analyzed singly (as a phylogeny or haplotype network) and none of them sort haplotypes according to species or mitochondrial DNA lineage. A multimarker approach (BAPS and *BEAST) on the other hand shows that not only the recognized species, but also the three mitochondrial DNA lineages represent discrete nuclear DNA gene pools. The only mismatch is found in the extreme northwest of Asiatic Turkey, where several populations identified as 'central *T. karelinii*' based on nuclear DNA possesses 'western *T. karelinii*' mitochondrial DNA. We invoke asymmetric mitochondrial DNA introgression to explain this pattern and support this with a historical biogeographical scenario. We suggest the three spatial groups in *T. karelinii* sensu lato should be regarded as distinct species.

Introduction

A single gene tree does not necessarily represent the true phylogenetic relationships among or within species (71). Phenomena like ancestral polymorphism and introgression cloud the evolutionary picture (77). To distil the true evolutionary history, multiple gene trees should be employed (71). The mitochondrial genome shows a linked inheritance and in effect behaves as a single gene tree. On the other hand, the nuclear genome, due to its recombining nature, represents a reticulation of evolutionary lineages. Despite this theoretical advantage of nuclear DNA, mitochondrial DNA is still the most regularly employed genetic marker in practice (232-234).

The crested newt (*Triturus cristatus*) superspecies comprises five parapatric species (Fig. 1). In a previous phylogeographical survey of the species traditionally referred to as '*T. karelinii*' (hereafter *T. karelinii* sensu lato), we uncovered three geographically structured mitochondrial DNA lineages. In terms of mitochondrial DNA divergence, these three lineages are as distinct from each other as recognized (non-*T. karelinii*) crested newt species are (65).

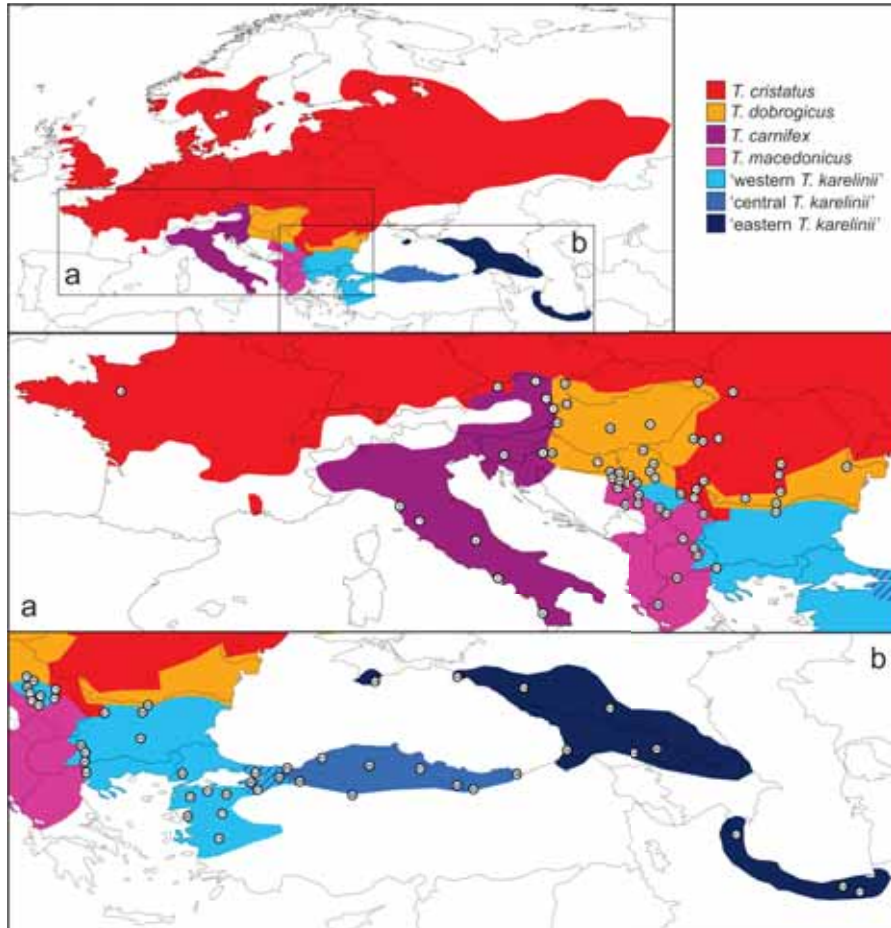


Figure 1 Distribution map of the crested newts. The inset shows the distribution of the recognized crested newt species and of the 'eastern,' 'central' and 'western *T. karelinii*' mitochondrial DNA lineages. Cut-out a shows the sampling for the recognized species and cut-out b for *T. karelinii* sensu lato. The hatched area in the cut-outs shows a region where 'central *T. karelinii*' newts as identified based on nuclear DNA contain 'western *T. karelinii*' mitochondrial DNA. Population numbers correspond to Appendix S1. This map is based on Wielstra and Arntzen (131).

The recognized crested newt species are known to differ based on morphological features and a battery of allozymes markers (132). On the other hand, range wide allozyme data is not available for *T. karelinii* sensu lato (112) and analysis of morphological features known to discriminate the recognized species did not reveal unequivocal differences among the three mitochondrial DNA lineages (63, 133). However, in terms of niche differentiation the three lineages are as distinct as recognized species (235).

We explore whether the three mitochondrial DNA lineages comprising *T. karelinii* sensu lato represent independent evolutionary trajectories. To this aim, we analyze three nuclear DNA markers, using both single and multi-locus analytical approaches. Throughout the present paper we refer to the three *T. karelinii* sensu lato candidate species as 'eastern,' 'central' and 'western *T. karelinii*' and acknowledge that their true distribution (and distinction) based on the nuclear genome might be different than suggested by mitochondrial DNA. To guide our interpretation, we compare the situation in *T. karelinii* sensu lato with that shown by the recognized crested newt species.

Methods

Sampling strategy, laboratory methods and data preparation

We included 302 crested newts from 106 populations (Fig. 1, Appendix S1). Our dataset includes a dense geographical sampling for the representatives of the three mitochondrial DNA lineages constituting *T. karelinii* sensu lato as well as for all the recognized non-*T. karelinii* crested newt species. For each crested newt species and lineage we sampled in the core of the range and near the contact zones with other species or lineages. We also added several newts from the type locality of '*T. karelinii arntzeni*' (locality 59 in Fig. 1) to our dataset to address the concern raised in Arntzen and Wielstra (112) that these newts may in fact represent *T. macedonicus*.

We obtained sequence data for three nuclear introns: β -Fibrinogen intron 7 (*β fibint7*), Calreticulin intron C (*CalintC*), Platelet-derived growth factor receptor α (*Pdgfra*). Furthermore, we include one mitochondrial protein coding gene: subunit 4 of the NADH dehydrogenase gene complex (ND4). Part of the data has been published before: all ND4 in (65, 132, 172, 216) and *β fibint7* and *CalintC* for the recognized crested newt species in (236). In order to make our dataset complete, all three nuclear markers were sequenced for the samples from Wielstra et al. (65) and *Pdgfra* sequences were obtained for the samples from (236). See Espregueira Themudo et al. (70) and Wielstra et al. (65) for details on laboratory methods.

For the nuclear markers, individuals possess two alleles, which may or may not be identical. We managed to retrieve the two alleles for each individual from direct sequencing products. If alleles were identical or differed only by one substitution, retrieving them was straightforward. For diploid individuals containing alleles of different length, these could be retrieved following the method outlined in Flot et al. (237). For alleles of identical length but differing at more than one base pair, allele specific walking primers were developed (cf. 238). Sequences were manually aligned and identical ones merged into haplotypes using MacClade 4.08 (92). For GenBank accession number, see Appendix S2.

Data analyses

Four indels in *CalintC* that could not be unambiguously aligned were excluded from the analysis, the remaining indels were included. We analyzed the data using single and multi-locus analytical approaches. Firstly, for each of the four markers we conducted a Neighbor Joining analysis with 1000 bootstrap replications in MEGA 5.05 (173). We included the marbled newt *T. marmoratus* to function as an outgroup (see Appendix S1 for sampling details). Furthermore, for each nuclear marker, a minimum spanning haplotype network was created with HapStar 0.5 (227), based on distance matrices produced with Arlequin 3.5 (174).

Secondly, we used a Bayesian analysis of population structure with the program BAPS v.5.3 (239). BAPS assigns individuals to distinct gene pools probabilistically, based upon multilocus genetic data, where each individual allele is coded as a haplotype (two alleles per marker, which may or may not belong to the same haplotype). BAPS does not make a priori assumptions about the number of gene pools (k) but a fixed number can be set. We used BAPS in two ways. First we enforced BAPS to partition the individuals in seven groups ($k = 7$), as we are dealing with four recognized species and three candidate species. Then we let BAPS determine the most probable number of distinct gene pools, evaluating k over a $2 \leq k \leq 106$ range.

Thirdly, we conducted Bayesian inference of the species tree using *BEAST (240), a multi-species coalescent model available in BEAST 1.7 (241). We conducted two 500 million generation runs in *BEAST, applied a sampling frequency of 0.0001 and discarded the first half of generations as burn-in. We determined the most appropriate model of sequence evolution based on the Akaike Information Criterion with MrModeltest 2.2 (94) for each marker: GTR+G for *βfibint7* and *Pdgfra* and HKY+G for *CalintC*. We applied a Yule process species tree prior, a piecewise linear and constant root population size model, a strict molecular clock and a random starting tree.

Tracer 1.5 (99) was used to make sure that runs had converged and effective samples sizes were at least 200. *BEAST requires individual sequences to be appointed to operational taxonomical units *a priori*. However, when testing for the presence of candidate species, such classification is not straight forward (and in the present case should be independent from the mitochondrial DNA signal). To deal with this limitation, we used the BAPS groups identified under a search for the optimal k as operational taxonomical units in *BEAST. Thus, for each marker, we partitioned haplotypes according to BAPS group and the same haplotype could be present in more than one BAPS group.

Results

For the distribution of haplotypes among the included individuals, see Appendix S1 and S2. The mitochondrial DNA sorts into seven distinct lineages, corresponding to the four recognized species and the three mitochondrial DNA lineages comprising *T. karelinii* sensu lato (Fig. 2). Mismatches between phenology and mitochondrial DNA type in the recognized species are generally restricted to the contact zones (see Appendix S1), though *T. macedonicus* contains 'western *T. karelinii*' mitochondrial DNA over a more extensive area. The phylogenies and haplotype networks of the different genetic markers show contrasting patterns (Figs. 3). Species and mitochondrial DNA lineages do not sort in reciprocally monophyletic groups and haplotypes are shared among them.

With BAPS enforcing seven groups, 13 out of 134 non-*T. karelinii* crested newts do not cluster according to the species they were appointed based on phenotype (Appendix S1). Six instances where BAPS appoints individuals to a different species concerns individuals from at the contact zone (Appendix S1). Furthermore, the seven *T. carnifex* individuals from outside Italy (from the Balkans and Austria) are clustered with *T. cristatus*. The five individuals from the type locality of '*T. karelinii arntzenii*' are grouped with *T. macedonicus*. The *T. karelinii* sensu lato individuals generally group according to mitochondrial DNA lineage, but four populations (locality 84-87 in the hatched area in Fig. 1), despite containing 'western *T. karelinii*' mitochondrial DNA (haplotypes in bold in Fig. 2), cluster with 'central *T. karelinii*' based on nuclear DNA. There is one exception: one individual from locality 85 is placed in 'western *T. karelinii*' (but see below). Two 'western *T. karelinii*' newts from the contact zone are classified as *T. macedonicus* by BAPS.

With BAPS allowing the optimal value of k , 41 genetic clusters are resolved, generally corresponding to the species they were appointed or, in the case of *T. karelinii* sensu lato, to 'eastern,' 'central' and 'western *T. karelinii*' as delimited by BAPS with $k = 7$.

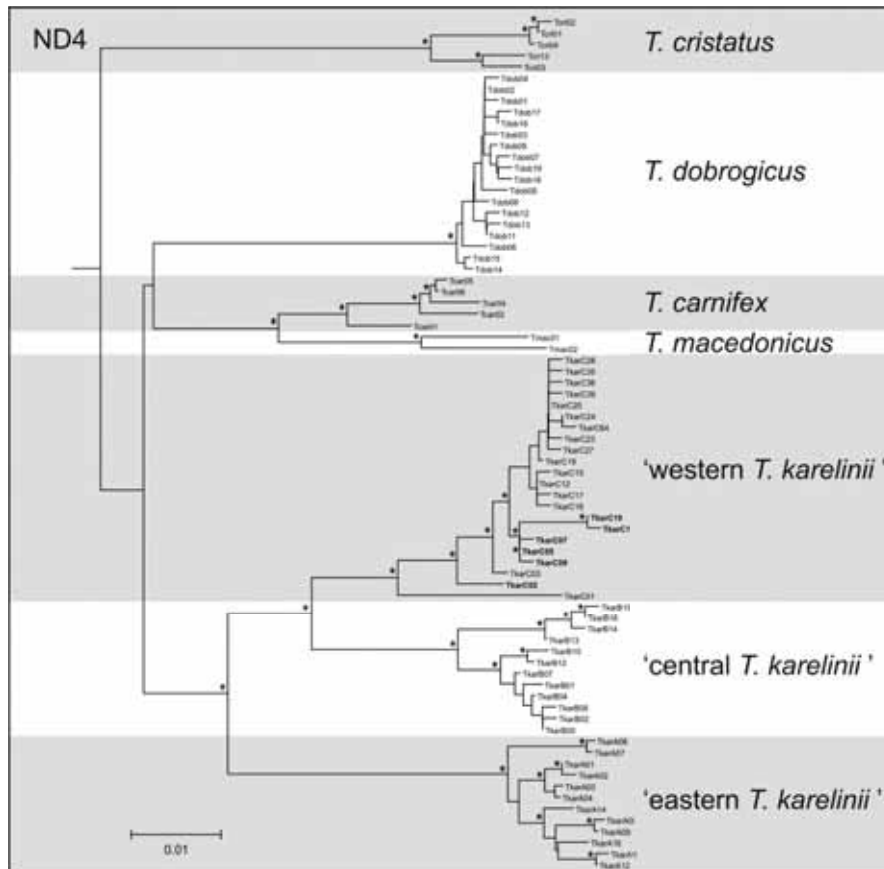


Fig. 2. Neighbor joining tree for the ND4 haplotypes. Branches supported with a bootstrap over 70 are marked with an asterisk. The *T. marmoratus* outgroup is not shown. Haplotype codes correspond to Appendix S1 and S2. 'Western *T. karelinii*' mitochondrial DNA haplotypes found in 'central *T. karelinii*' as delineated by nuclear DNA are shown in bold.

Two BAPS groups belong to *T. carnifex*, six to *T. cristatus*, nine to *T. dobrogicus*, five to *T. macedonicus*, six to 'western *T. karelinii*', eight to 'central *T. karelinii*' and five to 'eastern *T. karelinii*' (Appendix S1). The eight individuals from the contact zone that were clustered with a different species than their phenotype would suggest when using $k = 7$ are also found with $k = 41$. The seven *T. carnifex* that clustered with *T. cristatus* with $k = 7$ are now placed in a separate group, together with a single *T. cristatus* individual from the contact zone with *T. carnifex*. The individual from western Asiatic Turkey clustering with 'western *T. karelinii*' with $k = 7$ is appointed to a 'central *T. karelinii*' cluster with $k = 41$.

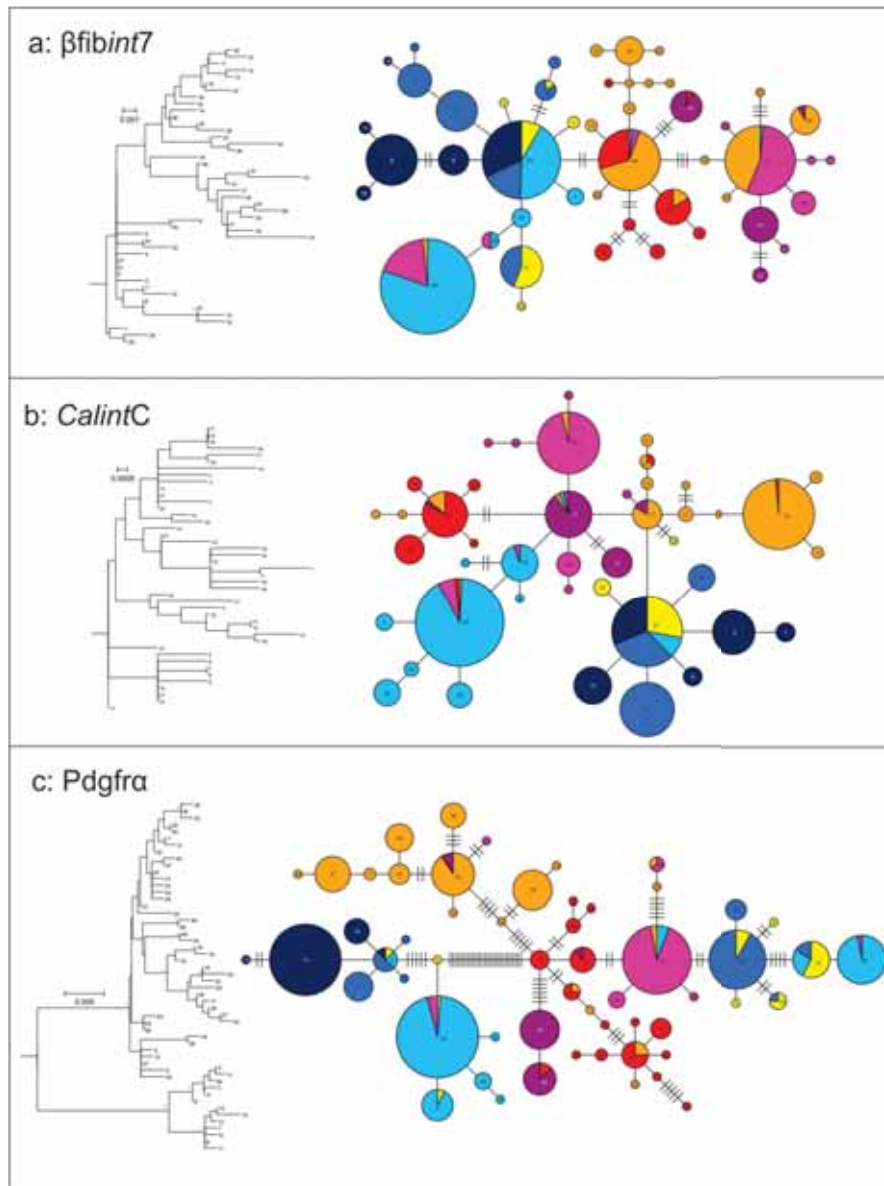


Figure 3 Neighbour joining trees and haplotype networks for each of the three nuclear markers. For the networks, the frequency is expressed by the diameter of the circles (see Appendix S2 for details). Colors (corresponding to Fig. 1) reflect the species in which each haplotype is found or, in the case of *T. karelinii* sensu lato, which mitochondrial DNA lineage they possess. Newts identified as 'central *T. karelinii*' based on nuclear DNA but containing 'western *T. karelinii*' mitochondrial DNA are colored yellow. Haplotype codes correspond to Appendix S1 and S2.

The species tree obtained with *BEAST is shown in Fig. 4. Monophyly of most (candidate) species is suggested, but support is not that high: pp. = 0.78 for *T. cristatus*, pp. = 0.97 for *T. dobrogicus*, pp. = 0.89 for 'central *T. karelinii*', and pp. = 0.93 for 'eastern *T. karelinii*'. Italian *T. carnifex* comprises only a single BAPS group (i.e. pp. is not applicable); the BAPS group comprising the *T. carnifex* individuals from outside of Italy is nested within *T. cristatus* (as already alluded to by BAPS itself when enforcing $k = 7$). Another peculiar result is the placement of *T. macedonicus*: most of the individuals are nested with 'western *T. karelinii*' in a relatively highly supported clade (pp. = 0.91). The remaining *T. macedonicus* BAPS group is nested in *T. dobrogicus* (this group, containing two *T. macedonicus* newts also contains one *T. dobrogicus* individual and occurs at the contact zone with that species).

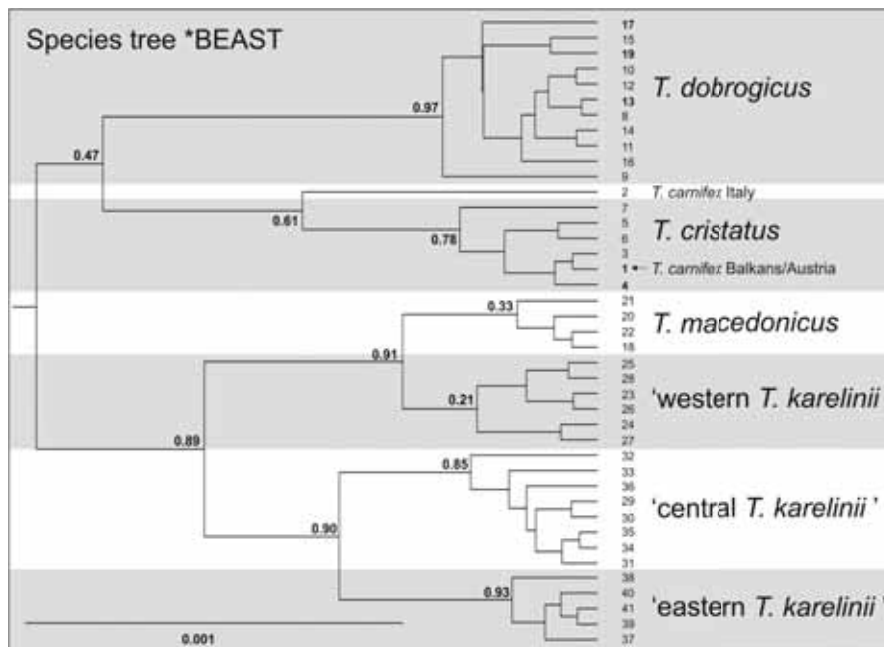


Figure 4 Species tree resulting from the *BEAST multi-species coalescent analysis based on the three nuclear DNA markers. Only posterior probabilities for (candidate) species and the relationships among them are shown; posterior probabilities within (candidate) species are $\ll 0.50$. Note that *BEAST does not require an outgroup. The numbers at the tips refer to BAPS groups and correspond to Appendix S1; bold numbers reflect BAPS groups that contain newts belonging to more than one species (see text).

There is no support for phylogenetic structure within the (candidate) species according to *BEAST. This also applies to the placement of *T. macedonicus* within 'western *T. karelinii*'; although the two are placed in two reciprocally monophyletic clades, support for each clade is low. Furthermore, there is no support for phylogenetic relationships among the recognized crested newt species. On the other hand, *T. karelinii* sensu lato shows support for phylogenetic structure among the three candidate species: 'eastern' and 'central *T. karelinii*' are each other's closest relatives (pp. = 0.90) and this clade is sister (pp. = 0.90) to 'western *T. karelinii*' (which, as noted above, includes the majority of *T. macedonicus* individuals).

Discussion

A single locus analysis reveals reticulated evolution

The different genetic markers show distinct patterns. Whereas the mitochondrial gene tree shows geographically distinct clades, this is not the case for the nuclear gene trees (Fig. 2 and 3). All three nuclear gene trees differ from each other and none of them shows reciprocally monophyletic groups corresponding to units identifiable based on other data such as morphology, mitochondrial DNA or allozymes (cf. 132). The complexity of the situation becomes clearer when the data is analyzed as haplotype networks (Fig. 3). On the one hand, haplotypes are often shared among several species and on the other haplotypes found in the same species are scattered throughout the network. It should be stressed that this does not only concern the three mitochondrial DNA lineages within *T. karelinii*, but also the four recognized crested newt species.

Our results show the importance to include the recognized species when assessing evolutionary independence of the three *T. karelinii* sensu lato candidate species. If we had not put the pattern shown in *T. karelinii* sensu lato into the context of the situation shown by the recognized species, we might have wrongly interpreted allele sharing and non-monophyly as evidence for the lack of a barrier to gene flow. Two phenomena can explain the confusing pattern shown by the individual markers. The sharing of alleles can partially be explained by ancestral polymorphism, retained from before the time that the different species split. However, the low frequency presence of haplotypes in one species, typically restricted to the contact zone with a neighboring species in which this haplotype is more abundant, suggests horizontal gene flow due to hybridization also occurred during crested newt evolution. To further unravel such a reticulated evolutionary pattern requires a multi-locus approach.

Classification based on multi-locus data sorts out crested newt (candidate) species

BAPS brings order to the chaos. When we force BAPS to partition the individual crested newts into seven groups (considering we have four recognized and three candidate species), BAPS manages to appoint the majority of newts to the species or mitochondrial DNA lineage they were *a priori* appointed to (based on phenotypical characteristics or molecular data). When BAPS is allowed to choose the optimal number of gene pools, the identified clusters again can be neatly grouped in the seven (candidate) species. Most mismatches identified are to be expected: they occur close to the contact zone with other species and can be explained by gene flow due to hybridization (cf. 132).

There is one peculiar finding: the *T. carnifex* populations outside of Italy, from the northern Balkan Peninsula and east of the Alps, are clustered with *T. cristatus*. Allozyme and morphological data shows that these newts definitely belong to *T. carnifex* (67, 132). When BAPS is allowed to determine the optimal number of gene pools, these newts are clustered in a unique group. However, the inclusion of one *T. cristatus* individual from the contact zone in this group and its placement in the species tree (see below) would suggest genetic influence of *T. cristatus* during the evolutionary history of this *T. carnifex* stock. A genome scale analysis is required to further explore this phenomenon.

In contrast to the nuclear phylogenetic trees and haplotype networks, BAPS supports the presence of three distinct gene pools in *T. karelinii* sensu lato. These groups almost fully correspond to the geographical pattern suggested by mitochondrial DNA. The only exception is that 'central *T. karelinii*' contains 'western *T. karelinii*' mitochondrial DNA in the westernmost part of its range (Fig. 1). This can be explained by mitochondrial DNA introgression: a phenomenon regularly observed in crested newts (132, 172). Newts from the type locality of '*T. karelinii arntzen*' do not belong to *T. karelinii* sensu lato but are grouped with *T. macedonicus*.

A species tree for Triturus based on multi-locus data

Our approach to treat BAPS groups as operational taxonomical units circumvents the arbitrariness in the *a priori* defining of 'species' required by *BEAST. The different BAPS groups generally cluster in (candidate) species as expected in the species tree produced by *BEAST. Support for the monophyly of each is suggestive, but in most cases not statistically significant.

It should be stressed that the recognized crested newt species are supported as discrete nuclear gene pools by allozyme data and we thus do not doubt their status as distinct species (132, whose sampling of individuals from recognized crested newt species largely overlaps with the current paper). Support for the monophyly of the three candidate species is relatively high compared with the recognized species.

To a certain extent low support might reflect a lack of resolution in the data, but we suspect gene flow due to hybridization (cf. section 4.1.) mainly influences our results. *BEAST assumes that there is no horizontal gene flow between 'species' (240). However, this assumption is likely to be violated for recently radiated species. Note that such groups would also be the ones that particularly benefit from the application of a multi-species coalescent approach as they are more likely to show ancestral polymorphism. The current inability to deal with gene flow is thus a considerable limitation and an important issue to be resolved in future development of multispecies coalescent models. As we have no objective way to correct for gene flow after speciation events, we have to take its adverse effects for granted here. BAPS groups containing combination of alleles derived from different species can be expected to be difficult to place in a species tree.

The peculiar situation involving the placement of *T. macedonicus* suggests that the geographical reach of horizontal gene flow can be extensive. Based on allozyme data it is clear that *T. macedonicus* and 'western *T. karelinii*' behave as distinct species (132). Similarly, BAPS manages to pull *T. macedonicus* and 'western *T. karelinii*' apart. However, *T. macedonicus* clusters together with 'western *T. karelinii*' in the species tree. It has been hypothesized that *T. macedonicus* has displaced 'western *T. karelinii*' over a large part of its former range (172). This process co-occurred with introgressive hybridization, reflected by the presence of 'western *T. karelinii*' mitochondrial DNA in *T. macedonicus*. We suggest the clustering of *T. macedonicus* with 'western *T. karelinii*' likely reflects asymmetric introgression of nuclear DNA into *T. macedonicus* as it displaced 'western *T. karelinii*' (cf. 160). To further explore this intriguing phenomenon, we recommend a denser sampling for *T. macedonicus* and 'western *T. karelinii*', in terms of both the number of populations and of nuclear DNA markers. Contrastingly, clustering with 'western *T. karelinii*' is not shown by the 'central *T. karelinii*' that contain asymmetrically introgressed 'western' mitochondrial DNA.

The *BEAST species tree constructed here does not provide insight into the phylogenetic relationships among the recognized crested newt species. It does so for the three candidate species comprising *T. karelinii* sensu lato. However, the suggested phylogeny differs from the one based on mitochondrial DNA (Fig. 2; cf. 65, 131).

Whereas mitochondrial DNA suggests 'central' and 'western *T. karelinii*' are more closely related to each other than each of them is to 'eastern *T. karelinii*', the *BEAST species tree clusters 'central' together with 'eastern *T. karelinii*' and suggests 'western *T. karelinii*' as their sister. Considering that low phylogenetic signal and gene flow hamper our estimation of the *Triturus* species tree here, we for now prefer the phylogenetic hypothesis for *Triturus* based on mitochondrial DNA. We recommend an approach using many more (i.e. 50-100) nuclear DNA markers to further explore the crested newt phylogeny and to explore clinal transition of individual markers across hybrid zones, especially for the 'western *T. karelinii* – *T. macedonicus* case.

*BEAST is typically applied to recognized species, known to be closely related (240). The program has up to now been only sparsely applied in a phylogeographical setting, densely sampling taxa potentially containing multiple species (242, 243; this study). *BEAST appears to perform reasonably well for the identification of distinct gene pools in multi-locus datasets and in this respect the program is a welcome addition to the phylogeographer's toolkit.

*The current (lack of) genetic interaction between *T. karelinii* clades*

'Eastern' and 'central *T. karelinii*' show no signs of recent genetic admixture. This is in line with their apparent current allopatry (cf. Fig. 1; 65). Historical records have been found on the Turkish side of the border with Georgia but could not be confirmed during recent fieldwork (reviewed in 65). We suspect these historical records concern 'eastern *T. karelinii*', considering the geographical proximity to known 'eastern *T. karelinii* localities' (locality 98 in Fig. 1); the distance to the nearest known 'central *T. karelinii* locality' (locality 96 in Fig. 1) is considerably larger. When newts on the Turkish sides of the border are re-discovered, their identity can easily be determined using the dataset and procedure presented in this paper.

'Western' and 'central *T. karelinii*' are parapatric (cf. Fig. 1). An earlier attempt to locate the contact zone between 'western' and 'central *T. karelinii*' (112) similarly found that 'central *T. karelinii*' was distributed more westerly than would be expected based on mitochondrial DNA. However, a more convoluted shape for the contact zone was suggested, with individuals identified as 'western *T. karelinii*' present close to our locality 91 (Fig. 1). However, the study by Arntzen and Wielstra (112) suffered from a very limited sampling of 'central *T. karelinii*' (and 'eastern *T. karelinii*' was not included at all). Therefore, we put more confidence in the present findings.

However, we do suggest a detailed hybrid zone analysis to be conducted, using a denser sampling in terms of more populations, more individuals per population and more nuclear DNA markers, to more thoroughly explore how sharp the transition between 'central' and 'western *T. karelinii*' is.

Different newts, comparative phylogeographical pattern

There is a striking similarity between the 'central *T. karelinii*' – 'western *T. karelinii*' and the *Lissotriton kosswigi* – *L. vulgaris* contact zones (244). Not only is the contact zone between the two pairs of newts positioned in the same region, but *L. kosswigi* also possesses *L. vulgaris* mitochondrial DNA in the same area where 'central *T. karelinii*' contains 'western *T. karelinii*' mitochondrial DNA. Furthermore, the temporal estimation of the split between both species pairs is similar (65, around 5.5 Ma; 244). We propose the following shared historical biogeographical scenario underlying the pattern shown by the two pairs of newts.

The reconnecting of the Black Sea with the Aegean Sea at the conclusion of the Messinian Salinity Crisis, around 5.33 Ma (117), caused the initial split between both pairs of newts. The route of this marine connection was re-ordered extensively on several occasions due to tectonic developments. Although the exact intermediate stages are not yet fully understood, the initial route across the Balkans (245) shifted and by the start of the Pleistocene (2.6Ma) incorporated the Marmara Sea (121). Until the beginning of the Holocene (11.7 Ka), a sea straight known as the İzmit Gulf – Lake Sapanca – Sakarya Valley waterway connected the Black Sea with the Sea of Marmora (121). Although the re-ordering of the Aegean Sea - Black Sea connection may have facilitated periodic geographical contact between the two pairs of newts prior to the Pleistocene, no ancient introgression could be identified.

We suggest the İzmit Gulf – Lake Sapanca – Sakarya Valley waterway separated the geographical ranges of both pairs of newts (cf. Fig. 5). After this waterway closed, 'central *T. karelinii*' and *L. kosswigi* expanded their ranges westwards, at the expense of 'western *T. karelinii*' and *L. vulgaris*. This displacement coincided with hybridization and mitochondrial DNA introgressed in the process (cf. 160). Both 'western' and 'central' '*T. karelinii*' mitochondrial DNA are currently found in syntopy at locality 84 (Fig. 1, Appendix S1), where the waterway was positioned. We predict that a denser sampling in *L. kosswigi* along the route of the ancient waterway will also reveal syntopy of *L. kosswigi* and *L. vulgaris* mitochondrial DNA. With the formation of the Bosphorus in the Holocene (11.7Ka to present), an alternative connection between the Marmara and Black Seas arose (121, 127), which prevented 'central *T. karelinii*' and *L. kosswigi* to colonize Europe (cf. Fig. 5).

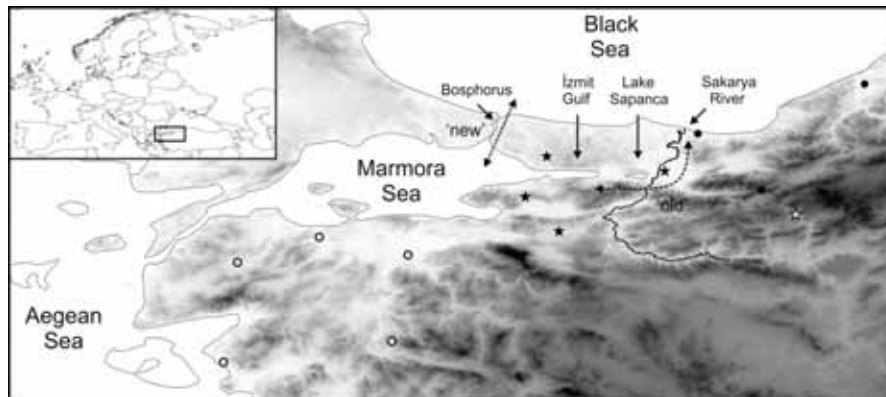


Figure 5 Map showing (paleo)geological features mentioned in the biogeographical scenario explaining the asymmetrical introgression of 'western *T. karelinii*' mitochondrial into 'central *T. karelinii*'. Closed circles reflect 'central *T. karelinii*' containing 'central' mitochondrial DNA and open circles 'western *T. karelinii*' containing 'western' mitochondrial DNA; closed stars reflect 'central *T. karelinii*' containing 'western' mitochondrial DNA and the white star a locality where both mitochondrial DNA types were found in syntopy in another study (216). Elevation is expressed as a continuous scale, running from light (low elevation) to dark (high elevation). Up to recently the Marmara Sea was connected to the Black Sea via an 'old' waterway, incorporating the İzmit Gulf, Lake Sapanca and the Sakarya Valley. At the beginning of the Holocene, a 'new' waterway, the Bosphorus, took over. With the former sea strait gone, 'central *T. karelinii*' expanded westwards, at the expense of 'western *T. karelinii*' and took up 'western' mitochondrial DNA in the process via introgressive hybridization (see text for details).

The İzmit Gulf – Lake Sapanca – Sakarya Valley waterway explains the observed pattern. The arid, high altitude Anatolian Plateau would further have acted as a barrier south of the waterway, contributing to the isolation of 'western' and 'central *T. karelinii*'. Wielstra et al. (216) found both 'western' and 'central *T. karelinii*' mitochondrial DNA in Seben, 30 km southeast of our locality 88 (noted in Fig. 5). This finding suggests that interaction between the two was possible via the upper reaches of the Sakarya River. Evidently, the extent of such interaction must have been limited. How 'central *T. karelinii*' and *L. kosswigi* managed to outcompete 'western *T. karelinii*' and *L. vulgaris* after the İzmit Gulf – Lake Sapanca – Sakarya Valley waterway closed and whether their current contact zones are in equilibrium or still moving are promising prospects for future research.

The outdated taxonomy of T. karelinii sensu lato

We have shown that the three mitochondrial DNA lineages we previously identified in *T. karelinii sensu lato* are also from a nuclear DNA perspective as distinct from each other as the recognized crested newt species are. Therefore we suggest the traditional '*T. karelinii*' should be treated as three distinct species. The type locality of '*T. karelinii*' is from Iran (close to locality 101 in Fig. 1) and *T. karelinii sensu stricto* should therefore be applied to 'eastern *T. karelinii*'. A different name needs to be applied to the two remaining species.

Although the name '*T. (karelinii) arntzeni*' has been applied to the 'western *T. karelinii*', our analysis shows that newts from the type locality are in fact *T. macedonicus*. This possibility was already alluded to by Arntzen and Wielstra (112) as the genome size is very different from *T. karelinii sensu lato* (including those from within the range of 'western *T. karelinii*') but completely overlaps with that of *T. macedonicus* (cf. 246). Furthermore, published pictures (247) of the throat and belly pattern of the holotype and paratypes of '*T. (karelinii) arntzeni*' and newts from the type locality observed by us in the field (pers. obs.) actually resemble *T. macedonicus* instead of *T. karelinii sensu lato*. We recommend that the name '*arntzeni*' is treated as a junior synonym of *T. macedonicus*. As a consequence, the name is not available for 'western *T. karelinii*'. For 'central *T. karelinii*', no name has been proposed yet. Both 'central' and 'western *T. karelinii*' are thus awaiting taxonomic treatment, which will be presented elsewhere.

Supplementary data

The supplementary data associated with this chapter can be found at <http://science.naturalis.nl/media/333572/ch6suppdata.zip>.

- Appendix S1: Details on sampling and the distribution of haplotypes across individuals.
- Appendix S2: GenBank accession numbers for haplotypes and the distribution of haplotypes across species and mitochondrial DNA lineages.

Synthesis

Background

Biogeography is the branch of Biology that seeks to understand the spatio-temporal distribution of biodiversity. With the advance of molecular approaches, a wealth of hitherto cryptic biodiversity has been revealed, hidden in organisms' genomes (10). Present day patterns of geographical genetic structuring are a derivative of past events and the field of phylogeography aims to untangle the complex history underlying intraspecific genetic structuring (12). The ecological niche of a species enfolds the suite of conditions under which it can maintain self-sustaining populations (5). In ecological niche modeling, the environmental requirements of a species are approximated, based on the range of climatic conditions experienced at known localities (30). By projecting the model on climate layers, the potential distribution of the species can be determined.

Both phylogeography and ecological niche modeling can provide insights into past distributions, independent of each other, and a tandem implementation is increasingly being promoted to improve historical biogeographical reconstructions (21, 22, 30). Although this joined approach it is still in the early stages, it has been successfully applied in biogeographical analyses: if both phylogeography and ecological niche modeling converge on the same result, confidence in a historical biogeographical hypothesis is strengthened (e.g. 57, 188). The aim of this thesis is to combine both techniques to increase the yield of biogeographical information from georeferenced genomes.

Findings

In this thesis, *Triturus* newts are used as a model system. We take a top down approach, first determining the relationships among species and subsequently the geographical structuring within species. We employ both genetic and ecological data to test species boundaries, to trace distribution back in time and to deduce past interspecific competition. This paragraph explains how the different chapters relate to each other and how the use of phylogeography and spatial ecology is interwoven.

The four morphotypes comprising the crested newt *T. cristatus* superspecies – the *T. karelinii* group, *T. carnifex* – *T. macedonicus*, *T. cristatus* and *T. dobrogicus* – differ in phenology: newts with sturdy bodies, reflected by a low number of rib-bearing pre-sacral vertebrae (NRBV), are associated with a relatively terrestrial way of life. Those with slender bodies, reflected by a high NRBV count, are associated with a more aquatic life style.

Given the explicit link with the phenetic and the phenological regime, it is of particular interest to understand the evolution of body build in crested newts. However, the tracing of character state changes has been hampered up to now by the lack of a resolved phylogeny. In [chapter 1](#) we, for the first time, manage to determine the phylogenetic relationships among the four morphotypes. To this aim we employ Bayesian phylogenetic inference of full mitogenomic sequences. The new phylogeny involves a maximally parsimonious interpretation of NRBV evolution: the more slender the morphotype, the later it was derived. The four morphotypes radiated in temporal proximity (determined with r8s and BEAST). As most splits cannot be aligned with geomorphological developments, we speculate that ecological differentiation in the form of adaptive shifts towards different water regimes (reflected by body shape differentiation) played a role during crested newt speciation.

The geographical genetic structuring of the three morphotypes confined to Europe has been relatively well studied. In contrast, the situation in the fourth morphotype, the Near Eastern *T. karelinii* group, is poorly understood. In [chapter 2](#) we conduct a dense mitochondrial phylogeographical survey, using both Bayesian and Maximum Likelihood inference. Based on temporal calibration of the phylogeographic framework (using both r8s and BEAST), we provide a paleogeographical scenario. The separation of the *T. karelinii* group from the remaining crested newts around is related to the separation of the Balkan and Anatolian landmasses. The *T. karelinii* group comprises three genetically distinct, geographically structured clades (eastern, central and western). We suggest the uplift of the Armenian Plateau to be responsible for the separation of the eastern clade, and the re-establishment of a marine connection between the Black Sea and the Mediterranean at the end of the Messinian Salinity Crisis to have caused the split between the central and western clade.

The three mitochondrial DNA lineages comprising the *T. karelinii* group are genetically as diverged as recognized crested newt species. In [chapter 3](#) we test whether these 'candidate species' are also ecologically differentiated. To interpret ecological divergence, we treat the ecological overlap among the recognized crested newts as a benchmark. To quantify niche differences among all crested newt (candidate) species and test hypotheses regarding niche evolution, we use a framework by Broennimann and colleagues written for R. We employ the two best performing techniques: principal component analysis calibrated on the entire environmental space of the study area and ecological niche factor analyses.

All (candidate) species occupy significantly different segments of environmental space. Niche overlap values for the three candidate species are not significantly higher than those for the recognized species. The three candidate crested newt species thus are, not only in terms of mitochondrial DNA genetic divergence, but also ecologically speaking, as diverged as the 'real' crested newt species. Our findings provide further support for the hypothesis that they represent true cryptic species.

The climatic oscillations during the Quaternary Ice Age heavily influenced the distribution of species and left their mark on intraspecific genetic diversity. In [chapter 4](#) we test the response of *Triturus* newts as the climate shifted from the previous glacial period (the Last Glacial Maximum, ~21Ka) to the current interglacial. We conduct a dense mitochondrial DNA phylogeography, visualizing genetic diversity within populations (based on nucleotide diversity determined with Arlequin) and divergence among populations (based on average sequence divergence determined with Alleles in Space). We produce species distribution models with Maxent using and project these on climate simulations for the Last Glacial Maximum. The two independent techniques provide insight in the glacial reduction and postglacial expansion of *Triturus*. For most species we manage to deduce the position of likely glacial refugia: areas which are predicted to have been suitable at the Last Glacial Maximum and which are genetically rich. A notable exception is provided by *T. dobrogicus*: both the mitochondrial DNA data and the species distribution models suggest this species has been severely bottlenecked. We also identify instances of a mismatch between species identity and mitochondrial DNA type, which we relate to shifting contact zones. We take a closer look to the most extreme situation in the next chapter.

If the geographical displacement of one species by another is accompanied by hybridization, mitochondrial DNA can introgress asymmetrically, from the outcompeted species into the invading species, over a large geographical extent. In [chapter 5](#) we trace a species overturn between two crested newt species. We first delimit a ca. 54,000 km² area in which *T. macedonicus* contains *T. karelinii* mitochondrial DNA. This introgression zone bisects the range of *T. karelinii*. Similarity of the introgressed mitochondrial DNA haplotypes suggests a recent transfer across the species boundary. We then use ecological niche modeling with Maxent to explore the suitability of the introgression zone under current and Last Glacial Maximum conditions. The introgression zone was inhospitable during the Last Glacial Maximum for both species, but has since that time become suitable. Together, these data support a scenario of postglacial outcompeting of *T. karelinii* by *T. macedonicus*.

The introgression zone was first colonized after the Last Glacial Maximum by *T. karelinii*. Subsequently, *T. karelinii* was outcompeted by *T. macedonicus*, which captured *T. karelinii* mitochondrial DNA via introgressive hybridization in the process. Once peripheral *T. macedonicus* populations contained *T. karelinii* mitochondrial DNA, this mitochondrial DNA could be spread into areas never populated by *T. karelinii* via a *T. macedonicus* host. This can explain the presence of *T. karelinii* mitochondrial DNA in areas predicted to be unsuitable for *T. karelinii* both at the Last Glacial Maximum and at the present.

Mitochondrial DNA represents just a single gene tree and, ideally, multiple nuclear DNA markers should be included in phylogeographical studies to distill the true evolutionary history. In [chapter 6](#), we conduct a multimarker phylogeography to explore the evolutionary independence of the three mitochondrial DNA lineages comprising the *T. karelinii* group. We include representatives of recognized crested newt species to guide our interpretation of the results. All markers show distinct patterns when analyzed singly (as a phylogeny or haplotype network) and none of them sort haplotypes according to species or mitochondrial DNA lineage. Multimarker approaches (BAPS and *BEAST) on the other hand show that not only the recognized species, but also the three mitochondrial DNA lineages represent discrete nuclear DNA gene pools. A historical range shift coinciding with asymmetric mitochondrial DNA introgression is invoked to explain a slight mismatch between the distribution of nuclear and mitochondrial DNA in the extreme northwest of Asiatic Turkey. This scenario is supported by paleogeological evidence and a striking concordant pattern in co-distributed *Lissotriton* newts. We suggest that the traditional '*T. karelinii*' in fact comprises three species, albeit that they are morphologically cryptic.

The different papers presented in this thesis link together. The mitochondrial DNA data suggest the presence of 'cryptic' species. Subsequently we show how niche divergence can be used as a criterion to test their status and finally explore nuclear DNA as an independent confirmation. Furthermore, we link geographical differentiation of genetic richness with predicted distribution at the Last Glacial Maximum to trace glacial refugia of the different *Triturus* species. Finally, we deduce a past species overturn from a 'genetic footprint' left by the outcompeted species and link this to competition in response to climate change. The combined use of species distribution modeling and mitochondrial phylogeography provides a more complete understanding of the historical biogeography of *Triturus* than both approaches would on their own.

Outlook

Triturus still has much more to teach us about evolutionary biology. An interesting development will be the prediction of potential distribution in deep time, covering the entire timeframe of *Triturus* evolution. This depends in the first place on the availability of paleoclimatic reconstructions. The oldest climate layers currently available cover the Last Interglacial at ca. 120-140Ka (248), a date next to nothing on a geological time scale. Over larger time spans, the role of geomorphological dynamics will start influencing the climate. The resolution of future datasets will necessarily be rough.

A conceptual challenge relevant to ecological niche modeling in deep time will involve the incorporation of niche evolution: how can ancestral niches, coalescing at internal nodes, be reconstructed? Previously applied assumptions of phylogenetic signal and niche conservatism have been criticized for merely representing a subset of possibilities (249). Furthermore, the validity of tracing extrinsic characters (i.e. not directly heritable, such as the niche approximation obtained by ecological niche modeling) over a phylogeny has been questioned (250). Because in *Triturus* the number of rib-bearing vertebrae appears to reflect ecology, this intrinsic character can be used as a surrogate for niche evolution, with each addition of a rib-bearing vertebrae corresponding to a niche shift away from the ancestral character niche. Now that we have succeeded in placing the number of rib-bearing vertebrae in a temporally calibrated phylogenetic context, we can interpret when adaptive shift occurred and what their direction was.

The genomic revolution has (up to now) largely passed salamanders (251). The sheer vastness of salamander genomes (252) make them particularly interesting, but also relatively complex to decipher. Genomic data is an as yet little explored source of information on *Triturus* evolution. First, incorporating (much) more gene trees will help to more accurately establish the *Triturus* phylogeny and in particular to more precisely extract the temporal setting of the species radiation (71). Secondly, genomic data can be employed to uncover the genetic machinery behind body build (253). An understanding of how body build became moldable by natural selection in the ancestral *Triturus*, eventually producing the range of body patterns observed today, can be obtained by comparing the developmental pathways encoded by the genomes of the different *Triturus* species. Finally genomic data will allow us to establish the degree of nuclear gene flow between species, not only at present, but also historically (254). An interesting question is whether different sections of the genome permeate the species boundary to a different degree (255).

Studies on the hybridization between *Triturus* species will further aid our understanding of speciation. Still little is known about postzygotic barriers (132). Given that gene flow between species is geographically restricted, hybrids likely show reduced viability and increased sterility, but the relative importance and the underlying causes are unknown. Even less is known about prezygotic barriers (132). Sexual isolation due to behavioral differences (e.g. in the elaborate 'mating dance' of crested newts) or phenotypical differences (e.g. in the secondary sex characteristics) may well reinforce assortative mating where species occur in syntopy. Of particular interest is the role of pheromones in mating: it is clear that they must play an important part, but what that part is, is yet unclear (256). Laboratory experiments, but also monitoring in the wild, will provide more insight into such barriers to gene flow.

To come back to the niche, field studies will also help us to better understand small-scale ecological differences among species. As the contact zones are the areas where species actively replace one another, these should be the point of focus. Are different species adapted to different microhabitats (cf. 202)? Do ecological characteristics such as phenology or habitat selection make species differentially suited to particular ecological backgrounds? How do different species interact? How do relative frequencies in syntopic populations fluctuate? An interesting aspect is whether the species at the current contact zones are in spatial equilibrium, or whether they are still in the process of displacing each other. Furthermore, how will potential future climate change influence the position of the contact zones? In this section we listed many exciting evolutionary and ecological questions waiting to be answered. *Triturus* is a suitable model system in studies helping to address these questions.

References

1. Lomolino MV, Riddle BR, Brown JH (2006) *Biogeography* (Sinauer Associates, Sunderland, Massachusetts).
2. Brown JH, Stevens GC, Kaufman DM (1996) The geographic range: Size, shape, boundaries, and internal structure. *Annual Review of Ecology and Systematics* 27: 597-623.
3. Wiens JJ, Donoghue MJ (2004) Historical biogeography, ecology and species richness. *Trends in Ecology & Evolution* 19: 639-644.
4. Riddle BR (2005) Is biogeography emerging from its identity crisis? *Journal of Biogeography* 32: 185-186.
5. Hutchinson GE (1957) Concluding remarks. *Cold Spring Harbor Symposia on Quantitative Biology* 22: 415-427.
6. Waters JM (2011) Competitive exclusion: phylogeography's 'elephant in the room'? *Molecular Ecology* 20: 4388-4394.
7. Dayan T, Simberloff D (2005) Ecological and community-wide character displacement: The next generation. *Ecology Letters* 8: 875-894.
8. Losos JB (2000) Ecological character displacement and the study of adaptation. *Proceedings of the National Academy of Sciences of the United States of America* 97: 5693-5695.
9. Guisan A, Thuiller W (2005) Predicting species distribution: Offering more than simple habitat models. *Ecology Letters* 8: 993-1009.
10. Avise JC (2004) *Molecular markers, natural history, and evolution* (Sinauer Associates, Sunderland).
11. Manel S, Schwartz MK, Luikart G, Taberlet P (2003) Landscape genetics: combining landscape ecology and population genetics. *Trends in Ecology & Evolution* 18: 189-197.
12. Avise JC (2000) *Phylogeography: The history and formation of species*. (Harvard University Press, Cambridge, Massachusetts).
13. Avise JC, Arnold J, Ball RM, Bermingham E, Lamb T, Neigel JE, Reeb CA, Saunders NC (1987) Intraspecific phylogeography: The mitochondrial DNA bridge between population genetics and systematics. *Annual Review of Ecology and Systematics* 18: 489-522.
14. Diniz-Filho JAF, De Campos Telles MP, Bonatto SL, Eizirik E, De Freitas TRO, De Marco P, Santos FR, Sole-Cava A, Soares TN (2008) Mapping the evolutionary twilight zone: Molecular markers, populations and geography. *Journal of Biogeography* 35: 753-763.
15. Losos JB, Glor RE (2003) Phylogenetic comparative methods and the geography of speciation. *Trends in Ecology & Evolution* 18: 220-227.
16. Edwards SV, Beerli P (2000) Perspective: Gene divergence, population divergence, and the variance in coalescence time in phylogeographic studies. *Evolution* 54: 1839-1854.
17. Ballard JWO, Whitlock MC (2004) The incomplete natural history of mitochondria. *Molecular Ecology* 13: 729-744.
18. Zhang D-X, Hewitt GM (2003) Nuclear DNA analyses in genetic studies of populations: practice, problems and prospects. *Molecular Ecology* 12: 563-584.
19. Arbogast BS, Kenagy GJ (2001) Comparative phylogeography as an integrative approach to historical biogeography. *Journal of Biogeography* 28: 819-825.
20. Bermingham E, Moritz C (1998) Comparative phylogeography: Concepts and applications. *Molecular Ecology* 7: 367-369.
21. Kidd DM, Ritchie MG (2006) Phylogeographic information systems: Putting the geography into phylogeography. *Journal of Biogeography* 33: 1851-1865.

References

22. Swenson NG (2008) The past and future influence of geographic information systems on hybrid zone, phylogeographic and speciation research. *Journal of Evolutionary Biology* 21: 421-434.
23. Knowles LL (2004) The burgeoning field of statistical phylogeography. *Journal of Evolutionary Biology* 17: 1-10.
24. Knowles LL, Maddison WP (2002) Statistical phylogeography. *Molecular Ecology* 11: 2623-2635.
25. Richards CL, Carstens BC, Lacey Knowles L (2007) Distribution modelling and statistical phylogeography: An integrative framework for generating and testing alternative biogeographical hypotheses. *Journal of Biogeography* 34: 1833-1845.
26. Kidd DM, Liu XH (2008) GEOPHYLOBUILDER 1.0: An ARCGIS extension for creating 'geophylogenies'. *Molecular Ecology Resources* 8: 88-91.
27. Hill AW, Guralnick RP (2010) GeoPhylo: An online tool for developing visualizations of phylogenetic trees in geographic space. *Ecography* 33: 633-636.
28. Janies D, Hill AW, Guralnick R, Habib F, Waltari E, Wheeler WC (2007) Genomic analysis and geographic visualization of the spread of avian influenza (H5N1). *Systematic Biology* 56: 321-329.
29. Parks DH, Porter M, Churcher S, Wang S, Blouin C, Whalley J, Brooks S, Beiko RG (2009) GenGIS: A geospatial information system for genomic data. *Genome Research* 19: 1896-1904.
30. Kozak KH, Graham CH, Wiens JJ (2008) Integrating GIS-based environmental data into evolutionary biology. *Trends in Ecology & Evolution* 23: 141-148.
31. Wisz MS, Hijmans RJ, Li J, Peterson AT, Graham CH, Guisan A, Group NPSDW (2008) Effects of sample size on the performance of species distribution models. *Diversity and Distributions* 14: 763-773.
32. Stockwell DRB, Peterson AT (2002) Effects of sample size on accuracy of species distribution models. *Ecological Modelling* 148: 1-13.
33. Hirzel AH, Hausser J, Chessel D, Perrin N (2002) Ecological-niche factor analysis:: How to compute habitat-suitability maps without absence data? *Ecology* 83: 2027-2036.
34. Elith J, Graham CH, P. Anderson R, Dudík M, Ferrier S, Guisan A, J. Hijmans R, Huettmann F, R. Leathwick J, Lehmann A, Li J, G. Lohmann L, A. Loiselle B, Manion G, Moritz C, Nakamura M, Nakazawa Y, McC. M. Overton J, Townsend Peterson A, J. Phillips S, Richardson K, Scachetti-Pereira R, E. Schapire R, Soberón J, Williams S, S. Wisz M, E. Zimmermann N (2006) Novel methods improve prediction of species' distributions from occurrence data. *Ecography* 29: 129-151.
35. Guisan A, Zimmermann NE (2000) Predictive habitat distribution models in ecology. *Ecological Modelling* 135: 147-186.
36. Dormann CF (2007) Promising the future? Global change projections of species distributions. *Basic and Applied Ecology* 8: 387-397.
37. Pearson RG, Dawson TP (2003) Predicting the impacts of climate change on the distribution of species: Are bioclimate envelope models useful? *Global Ecology and Biogeography* 12: 361-371.
38. Wiens JJ, Graham CH (2005) Niche conservatism: Integrating evolution, ecology, and conservation biology. *Annual Review of Ecology, Evolution, and Systematics* 36: 519-539.
39. Warren DL, Glor RE, Turelli M (2008) Environmental niche equivalency versus conservatism: Quantitative approaches to niche evolution. *Evolution* 62: 2868-2883.
40. Peterson AT, Nyári ÁS (2008) Ecological niche conservatism and Pleistocene refugia in the thrush-like mourner, *Schiffornis* sp., in the Neotropics. *Evolution* 62: 173-183.
41. Kozak KH, Wiens JJ (2006) Does niche conservatism promote speciation? A case study in North American salamanders. *Evolution* 60: 2604-2621.

42. Peterson AT, Soberón J, Sánchez-Cordero V (1999) Conservatism of ecological niches in evolutionary time. *Science* 285: 1265-1267.
43. Davis EB (2005) Comparison of climate space and phylogeny of *Marmota* (Mammalia: Rodentia) indicates a connection between evolutionary history and climate preference. *Proceedings of the Royal Society B: Biological Sciences* 272: 519-526.
44. Kambhampati S, Peterson AT (2007) Ecological niche conservation and differentiation in the wood-feeding cockroaches, *Cryptocercus*, in the United States. *Biological Journal of the Linnean Society* 90: 457-466.
45. Prinzing A (2001) The niche of higher plants: Evidence for phylogenetic conservatism. *Proceedings of the Royal Society of London. Series B: Biological Sciences* 268: 2383-2389.
46. Yesson C, Culham A (2006) Phyoclimatic modeling: Combining phylogenetics and bioclimatic modeling. *Systematic Biology* 55: 785-802.
47. Davis MB, Shaw RG (2001) Range shifts and adaptive responses to Quaternary climate change. *Science* 292: 673-679.
48. Graham CH, Ron SR, Santos JC, Schneider CJ, Moritz C (2004) Integrating phylogenetics and environmental niche models to explore speciation mechanisms in dendrobatid frogs. *Evolution* 58: 1781-1793.
49. Losos JB, Leal M, Glor RE, de Queiroz K, Hertz PE, Rodriguez Schettino L, Chamizo Lara A, Jackman TR, Larson A (2003) Niche lability in the evolution of a Caribbean lizard community. *Nature* 424: 542-545.
50. Knouft JH, Losos JB, Glor RE, Kolbe JJ (2006) Phylogenetic analysis of the evolution of the niche in lizards of the *Anolis sagrei* group. *Ecology* 87: 29-38.
51. Peterson AT, Holt RD (2003) Niche differentiation in Mexican birds: Using point occurrences to detect ecological innovation. *Ecology Letters* 6: 774-782.
52. Rice NH, Martínez-Meyer E, Peterson AT (2003) Ecological niche differentiation in the *Aphelocoma* jays: A phylogenetic perspective. *Biological Journal of the Linnean Society* 80: 369-383.
53. Martínez-Meyer E, Peterson AT (2006) Conservatism of ecological niche characteristics in North American plant species over the Pleistocene-to-Recent transition. *Journal of Biogeography* 33: 1779-1789.
54. Martínez-Meyer E, Townsend Peterson A, Hargrove WW (2004) Ecological niches as stable distributional constraints on mammal species, with implications for Pleistocene extinctions and climate change projections for biodiversity. *Global Ecology and Biogeography* 13: 305-314.
55. Davis AJ, Jenkinson LS, Lawton JH, Shorrocks B, Wood S (1998) Making mistakes when predicting shifts in species range in response to global warming. *Nature* 391: 783-786.
56. Araújo MB, Luoto M (2007) The importance of biotic interactions for modelling species distributions under climate change. *Global Ecology and Biogeography* 16: 743-753.
57. Waltari E, Hijmans RJ, Peterson AT, Nyári ÁS, Perkins SL, Guralnick RP (2007) Locating Pleistocene refugia: Comparing phylogeographic and ecological niche model predictions. *PLoS ONE* 2: e563.
58. Stigall AL, Lieberman BS (2006) Quantitative palaeobiogeography: GIS, phylogenetic biogeographical analysis, and conservation insights. *Journal of Biogeography* 33: 2051-2060.
59. Peterson AT, Martínez-Meyer E, González-Salazar C (2004) Reconstructing the Pleistocene geography of the *Aphelocoma* jays (Corvidae). *Diversity and Distributions* 10: 237-246.
60. Hilbert DW, Bradford M, Parker T, Westcott DA (2004) Golden bowerbird (*Prionodura newtonia*) habitat in past, present and future climates: Predicted extinction of a

- vertebrate in tropical highlands due to global warming. *Biological Conservation* 116: 367-377.
61. Leroy SAG, Arpe K (2007) Glacial refugia for summer-green trees in Europe and south-west Asia as proposed by ECHAM3 time-slice atmospheric model simulations. *Journal of Biogeography* 34: 2115-2128.
 62. Peterson AT (2006) Uses and requirements of ecological niche models and related distributional models. *Biodiversity Informatics* 3: 59-72.
 63. Arntzen JW (2003) *Triturus cristatus* Superspecies - Kammolch-Artenkreis (*Triturus cristatus* (Laurenti, 1768) - Nördlicher Kammolch, *Triturus carnifex* (Laurenti, 1768) - Italienischer Kammolch, *Triturus dobrogicus* (Kiritzescu, 1903) - Donau-Kammolch, *Triturus karelinii* (Strauch, 1870) - Südlicher Kammolch). *Handbuch der Reptilien und Amphibien Europas. Schwanzlurche IIA*, eds Grossenbacher K & Thiesmeier B (Aula-Verlag, Wiebelsheim), pp 421-514.
 64. Whitfield JB, Lockhart PJ (2007) Deciphering ancient rapid radiations. *Trends in Ecology & Evolution* 22: 258-265.
 65. Wielstra B, Espregueira Themudo G, Güclü Ö, Olgun K, Poyarkov NA, Arntzen JW (2010) Cryptic crested newt diversity at the Eurasian transition: The mitochondrial DNA phylogeography of Near Eastern *Triturus* newts. *Molecular Phylogenetics and Evolution* 56: 888-896.
 66. Arntzen JW, Espregueira Themudo G, Wielstra B (2007) The phylogeny of crested newts (*Triturus cristatus* superspecies): Nuclear and mitochondrial genetic characters suggest a hard polytomy, in line with the paleogeography of the centre of origin. *Contributions to Zoology* 76: 261-278.
 67. Arntzen JW, Wallis GP (1999) Geographic variation and taxonomy of crested newts (*Triturus cristatus* superspecies): Morphological and mitochondrial data. *Contributions to Zoology* 68: 181-203.
 68. Arntzen JW, Wallis GP (1994) The 'Wolterstorff Index' and its value to the taxonomy of the crested newt superspecies. *Abhandlungen und Berichte für Naturkunde* 17: 57-66.
 69. Wallis GP, Arntzen JW (1989) Mitochondrial-DNA variation in the crested newt superspecies: Limited cytoplasmic gene flow among species. *Evolution* 43: 88-104.
 70. Espregueira Themudo G, Wielstra B, Arntzen JW (2009) Multiple nuclear and mitochondrial genes resolve the branching order of a rapid radiation of crested newts (*Triturus*, Salamandridae). *Molecular Phylogenetics and Evolution* 52: 321-328.
 71. Edwards SV (2009) Is a new and general theory of molecular systematics emerging? *Evolution* 63: 1-19.
 72. Cummings MP, Otto SP, Wakeley J (1995) Sampling properties of DNA-sequence data in phylogenetic analysis. *Molecular Biology and Evolution* 12: 814-822.
 73. Alfaro ME, Zoller S, Lutzoni F (2003) Bayes or bootstrap? A simulation study comparing the performance of Bayesian Markov chain Monte Carlo sampling and bootstrapping in assessing phylogenetic confidence. *Molecular Biology and Evolution* 20: 255-266.
 74. Degnan JH, Rosenberg NA (2009) Gene tree discordance, phylogenetic inference and the multispecies coalescent. *Trends in Ecology & Evolution* 24: 332-340.
 75. Maddison WP, Knowles LL (2006) Inferring phylogeny despite incomplete lineage sorting. *Systematic Biology* 55: 21-30.
 76. Moore WS (1995) Inferring phylogenies from mtDNA variation - Mitochondrial-gene trees versus nuclear-gene trees. *Evolution* 49: 718-726.
 77. Funk DJ, Omland KE (2003) Species-level paraphyly and polyphyly: Frequency, causes, and consequences, with insights from animal mitochondrial DNA. *Annual Review of Ecology Evolution and Systematics* 34: 397-423.

78. Dermitzakis DM, Papanikolaou DJ (1981) Paleogeography and geodynamics of the Aegean region during the Neogene. *Annales Géologiques des Pays Helléniques* 30: 245-289.
79. Popov SV, Rögl F, Rozanov AY, Steiniger FF, Shcherba IG, Kovac M (2004) Lithological-paleogeographic maps of Paratethys: 10 maps Late Eocene to Pliocene. *Courier Forschungsinstitut Senckenberg* 250: 1-46.
80. Babik W, Branicki W, Crnobrnja-Isailovic J, Cogalniceanu D, Sas I, Olgun K, Poyarkov NA, Garcia-Paris M, Arntzen JW (2005) Phylogeography of two European newt species - Discordance between mtDNA and morphology. *Molecular Ecology* 14: 2475-2491.
81. Sotiropoulos K, Eleftherakos K, Dzukic G, Kaiezic ML, Legakis A, Polymeni RM (2007) Phylogeny and biogeography of the alpine newt *Mesotriton alpestris* (Salamandridae, Caudata), inferred from mtDNA sequences. *Molecular Phylogenetics and Evolution* 45: 211-226.
82. Coyne JA, Orr HA (2004) *Speciation* (Sinauer Associates, Sunderland).
83. Schluter D (2001) Ecology and the origin of species. *Trends in Ecology & Evolution* 16: 372-380.
84. Rundle HD, Nosil P (2005) Ecological speciation. *Ecology Letters* 8: 336-352.
85. Sobel JM, Chen GF, Watt LR, Schemske DW (2010) The biology of speciation. *Evolution* 64: 295-315.
86. Carey C, Alexander MA (2003) Climate change and amphibian declines: Is there a link? *Diversity and Distributions* 9: 111-121.
87. Eronen JT, Ataabadia MM, Micheelsb A, Karme A, Bernor RL, Fortelius M (2009) Distribution history and climatic controls of the Late Miocene Pikermian chronofauna. *Proceedings of the National Academy of Sciences of the United States of America* 106: 11867-11871.
88. Wake DB (2009) What salamanders have taught us about evolution. *Annual Review of Ecology, Evolution, and Systematics* 40: 333-352.
89. Parra-Olea G, Wake DB (2001) Extreme morphological and ecological homoplasy in tropical salamanders. *Proceedings of the National Academy of Sciences of the United States of America* 98: 7888-7891.
90. Gvoždík L, van Damme R (2006) *Triturus* newts defy the running-swimming dilemma. *Evolution* 60: 2110-2121.
91. Zhang P, Papenfuss TJ, Wake MH, Qu LH, Wake DB (2008) Phylogeny and biogeography of the family Salamandridae (Amphibia: Caudata) inferred from complete mitochondrial genomes. *Molecular Phylogenetics and Evolution* 49: 586-597.
92. Maddison DR, Maddison WP (2005) MacClade 4: Analysis of phylogeny and character evolution, version 4.08. *Sunderland (Massachusetts): Sinauer Associates*.
93. Mueller RL, Macey JR, Jaekel M, Wake DB, Boore JL (2004) Morphological homoplasy, life history evolution, and historical biogeography of plethodontid salamanders inferred from complete mitochondrial genomes. *Proceedings of the National Academy of Sciences of the United States of America* 101: 13820-13825.
94. Nylander JAA: MrModelTest2. [<http://www.abc.se/~nylander>].
95. Brandley MC, Schmitz A, Reeder TW (2005) Partitioned Bayesian analyses, partition choice, and the phylogenetic relationships of scincid lizards. *Systematic Biology* 54: 373-390.
96. Nylander JAA, Ronquist F, Huelsenbeck JP, Nieves-Aldrey JL (2004) Bayesian phylogenetic analysis of combined data. *Systematic Biology* 53: 47-67.
97. Kass RE, Raftery AE (1995) Bayes factors. *Journal of the American Statistical Association* 90: 773-795.

References

98. Ronquist F, Huelsenbeck JP (2003) MrBayes 3: Bayesian phylogenetic inference under mixed models. *Bioinformatics* 19: 1572-1574.
99. Rambaut A, Drummond AJ: Tracer. [<http://beast.bio.ed.ac.uk/tracer>].
100. Stamatakis A (2006) RAxML-VI-HPC: Maximum Likelihood-based phylogenetic analyses with thousands of taxa and mixed models. *Bioinformatics* 22: 2688-2690.
101. Miller MA, Holder MT, Vos R, Midford PE, Liebowitz T, Chan L, Hoover P, Warnow T: The CIPRES Portals. [http://www.phylo.org/sub_sections/portal]
102. Steinfartz S, Vicario S, Arntzen JW, Caccone A (2007) A Bayesian approach on molecules and behavior: Reconsidering phylogenetic and evolutionary patterns of the Salamandridae with emphasis on *Triturus* newts. *Journal of Experimental Zoology Part B: Molecular and Developmental Evolution* 308B: 139-162.
103. Sanderson MJ (2003) r8s: Inferring absolute rates of molecular evolution and divergence times in the absence of a molecular clock. *Bioinformatics* 19: 301-302.
104. Drummond AJ, Rambaut A (2007) BEAST: Bayesian evolutionary analysis by sampling trees. *BMC Evolutionary Biology* 7: 214.
105. Riddle BR, Dawson MN, Hadly EA, Hafner DJ, Hickerson MJ, Mantooth SJ, Yoder AD (2008) The role of molecular genetics in sculpting the future of integrative biogeography. *Progress in Physical Geography* 32: 173-202.
106. Meulenkamp JE, Sissingh W (2003) Tertiary palaeogeography and tectonostratigraphic evolution of the Northern and Southern Peri-Tethys platforms and the intermediate domains of the African-Eurasian convergent plate boundary zone. *Palaeogeography, Palaeoclimatology, Palaeoecology* 196: 209-228.
107. Rögl F (1998) Palaeogeographic considerations for Mediterranean and Paratethys Seaways (Oligocene to Miocene). *Annalen des Naturhistorischen Museums in Wien* 99: 279-310.
108. Mittermeier RA, Gil PR, Hoffmann M, Pilgrim J, Brooks T, Mittermeier CG, Lamoreux J, Da Fonseca GAB (2005) *Hotspots revisited: Earth's biologically richest and most endangered terrestrial ecoregions* (The University of Chicago Press, Chicago).
109. Myers N, Mittermeier RA, Mittermeier CG, da Fonseca GAB, Kent J (2000) Biodiversity hotspots for conservation priorities. *Nature* 403: 853-858.
110. Beheregaray LB (2008) Twenty years of phylogeography: The state of the field and the challenges for the Southern Hemisphere. *Molecular Ecology* 17: 3754-3774.
111. Zeisset I, Beebee TJC (2008) Amphibian phylogeography: A model for understanding historical aspects of species distributions. *Heredity* 101: 109-119.
112. Arntzen JW, Wielstra B (2010) Where to draw the line? A nuclear genetic perspective on proposed range boundaries of the crested newts *Triturus karelinii* and *T. arntzeni*. *Amphibia-Reptilia* 31: 311-322.
113. Arévalo E, Davis SK, Sites JW, Jr. (1994) Mitochondrial DNA sequence divergence and phylogenetic relationships among eight chromosome races of *Sceloporus grammicus* complex (Phrynosomatidae) in Central Mexico. *Systematic Biology* 43: 387 - 418.
114. Steininger FF, Rögl F (1984) Paleogeography and palinspastic reconstruction of the Neogene of the Mediterranean and Paratethys. *The Geological Evolution of the Eastern Mediterranean*, eds Dixon JE & Robertson AHF (Blackwell Science, Oxford), pp 659-668.
115. Popov SV, Shcherba IG, Ilyina LB, Nevesskaya LA, Paramonova NP, Khondkarian SO, Magyar I (2006) Late Miocene to Pliocene palaeogeography of the Paratethys and its relation to the Mediterranean. *Palaeogeography, Palaeoclimatology, Palaeoecology* 238: 91-106.
116. Chepalyga AL (1995) East Paratethys - Tethys marine connections along Euphrat Passage during Neogene. *Romanian Journal of Stratigraphy* 76 (Suppl. 7): 149-150.

117. Krijgsman W, Hilgen FJ, Raffi I, Sierro FJ, Wilson DS (1999) Chronology, causes and progression of the Messinian salinity crisis. *Nature* 400: 652-655.
118. Çağatay MN, Görür N, Flecker R, Sakinç M, Tünoğlu C, Ellam R, Krijgsman W, Vincent S, Dikbaş A (2006) Paratethyan-Mediterranean connectivity in the Sea of Marmara region (NW Turkey) during the Messinian. *Sedimentary Geology* 188: 171-187.
119. Sakinç M, Yaltırak C (2005) Messinian crisis: What happened around the northeastern Aegean? *Marine Geology* 221: 423-436.
120. Clauzon G, Suc JP, Popescu SM, Marunteanu M, Rubino JL, Marinescu F, Melinte MC (2005) Influence of Mediterranean sea-level changes on the Dacic Basin (Eastern Paratethys) during the late Neogene: The Mediterranean Lago Mare facies deciphered. *Basin Research* 17: 437-462.
121. Elmas A (2003) Late Cenozoic tectonics and stratigraphy of northwestern Anatolia: The effects of the North Anatolian Fault to the region. *International Journal of Earth Sciences* 92: 380-396.
122. Ryan WBF, Major CO, Lericolais G, Goldstein SL (2003) Catastrophic flooding of the Black Sea. *Annual Review of Earth and Planetary Sciences* 31: 525-554.
123. Lambeck K, Esat TM, Potter EK (2002) Links between climate and sea levels for the past three million years. *Nature* 419: 199-206.
124. Tugolesov DA, Gorshkov AS, Meisner LB, V. SV, Khakhalev EM (1985) Tectonics of the Black Sea depression. *Geotektonika* 6: 3-20.
125. Lemmon EM, Lemmon AR, Cannatella DC (2007) Geological and climatic forces driving speciation in the continentally distributed trilling chorus frogs (pseudacris). *Evolution* 61: 2086-2103.
126. Pauly GB, Piskurek O, Shaffer HB (2007) Phylogeographic concordance in the southeastern United States: The flatwoods salamander, *Ambystoma cingulatum*, as a test case. *Molecular Ecology* 16: 415-429.
127. Kerey IE, Meric E, Tunoglu C, Kelling G, Brenner RL, Dogan AU (2004) Black Sea-Marmara Sea Quaternary connections: New data from the Bosphorus, Istanbul, Turkey. *Palaeogeography, Palaeoclimatology, Palaeoecology* 204: 277-295.
128. Ballard JWO, Rand DM (2005) The population biology of mitochondrial DNA and its phylogenetic implications. *Annual Review of Ecology Evolution and Systematics* 36: 621-642.
129. Broennimann O, Fitzpatrick MC, Pearman PB, Petitpierre B, Pellissier L, Yoccoz NG, Thuiller W, Fortin M-J, Randin C, Zimmermann NE, Graham CH, Guisan A (2012) Measuring ecological niche overlap from occurrence and spatial environmental data. *Global Ecology and Biogeography* 21: 481-497.
130. Funk DJ, Nosil P, Etges WJ (2006) Ecological divergence exhibits consistently positive associations with reproductive isolation across disparate taxa. *Proceedings of the National Academy of Sciences of the United States of America* 103: 3209-3213.
131. Wielstra B, Arntzen JW (2011) Unraveling the rapid radiation of crested newts (*Triturus cristatus* superspecies) using complete mitogenomic sequences. *BMC Evolutionary Biology* 11: 162.
132. Arntzen JW, Wallis GP, Wielstra B (submitted) Spatial patterns of nuclear, mitochondrial and morphological transition in *Triturus* newts.
133. Ivanović A, Üzüm N, Wielstra B, Olgun K, Litvinchuk SN, Kalezić ML, Arntzen JW (2012) Is mitochondrial DNA divergence of Near Eastern crested newts (*Triturus karelinii* group) reflected by differentiation of skull shape? *Zoologischer Anzeiger*: TBA.
134. Hijmans RJ, Cameron SE, Parra JL, Jones PG, Jarvis A (2005) Very high resolution interpolated climate surfaces for global land areas. *International Journal of Climatology* 25: 1965-1978.

135. Austin M (2007) Species distribution models and ecological theory: A critical assessment and some possible new approaches. *Ecological Modelling* 200: 1-19.
136. Warren DL, Glor RE, Turelli M (2010) ENMTools: A toolbox for comparative studies of environmental niche models. *Ecography* 33: 607-611.
137. VanDerWal J, Shoo LP, Graham C, Williams SE (2009) Selecting pseudo-absence data for presence-only distribution modeling: How far should you stray from what you know? *Ecological Modelling* 220: 589-594.
138. Team RDC (2010) *R: A language and environment for statistical computing* (R Foundation for Statistical Computing, Vienna).
139. Schoener TW (1970) Nonsynchronous spatial overlap of lizards in patchy habitats. *Ecology* 51: 408-418.
140. Vukov TD, Sotiropoulos K, Wielstra B, Džukić G, Kalezić ML (2011) The evolution of the adult body form of the crested newt (*Triturus cristatus* superspecies, Caudata, Salamandridae). *Journal of Zoological Systematics and Evolutionary Research* 49: 324-334.
141. Ivanović A, Džukić G, Kalezić ML (2012) A phenotypic point of view of the adaptive radiation of crested newts (*Triturus cristatus* superspecies, Caudata, Amphibia). *International Journal of Evolutionary Biology* 2012: Article ID 740605.
142. Soberón J, Nakamura M (2009) Niches and distributional areas: Concepts, methods, and assumptions. *Proceedings of the National Academy of Sciences of the United States of America* 106: 19644-19650.
143. Wolterstorff W (1923) Übersicht den Unterarten und Formen des *Triton cristatus* Laur. *Blätter für Aquarien-und Terrarienkunde* 34: 120-126.
144. Bucci-Innocenti S, Ragghianti M, Mancino G (1983) Investigations of karyology and hybrids in *Triturus boscai* and *T. vittatus*, with a reinterpretation of the species groups within *Triturus* (Caudata: Salamandridae). *Copeia* 1983: 662-672.
145. Raxworthy CJ, Ingram CM, Rabibisoa N, Pearson RG (2007) Applications of ecological niche modeling for species delimitation: A review and empirical evaluation using day geckos (*Phelsuma*) from Madagascar. *Systematic Biology* 56: 907-923.
146. Rissler LJ, Apodaca JJ (2007) Adding more ecology into species delimitation: Ecological niche models and phylogeography help define cryptic species in the black salamander (*Aneides flavipunctatus*). *Systematic Biology* 56: 924-942.
147. Graham CH, Ferrier S, Huettman F, Moritz C, Peterson AT (2004) New developments in museum-based informatics and applications in biodiversity analysis. *Trends in Ecology & Evolution* 19: 497-503.
148. Hewitt G (2000) The genetic legacy of the Quaternary ice ages. *Nature* 405: 907-913.
149. Keppel G, Van Niel KP, Wardell-Johnson GW, Yates CJ, Byrne M, Mucina L, Schut AGT, Hopper SD, Franklin SE (2012) Refugia: identifying and understanding safe havens for biodiversity under climate change. *Global Ecology and Biogeography* 21: 393-404.
150. Schmitt T (2007) Molecular biogeography of Europe: Pleistocene cycles and postglacial trends. *Frontiers in Zoology* 4: 11.
151. Cane MA, Braconnot P, Clement A, Gildor H, Joussaume S, Kageyama M, Khodri M, Paillard D, Tett S, Zorita E (2006) Progress in paleoclimate modeling. *Journal of Climate* 19: 5031-5057.
152. Hofreiter M, Stewart J (2009) Ecological change, range fluctuations and population dynamics during the Pleistocene. *Current Biology* 19: R584-R594.
153. Hof C, Levinsky I, Araújo MB, Rahbek C (2011) Rethinking species' ability to cope with rapid climate change. *Global Change Biology* 17: 2987-2990.

154. Ohlemüller R, Huntley B, Normand S, Svenning J-C (2011) Potential source and sink locations for climate-driven species range shifts in Europe since the Last Glacial Maximum. *Global Ecology and Biogeography* 21: 152–163.
155. Hoffmann AA, Sgro CM (2011) Climate change and evolutionary adaptation. *Nature* 470: 479–485.
156. Provan J, Bennett KD (2008) Phylogeographic insights into cryptic glacial refugia. *Trends in Ecology & Evolution* 23: 564–571.
157. Stewart JR, Lister AM, Barnes I, Dalen L (2010) Refugia revisited: Individualistic responses of species in space and time. *Proceedings of the Royal Society B-Biological Sciences* 277: 661–671.
158. Bennett KD, Provan J (2008) What do we mean by 'refugia'? *Quaternary Science Reviews* 27: 2449–2455.
159. Excoffier L, Foll M, Petit RJ (2009) Genetic consequences of range expansions. *Annual Review of Ecology, Evolution, and Systematics* 40: 481–501.
160. Currat M, Ruedi M, Petit RJ, Excoffier L (2008) The hidden side of invasions: Massive introgression by local genes. *Evolution* 62: 1908–1920.
161. Svenning J-C, Fløjgaard C, Marske KA, Nógues-Bravo D, Normand S (2011) Applications of species distribution modeling to paleobiology. *Quaternary Science Reviews* 30: 2930–2947.
162. Peterson AT (2011) Ecological niche conservatism: a time-structured review of evidence. *Journal of Biogeography* 38: 817–827.
163. Buckley LB, Jetz W (2008) Linking global turnover of species and environments. *Proceedings of the National Academy of Sciences of the United States of America* 105: 17836–17841.
164. Vieites DR, Nieto-Román S, Wake DB (2009) Reconstruction of the climate envelopes of salamanders and their evolution through time. *Proceedings of the National Academy of Sciences of the United States of America* 106: 19715–19722.
165. Araujo MB, Nogués-Bravo D, Diniz-Filho JAF, Haywood AM, Valdes PJ, Rahbek C (2008) Quaternary climate changes explain diversity among reptiles and amphibians. *Ecography* 31: 8–15.
166. Araujo MB, Thuiller W, Pearson RG (2006) Climate warming and the decline of amphibians and reptiles in Europe. *Journal of Biogeography* 33: 1712–1728.
167. Herrero P, Montori A, Arano B (2003) *Triturus marmoratus* (Latreille, 1800) - Nördlicher Marmormolch. *Handbuch der Reptilien und Amphibien Europas. Schwanzlurche IIA*, eds Grossenbacher K & Thiesmeier B (Aula-Verlag, Wiebelsheim), pp 515–541.
168. Herrero P, Montori A, Arano B (2003) *Triturus pygmaeus* (Wolterstorff, 1905) - Südlicher Marmormolch. *Handbuch der Reptilien und Amphibien Europas. Schwanzlurche IIA*, eds Grossenbacher K & Thiesmeier B (Aula-Verlag, Wiebelsheim), pp 543–553.
169. Hewitt GM (2004) Genetic consequences of climatic oscillations in the Quaternary. *Philosophical Transactions of the Royal Society of London Series B-Biological Sciences* 359: 183–195.
170. Canestrelli D, Salvi D, Maura M, Bologna M, Nascetti G (2012) One species, three Pleistocene evolutionary histories: Phylogeography of the crested newt *Triturus carnifex*. *PLoS ONE* 7: e41754.
171. Espregueira Themudo G, Nieman A, Arntzen JW (accepted) Is dispersal guided by the environment? A comparison of interspecific gene flow estimates among differentiated regions of a newt hybrid zone. *Molecular Ecology*: TBA.
172. Wielstra B, Arntzen JW (2012) The shifting interchange of two species of *Triturus* newts deduced from asymmetrically introgressed mitochondrial DNA. *BMC Evolutionary Biology* 12: 161.

173. Tamura K, Peterson D, Peterson N, Stecher G, Nei M, Kumar S (2011) MEGA5: Molecular evolutionary genetics analysis using maximum likelihood, evolutionary distance, and maximum parsimony methods. *Molecular Biology and Evolution* 28: 2731-2739.
174. Excoffier L, Lischer HEL (2010) Arlequin suite ver 3.5: A new series of programs to perform population genetics analyses under Linux and Windows. *Molecular Ecology Resources* 10: 564-567.
175. Miller MP (2005) Alleles In Space (AIS): Computer software for the joint analysis of interindividual spatial and genetic information. *Journal of Heredity* 96: 722-724.
176. Fijarczyk A, Nadachowska K, Hofman S, Litvinchuk SN, Babik W, Stuglik M, Gollmann G, Choleva L, Cogălniceanu DAN, Vukov T, Džukić G, Szymura JM (2011) Nuclear and mitochondrial phylogeography of the European fire-bellied toads *Bombina bombina* and *Bombina variegata* supports their independent histories. *Molecular Ecology* 20: 3381-3398.
177. Rödder D, Schmidlein S, Veith M, Lötters S (2009) Alien invasive slider turtle in unpredicted habitat: A matter of niche shift or of predictors studied? *PLoS ONE* 4: e7843.
178. Braconnot P, Otto-Bliesner B, Harrison S, Joussaume S, Peterchmitt JY, Abe-Ouchi A, Crucifix M, Driesschaert E, Fichefet T, Hewitt CD, Kageyama M, Kitoh A, Laine A, Loutre MF, Marti O, Merkel U, Ramstein G, Valdes P, Weber SL, Yu Y, Zhao Y (2007) Results of PMIP2 coupled simulations of the Mid-Holocene and Last Glacial Maximum - Part 1: experiments and large-scale features. *Climate of the Past* 3: 261-277.
179. Collins WD, Bitz CM, Blackmon ML, Bonan GB, Bretherton CS, Carton JA, Chang P, Doney SC, Hack JJ, Henderson TB, Kiehl JT, Large WG, McKenna DS, Santer BD, Smith RD (2006) The Community Climate System Model Version 3 (CCSM3). *Journal of Climate* 19: 2122-2143.
180. Phillips SJ, Anderson RP, Schapire RE (2006) Maximum entropy modeling of species geographic distributions. *Ecological Modelling* 190: 231-259.
181. Elith J, Kearney M, Phillips S (2010) The art of modelling range-shifting species. *Methods in Ecology and Evolution* 1: 330-342.
182. Stokland JN, Halvorsen R, Støa B (2011) Species distribution modelling - Effect of design and sample size of pseudo-absence observations. *Ecological Modelling* 222: 1800-1809.
183. Elith J, Phillips SJ, Hastie T, Dudik M, Chee YE, Yates CJ (2011) A statistical explanation of MaxEnt for ecologists. *Diversity and Distributions* 17: 43-57.
184. Barve N, Barve V, Jiménez-Valverde A, Lira-Noriega A, Maher SP, Peterson AT, Soberón J, Villalobos F (2011) The crucial role of the accessible area in ecological niche modeling and species distribution modeling. *Ecological Modelling* 222: 1810-1819.
185. Raes N, ter Steege H (2007) A null-model for significance testing of presence-only species distribution models. *Ecography* 30: 727-736.
186. Carstens BC, Richards CL (2007) Integrating coalescent and ecological niche modeling in comparative phylogeography. *Evolution* 61: 1439-1454.
187. Knowles LL, Carstens BC, Keat Marcia L (2007) Coupling genetic and ecological-niche models to examine how past population distributions contribute to divergence. *Current Biology* 17: 940-946.
188. Hugall A, Moritz C, Moussalli A, Stanicic J (2002) Reconciling paleodistribution models and comparative phylogeography in the Wet Tropics rainforest land snail *Gnarosiphia bellendenkerensis* (Brazier 1875). *Proceedings of the National Academy of Sciences of the United States of America* 99: 6112-6117.
189. Tarkhnishvili D, Gavashelishvili A, Mumladze L (2012) Palaeoclimatic models help to understand current distribution of Caucasian forest species. *Biological Journal of the Linnean Society* 105: 231-248.

190. Arntzen JW (2001) Genetic variation in the Italian crested newt, *Triturus carnifex*, and the origin of a non-native population north of the Alps. *Biodiversity and Conservation* 10: 971-987.
191. Arntzen JW, Thorpe RS (1999) Italian crested newts (*Triturus carnifex*) in the Basin of Geneva: Distribution and genetic interactions with autochthonous species. *Herpetologica* 55: 423-433.
192. Bogaerts S (2002) Italian crested newts, *Triturus carnifex*, on the Veluwe, Netherlands. *Zeitschrift für Feldherpetologie* 9: 217-226.
193. Brede EG, Thorpe RS, Arntzen JW, Langton TES (2000) A morphometric study of a hybrid newt population (*Triturus cristatus*/*T. carnifex*): Beam Brook Nurseries, Surrey, U.K. *Biological Journal of the Linnean Society* 70: 685-695.
194. Maletzky A, Mikulíček P, Franzen M, Goldschmid A, Gruber H-J, Horák A, Kyek M (2008) Hybridization and introgression between two species of crested newts (*Triturus cristatus* and *T. carnifex*) along contact zones in Germany and Austria: morphological and molecular data. *The Herpetological Journal* 18: 1-15.
195. McGuire JA, Linkem CW, Koo MS, Hutchison DW, Lappin AK, Orange DI, Lemos-Espinal J, Riddle BR, Jaeger JR (2007) Mitochondrial introgression and incomplete lineage sorting through space and time: Phylogenetics of crotaphytid lizards. *Evolution* 61: 2879-2897.
196. Bryson JRW, De Oca AN-M, Jaeger JR, Riddle BR (2010) Elucidation of cryptic diversity in a widespread Nearctic treefrog reveals episodes of mitochondrial gene capture as frogs diversified across a dynamic landscape. *Evolution* 64: 2315-2330.
197. Liu K, Wang F, Chen W, Tu L, Min M-S, Bi K, Fu J (2010) Rampant historical mitochondrial genome introgression between two species of green pond frogs, *Pelophylax nigromaculatus* and *P. plancyi*. *BMC Evolutionary Biology* 10: 201.
198. Espregueira Themudo G, Arntzen JW (2007) Newts under siege: range expansion of *Triturus pygmaeus* isolates populations of its sister species. *Diversity and Distributions* 13: 580-586.
199. Arntzen JW, Espregueira Themudo G (2008) Environmental parameters that determine species geographical range limits as a matter of time and space. *Journal of Biogeography* 35: 1177-1186.
200. Krosby M, Rohwer S (2009) A 2000 km genetic wake yields evidence for northern glacial refugia and hybrid zone movement in a pair of songbirds. *Proceedings of the Royal Society B-Biological Sciences* 276: 615-621.
201. Jehle R, Bouma P, Sztatecsny M, Arntzen JW (2000) High aquatic niche overlap in the newts *Triturus cristatus* and *T. marmoratus* (Amphibia, Urodela). *Hydrobiologia* 437: 149-155.
202. Arntzen JW, Wallis GP (1991) Restricted gene flow in a moving hybrid zone of the newts *Triturus cristatus* and *T. marmoratus* in western France. *Evolution* 45: 805-826.
203. Schoorl J, Zuiderwijk A (1980) Ecological Isolation in *Triturus cristatus* and *Triturus marmoratus* (Amphibia: Salamandridae). *Amphibia-Reptilia* 1: 235-252.
204. Arntzen JW, Hedlund L (1990) Fecundity of the newts *Triturus cristatus*, *T. marmoratus* and their natural hybrids in relation to species coexistence. *Holarctic Ecology* 13: 325-332.
205. Arntzen JW, Jehle R, Bardakci F, Burke T, Wallis GP (2009) Asymmetric viability of reciprocal-cross hybrids between crested and marbled newts (*Triturus cristatus* and *T. marmoratus*). *Evolution* 63: 1191-1202.
206. Estes R (1981) Gymnophiona, Caudata. *Handbuch der Paläoherpetologie, Part 2*, ed P W (Gustav Fischer, Stuttgart), pp 1-15.

References

207. Arntzen JW, Bugter RJF, Cogalniceanu D, Wallis GP (1997) The distribution and conservation status of the Danube crested newt, *Triturus dobrogicus*. *Amphibia-Reptilia* 18: 133-142.
208. Vörös J, Arntzen JW (2010) Weak population structuring in the Danube crested newt, *Triturus dobrogicus*, inferred from allozymes. *Amphibia-Reptilia* 31: 339-346.
209. Georgievski G, Stanev E (2006) Paleo-evolution of the Black Sea watershed: Sea level and water transport through the Bosphorus Straits as an indicator of the Lateglacial–Holocene transition. *Climate Dynamics* 26: 631-644.
210. Vörös J, Mikuliček P, Major Á, Recuero-Gil E, Arntzen JW (in prep.) Down by the river: Phylogeography and population genetic structure of the Danube crested newt, *Triturus dobrogicus* (Kiritzescu, 1903).
211. Perissoratis C, Conispoliatis N (2003) The impacts of sea-level changes during latest Pleistocene and Holocene times on the morphology of the Ionian and Aegean seas (SE Alpine Europe). *Marine Geology* 196: 145-156.
212. Kvasov DD (1975) *The Late Quaternary history of large lakes and inland seas of eastern Europe*. (Leningrad) p 248.
213. Chan KMA, Levin SA (2005) Leaky prezygotic isolation and porous genomes: Rapid introgression of maternally inherited DNA. *Evolution* 59: 720-729.
214. Petit RJ, Excoffier L (2009) Gene flow and species delimitation. *Trends in Ecology & Evolution* 24: 386-393.
215. Galtier N, Nabholz B, Glemin S, Hurst GDD (2009) Mitochondrial DNA as a marker of molecular diversity: A reappraisal. *Molecular Ecology* 18: 4541-4550.
216. Wielstra B, Crnobrnja-Isailović J, Litvinchuk SN, Reijnen B, Skidmore AK, Sotiropoulis K, Toxopeus AG, Tzankov N, Vukov T, Arntzen JW (submitted) Tracing glacial refugia of *Triturus* newts based on mitochondrial DNA phylogeography and species distribution modeling.
217. Bossu CM, Near TJ (2009) Gene trees reveal repeated instances of mitochondrial DNA introgression in orangethroat darters (Percidae: *Etheostoma*). *Systematic Biology* 58: 114-129.
218. García-París M, Alcobendas M, Buckley D, Wake DB (2003) Dispersal of viviparity across contact zones in Iberian populations of fire salamanders (*Salamandra*) inferred from discordance of genetic and morphological traits. *Evolution* 57: 129-143.
219. Alley RB, Ágústssdóttir AM (2005) The 8k event: cause and consequences of a major Holocene abrupt climate change. *Quaternary Science Reviews* 24: 1123-1149.
220. Steig EJ (1999) Mid-Holocene climate change. *Science* 286: 1485-1487.
221. Mayewski PA, Rohling EE, Curt Stager J, Karlén W, Maasch KA, David Meecker L, Meyerson EA, Gasse F, van Kreveland S, Holmgren K, Lee-Thorp J, Rosqvist G, Rack F, Staubwasser M, Schneider RR, Steig EJ (2004) Holocene climate variability. *Quaternary Research* 62: 243-255.
222. Lamb T, Avise JC (1986) Directional introgression of mitochondrial DNA in a hybrid population of tree frogs: The influence of mating behavior. *Proceedings of the National Academy of Sciences of the United States of America* 83: 2526-2530.
223. Rand DM (2001) The units of selection on mitochondrial DNA. *Annual Review of Ecology and Systematics* 32: 415-448.
224. Niki Y, Chigusa SI, Matsuura ET (1989) Complete replacement of mitochondrial DNA in *Drosophila*. *Nature* 341: 551-552.
225. Irwin DE, Rubtsov AS, Panov EN (2009) Mitochondrial introgression and replacement between yellowhammers (*Emberiza citrinella*) and pine buntings (*Emberiza*

- leucocephalos*) (Aves: Passeriformes). *Biological Journal of the Linnean Society* 98: 422-438.
226. Plötner J, Uzzell T, Beerli P, Spolsky C, Ohst T, Litvinchuk SN, Guex GD, Reyer HU, Hotz H (2008) Widespread unidirectional transfer of mitochondrial DNA: a case in western Palearctic water frogs. *Journal of Evolutionary Biology* 21: 668-681.
227. Teacher AGF, Griffiths DJ (2011) HapStar: Automated haplotype network layout and visualization. *Molecular Ecology Resources* 11: 151-153.
228. Librado P, Rozas J (2009) DnaSP v5: A software for comprehensive analysis of DNA polymorphism data. *Bioinformatics* 25: 1451-1452.
229. Rogers AR, Harpending H (1992) Population growth makes waves in the distribution of pairwise genetic differences. *Molecular Biology and Evolution* 9: 552-569.
230. Ramos-Onsins SE, Rozas J (2002) Statistical properties of new neutrality tests against population growth. *Molecular Biology and Evolution* 19: 2092-2100.
231. Hasumi H, Emori S: K-1 coupled GCM (MIROC) description. [<http://www.ccsr.u-tokyo.ac.jp/kyosei/hasumi/MIROC/techrepo.pdf>].
232. Edwards S, Bensch S (2009) Looking forwards or looking backwards in avian phylogeography? A comment on Zink and Barrowclough 2008. *Molecular Ecology* 18: 2930-2933.
233. Zink RM, Barrowclough GF (2008) Mitochondrial DNA under siege in avian phylogeography. *Molecular Ecology* 17: 2107-2121.
234. Barrowclough GF, Zink RM (2009) Funds enough, and time: mtDNA, nuDNA and the discovery of divergence. *Molecular Ecology* 18: 2934-2936.
235. Wielstra B, Beukema W, Arntzen JW, Skidmore AK, Toxopeus AG, Raes N (submitted) Niche differentiation among cryptic crested newts: candidate species separate in environmental space as recognized species do.
236. Arntzen JW, Baird AB, Espregueira Themudo G, Wielstra B (in prep.) Phylogenetic mismatch analysis to identify incomplete lineage sorting and introgression events, with case studies in newts and lizards.
237. Flot J-F, Tillier A, Samadi S, Tillier S (2006) Phase determination from direct sequencing of length-variable DNA regions. *Molecular Ecology Notes* 6: 627-630.
238. Baird AB, Hillis DM, Patton JC, Bickham JW (2009) Speciation by monobrachial centric fusions: A test of the model using nuclear DNA sequences from the bat genus *Rhogeessa*. *Molecular Phylogenetics and Evolution* 50: 256-267.
239. Corander J, Marttinen P, Siren J, Tang J (2009) Enhanced Bayesian modelling in BAPS software for learning genetic structures of populations. *BMC Bioinformatics* 9: 539.
240. Heled J, Drummond AJ (2010) Bayesian inference of species trees from multilocus data. *Molecular Biology and Evolution* 27: 570-580.
241. Drummond AJ, Suchard MA, Xie D, Rambaut A (2012) Bayesian phylogenetics with BEAUti and the BEAST 1.7. *Molecular Biology and Evolution*.
242. Hung C-M, Drovetski S, Zink RM (2012) Multilocus coalescence analyses support a mtDNA-based phylogeographic history for a widespread Palearctic passerine bird, *Sitta europaea*. *Evolution*: no-no.
243. Tavares E, de Kroon G, Baker A (2010) Phylogenetic and coalescent analysis of three loci suggest that the Water Rail is divisible into two species, *Rallus aquaticus* and *R. indicus*. *BMC Evolutionary Biology* 10: 226.
244. Nadachowska K, Babik W (2009) Divergence in the face of gene flow: The case of two newts (Amphibia: Salamandridae). *Molecular Biology and Evolution* 26: 829-841.
245. Suc J-P, Do Couto D, Melinte-Dobrinescu MC, Macaleț R, Quillévéré F, Clauzon G, Csato I, Rubino J-L, Popescu S-M (2011) The Messinian Salinity Crisis in the Dacic Basin (SW

References

- Romania) and early Zanclean Mediterranean–Eastern Paratethys high sea-level connection. *Palaeogeography, Palaeoclimatology, Palaeoecology* 310: 256-272.
246. Litvinchuk SN, Borkin LJ, Džukić G, Kalezić ML, Khalturin MD, Rosanov JM (1999) Taxonomic status of *Triturus karelinii* on the Balkans, with some comments about other crested newt taxa. *Russian Journal of Herpetology* 6: 153-163.
247. Litvinchuk SN, Borkin LJ (2009) *Evolution, systematics and distribution of crested newts (Triturus cristatus complex) in Russia and adjacent countries* (Evropeisky Dom Press, St. Petersburg) p 592.
248. Otto-Bliesner BL, Marshall SJ, Overpeck JT, Miller GH, Hu A, members CLIP (2006) Simulating Arctic Climate Warmth and Icefield Retreat in the Last Interglaciation. *Science* 311: 1751-1753.
249. Losos JB (2008) Phylogenetic niche conservatism, phylogenetic signal and the relationship between phylogenetic relatedness and ecological similarity among species. *Ecology Letters* 11: 995-1003.
250. Grandcolas P, Nattier R, Legendre F, Pellens R (2011) Mapping extrinsic traits such as extinction risks or modelled bioclimatic niches on phylogenies: does it make sense at all? *Cladistics* 27: 181-185.
251. Calboli FCF, Fisher MC, Garner TWJ, Jehle R (2011) The need for jumpstarting amphibian genome projects. *Trends in Ecology & Evolution* 26: 378-379.
252. Orgel LE, Crick FHC (1980) Selfish DNA: The ultimate parasite. *Nature* 284: 604-607.
253. White KP (2001) Functional genomics and the study of development, variation and evolution. *Nature Reviews. Genetics* 2: 528-537.
254. Smadja CM, Butlin RK (2011) A framework for comparing processes of speciation in the presence of gene flow. *Molecular Ecology* 20: 5123-5140.
255. Wu C-I, Ting C-T (2004) Genes and speciation. *Nature Reviews Genetics* 5: 114-122.
256. Jehle R, Thiesmeier B, Foster J (2011) *The crested newt: A dwindling pond-dweller* (Laurenti Verlag, Kock, Bielefeld).

Summary

Both phylogeography and spatial ecology provide insight into the spatio-temporal distribution dynamics of species. We employ these two independent techniques. As a model system we use *Triturus* newts. We determine the phylogenetic relationships among and within *Triturus* species based on mitochondrial DNA. This reveals three genetically diverged but morphologically cryptic candidate species. We show that niche divergence among candidate species is comparable to that among recognized *Triturus* species. By employing three nuclear DNA markers we test whether barriers to gene flow are present and prove that candidate species actually behave as real species. Based on species distribution modeling and geographical genetic structuring, we explore *Triturus* responses to the Last Glacial Maximum. Both approaches agree on the position of glacial refugia and postglacially colonized area. By exploiting asymmetrically introgressed mitochondrial DNA we deduce the postglacial outcompeting of one newt species by another. This thesis shows that the concerted application of phylogeographical and spatial ecological approaches improves the ability to reconstruct historical biogeographical processes.

Samenvatting

Zowel fylogeografie als ruimtelijke ecologie bieden inzicht in de verspreidingsdynamiek van soorten in tijd en ruimte. Wij passen deze twee onafhankelijke technieken toe. Als model gebruiken we *Triturus* salamanders. Op basis van van mitochondriaal DNA bepalen we de fylogenetische verwantschappen tussen en binnen *Triturus* soorten. Dit onthult drie genetisch gedivergeerde maar morfologisch cryptische kandidaatsoorten. Nichedivergentie tussen kandidaatsoorten is vergelijkbaar met die tussen erkende *Triturus* soorten. Met drie nucleaire DNA markers testen we de aanwezigheid van gene flow-barrières en tonen aan dat de kandidaatsoorten zich in feite als echte soorten gedragen. Aan de hand van gemodelleerde soortverspreiding en geografische genetische structuur onderzoeken we de respons van *Triturus* op het Laatste Glaciale Maximum. De positie van glaciale refugia en postglaciaal gekoloniseerd gebied komt voor beide methoden overeen. Gebruikmakend van asymmetrisch geïntrogressieerd mitochondriaal DNA leiden we het postglaciale verdringen van de ene salamandersoort door de andere af. Dit proefschrift toont aan dat de gezamenlijke toepassing van fylogeografie en ruimtelijk ecologie de reconstructie van historisch biogeografische processen bevordert.